



**UNIVERSITÀ
DEGLI STUDI
DI PADOVA**

UNIVERSITÀ DEGLI STUDI DI PADOVA

DIPARTIMENTO DI SCIENZE CHIRURGICHE, ONCOLOGICHE E
GASTROENTEROLOGICHE

CORSO DI DOTTORATO DI RICERCA IN
ONCOLOGIA CLINICA E SPERIMENTALE E IMMUNOLOGIA
XXXI CICLO

**EPITHELIAL OVARIAN CANCER: A STUDY ON THE
AUTOPHAGIC AND MICROENVIRONMENTAL
REGULATION OF CANCER STEM CELLS AND THE PRO-
TUMORIGENIC ROLE OF CASEIN KINASE 1 DELTA**

Coordinatrice: Prof.ssa Paola Zanovello

Supervisore: Prof. Alberto Amadori

Dottoranda: Elena Laura Mazzoldi

INDEX

| | |
|---|----|
| ABSTRACT..... | 7 |
| RIASSUNTO | 9 |
| Chapter 1 | |
| OVARIAN CANCER | 11 |
| 1.1. Ovarian cancer: an overview..... | 12 |
| 1.2. Epithelial ovarian cancer..... | 13 |
| 1.2.1. Epidemiology and risk factors..... | 13 |
| 1.2.2. Staging and grading..... | 16 |
| 1.2.3. Symptoms, diagnosis, and screening challenges..... | 17 |
| 1.2.4. Therapeutic strategies..... | 20 |
| 1.2.5. Innovative therapies..... | 21 |
| Chapter 2 | |
| CANCER STEM CELLS | 26 |
| 2.1. History of CSC research..... | 28 |
| 2.2. CSC features..... | 29 |
| 2.3. Stemness master genes..... | 33 |
| 2.4. Stemness-promoting signaling pathways..... | 34 |
| 2.5. Surface and functional markers for CSC identification..... | 37 |
| 2.6. CSC metabolism..... | 39 |
| 2.7. CSC niche and tumor microenvironment contribution to stemness..... | 42 |
| 2.8. CSC as a therapeutic target..... | 43 |
| Chapter 3 | |
| OVARIAN CANCER STEM CELLS..... | 47 |
| Chapter 4 | |
| SCF/c-KIT AXIS..... | 53 |
| Chapter 5 | |
| AUTOPHAGY IN CANCER AND CANCER STEM CELLS..... | 61 |
| Chapter 6 | |
| CASEIN KINASE 1 AND TUMORIGENESIS..... | 69 |
| Chapter 7 | |
| AIM OF THE THESIS..... | 77 |

Chapter 8

| | |
|--|----|
| MATERIALS AND METHODS..... | 81 |
| 8.1. EOC primary samples, cell lines, and <i>in vitro</i> culture..... | 82 |
| 8.2. Lentiviral vector production and cell transduction..... | 83 |
| 8.3. PDX generation and <i>in vivo</i> experiments..... | 84 |
| 8.4. Extreme limiting dilution assay (ELDA)..... | 85 |
| 8.5. Flow cytometry analysis and FACS-sorting..... | 85 |
| 8.6. Western blotting (WB)..... | 87 |
| 8.7. RNA extraction, reverse transcription, and quantitative RT-PCR..... | 88 |
| 8.8. PBMC purification, monocyte isolation, and macrophage differentiation and polarization..... | 88 |
| 8.9. Enzyme-linked immunosorbent assay (ELISA)..... | 89 |
| 8.10. Proliferation assay..... | 89 |
| 8.11. <i>In vitro</i> migration assays..... | 89 |
| 8.12. Statistical analysis..... | 90 |

Chapter 9

| | |
|--|-----|
| RESULTS..... | 91 |
| 9.1. Autophagy inhibition reduces chemoresistance and tumorigenic potential of ovarian CSC..... | 93 |
| 9.1.1. Ovarian CD44 ⁺ CD117 ⁺ CSC display higher basal autophagy compared to bulk tumor cells..... | 93 |
| 9.1.2. Inhibition of autophagy affects canonical CSC properties..... | 96 |
| 9.1.3. Autophagy blockade reduces CSC ability to resist <i>in vitro</i> and <i>in vivo</i> chemotherapy treatment..... | 97 |
| 9.2. SCF is abundant in EOC ascites, it is produced by fibroblasts and macrophages, and it activates the downstream pathway in CD117 ⁺ cells..... | 101 |
| 9.2.1. SCF soluble form is produced by tumor-associated fibroblasts and macrophages..... | 101 |
| 9.2.2. Monocyte-to-macrophage differentiation induces SCF expression, irrespective of M1 or M2 polarization..... | 104 |
| 9.2.3. SCF 248 and SCF 220 activate the PI3K/Akt pathway in CD117 ⁺ cells through c-Kit activation..... | 108 |
| 9.2.4. SCF stimulation affects the canonical properties of ovarian CSC..... | 111 |
| 9.3. CK1δ plays a role in the regulation of cell proliferation, response to chemotherapy and migration in ovarian cancer cells..... | 114 |

| | |
|--|-----|
| 9.3.1. CK1 δ knockdown causes morphological changes in OVCAR3 cells and a growth braking in OVCAR3 and IGROV1 cells | 114 |
| 9.3.2. CK1 δ knockdown is associated with p21 downregulation and sensitization to carboplatin treatment | 119 |
| 9.3.3. CK1 δ knockdown affects migration in ovarian cancer cells | 121 |
| Chapter 10 | |
| DISCUSSION AND CONCLUSIONS | 127 |
| AKNOWLEDGMENTS | 135 |
| REFERENCES | 137 |

ABSTRACT

Epithelial ovarian cancer (EOC), the most lethal gynecological malignancy, is normally treated with surgery followed by platinum and taxane-based chemotherapy. Despite an initial high response rate, the majority of patients eventually relapse and die. The cause could be ascribed to a subpopulation of cancer cells, named cancer stem cells (CSC), endowed with self-renewal, high tumorigenic and metastatic potential, and drug resistance. Therefore, CSC eradication could be envisioned as a successful treatment. Part of the work included in this thesis stemmed from the idea that ovarian CSC could enjoy some growth advantage, deriving from intrinsic properties or from autocrine/paracrine circuits operating in tumor microenvironment.

Our group and others demonstrated that CD44⁺CD117⁺ cells are likely EOC CSC. Recent studies indicated autophagy as a mechanism to survive chemotherapy and that CSC in particular could rely on this metabolic process. For this reason, we decided to evaluate autophagy activation and the effects of its perturbation in CSC from EOC ascitic effusions and from patient-derived xenografts (PDX) and we found that they presented a higher basal autophagy level compared to non-CSC. Autophagy blockade with chloroquine impaired CSC viability, *in vitro* spheroid growth, and *in vivo* tumorigenic potential. In addition, autophagy inhibition and carboplatin treatment had a synergistic effect both *in vitro* and *in vivo*. Our results suggest a possible clinical application of the combined therapy in EOC as this approach would counteract tumor growth and impair the CSC compartment at the same time, thus reducing tumor relapse. As the microenvironment contribution to CSC maintenance is revealing its growing importance, we focused on SCF, the ligand of CD117 (or c-Kit). Indeed, the SCF/c-Kit axis regulates cell viability, proliferation and differentiation both in physiological conditions and in cancer. Notably, SCF exists both as a soluble and transmembrane protein. We found that the EOC ascites contained high amounts of the cytokine. Soluble SCF was detected only in tumor-associated fibroblasts and macrophages supernatants, whereas the membrane isoform was also expressed by cancer cells. Both SCF isoforms were effective in activating Akt pathway in CD117⁺ cells, while the tyrosine kinase inhibitor imatinib abolished this effect. Accordingly, results obtained in spheroid assays suggest that SCF stimulation could enhance the canonical CSC properties and imatinib pre-treatment inhibited them. Overall, SCF stimulation might help CSC to survive in selective culture conditions and, more extensively, could support CSC survival in patient ascitic fluid.

Besides the role played by CSC in tumor outgrowth, the malignant cells forming the tumor bulk are sustained by pro-tumorigenic protein activation. Thus, we investigated the role of casein kinase 1 delta (CK1δ), member of a kinase family involved in many cellular processes, which

is genetically amplified in ovarian cancer and overexpressed in other cancer types. Since CK1 δ inhibition induced cell cycle arrest and apoptosis in a variety of tumor cell lines and delayed tumor growth *in vivo*, we evaluated the effects of CK1 δ knockdown on two EOC cell lines (OVCAR3 and IGROV1) both *in vitro* and *in vivo*. Silenced cells grew more slowly and were less tumorigenic *in vivo*. Moreover, CK1 δ knockdown sensitized ovarian cancer cells to carboplatin treatment. Interestingly, CK1 δ -depleted OVCAR3 cells resulted more prone to migrate *in vitro* and more metastatic *in vivo*, but these results need further confirmation in IGROV1 cells. Since numerous small molecule inhibitors targeting CK1 δ have been synthesized and tested, it would be important to unveil the molecular mechanism linking CK1 δ to metastatic potential before these compounds enter the clinic for EOC management.

This thesis encompasses three different topics, characterized by the common aim of investigating EOC biology from different perspectives, in order to highlight novel weak points of this deadly disease.

RIASSUNTO

Il carcinoma ovarico (EOC) è solitamente trattato tramite chirurgia e chemioterapia a base di platino e taxani. Nonostante un'iniziale risposta, nella maggior parte delle pazienti l'esito è la ricaduta e la morte. La causa può essere legata ad una popolazione di cellule cancerose, le cellule staminali tumorali (CSC), dotate di capacità di autorinnovamento, grande potenziale tumorigenico e metastatico e resistenza ai chemioterapici. Per questo, la loro eradicazione potrebbe essere una strategia terapeutica molto efficace. Parte di questo lavoro deriva dall'idea che le CSC godano di un vantaggio di crescita dovuto a caratteristiche intrinseche o a circuiti paracrini che si instaurano nel microambiente neoplastico.

Il nostro gruppo ha dimostrato che le cellule $CD44^+CD117^+$ sono verosimilmente le CSC nell'EOC. Studi recenti hanno dimostrato che l'autofagia è un meccanismo di sopravvivenza alla chemioterapia e che le CSC potrebbero dipendere da questo processo. Abbiamo quindi valutato i livelli di autofagia e gli effetti causati da sue alterazioni su CSC isolate da asciti di pazienti con EOC e da xenotrapianti. Le CSC presentano un livello autofagico basale più alto rispetto alle non-CSC. Il blocco dell'autofagia compromette la vitalità delle CSC, la formazione di sferoidi *in vitro* e il loro potenziale tumorigenico *in vivo*. Inoltre, l'inibizione dell'autofagia e il trattamento con carboplatino (CPT) mostrano un effetto sinergico sia *in vitro* che *in vivo*. I nostri risultati suggeriscono una possibile applicazione clinica nell'EOC di tale terapia combinata, in quanto contrasterebbe la crescita tumorale colpendo al contempo il compartimento staminale, riducendo così il rischio di recidiva.

Visto il contributo dato dal microambiente al mantenimento delle CSC, abbiamo posto la nostra attenzione su SCF, il ligando di CD117 (c-Kit). Infatti, l'asse SCF/c-Kit controlla la vitalità, la proliferazione e il differenziamento cellulare sia in contesti fisiologici che nel cancro. SCF esiste sia in forma solubile che associata alla membrana plasmatica. Abbiamo misurato alte concentrazioni della citochina in asciti delle pazienti affette da EOC. La forma solubile è rilevabile solo in surnatanti di macrofagi e fibroblasti associati al tumore, mentre quella di membrana è espressa anche da cellule tumorali. Entrambe le isoforme possono attivare la via di Akt in cellule $CD117^+$, mentre l'inibitore tirosin-chinasico imatinib blocca questo effetto. Similmente, i saggi su sferoidi suggeriscono che la stimolazione mediata da SCF può potenziare le proprietà canoniche delle CSC, inibite dal pretrattamento con imatinib. La stimolazione da parte di SCF può quindi favorire la sopravvivenza delle CSC, e supportarle all'interno dell'ascite.

A parte le CSC, il cancro è sostenuto dall'attivazione di proteine pro-tumorali. Per questo, abbiamo indagato il ruolo della casein chinasi 1 delta (CK1 δ), coinvolta in molteplici processi

cellulari, la cui amplificazione genica o iperespressione è stata descritta nell'EOC e in molte altre neoplasie. Poiché è noto che l'inibizione di CK1 δ induce arresto del ciclo cellulare e apoptosi in linee cellulari tumorali e rallenta la crescita dei tumori *in vivo*, abbiamo valutato *in vitro* e *in vivo* gli effetti del silenziamento della CK1 δ su due linee cellulari di carcinoma ovarico (OVCAR3 e IGROV1). Le cellule silenziate crescono più lentamente e sono meno tumorigeniche. Inoltre, il silenziamento di CK1 δ sensibilizza le cellule al trattamento con CPT. Inoltre, le cellule OVCAR3 silenziate per CK1 δ risultano più prone a migrare *in vitro* e più metastatiche *in vivo*. Poiché sono state sintetizzate numerose molecole che inibiscono la CK1 δ , sarebbe importante delineare il meccanismo molecolare che lega la CK1 δ al potenziale metastatico prima che questi composti possano entrare nella pratica clinica per il trattamento dell'EOC.

Questa tesi è comprensiva di tre differenti macroaree, caratterizzate dal comune scopo di studiare la biologia dell'EOC da differenti punti di vista, al fine di portare alla luce nuovi punti deboli di questa malattia mortale.

Chapter 1

OVARIAN CANCER

1.1. Ovarian cancer: an overview

Ovarian cancer is a heterogeneous group of neoplasms of the ovary, both benign and malignant. According to the histology, ovarian tumors can be classified in germ cell, stromal, or epithelial (1).

Germ cell ovarian tumors originate from the ova, and include dysgerminomas, yolk sac tumors/endodermal sinus tumors, embryonal carcinomas, polyembryomas, choriocarcinomas, immature and mature teratomas (2).

They are mainly diagnosed in young women and girls, being the most common ovarian tumor in women under 30. Germ cell tumors are mostly benign, accounting for the 25% of benign ovarian tumors, with mature teratoma (or dermoid cyst) being the most frequent subtype among them. Only 2-3% of germ cell tumors are malignant (3); the most common germ cell cancer is dysgerminoma, followed by immature teratoma. They are characterized by favorable prognosis, even if diagnosed in advanced stage (2).

Sex-cord stromal tumors originate from the stroma of the ovary or from the gonadal sex cord cells, and include granulosa cell tumors (adult and juvenile types), thecomas, fibromas, fibrosarcomas, sclerosing stromal tumors, Signet-ring stromal tumors, and Sertoli-Leydig cell tumors (2).

This category encompasses both benign and malignant types and accounts for the 5-8% of all ovarian tumors. The most common type is granulosa cell tumor (90% of sex-cord stromal tumors, 5% of all ovarian cancers), which is malignant. Any ages are involved, but the peak of incidence is at the age of 52 years. Sex-cord stromal tumors are usually indolent and slow-growing; the prognosis is often good, but more aggressive cases may occur (2, 4, 5).

Granulosa cell tumor produces estrogens, and this causes its typical symptoms: menometrorrhagia or post-menopausal bleeding, precocious puberty (in the juvenile case) and endometrial hyperplasia.

Sertoli-Leydig cell tumor occurs in younger patients (mean 25 years), and it is characterized by androgen production, which causes virilization (2, 5). Thecomas and fibromas are benign stromal tumors (1).

Epithelial ovarian tumors originate from the surface epithelium of the ovary, and include serous, mucinous, endometrioid, clear cell, and Brenner (or transitional) tumors (6).

Most of epithelial tumors are benign, and include serous and mucinous cystadenomas and Brenner tumors (1). Also low malignant potential (or borderline) epithelial ovarian cancers are observed (7).

Malignant carcinoma includes the serous, mucinous, endometrioid, transitional, squamous cell and clear cells subtypes (plus the undifferentiated one), with the serous cancer being the most frequent, as it accounts for 70-80% of epithelial ovarian cancers (3, 8).

Since it is the most common type of this malignancy, epithelial ovarian cancer (EOC) is often merely referred to as ovarian cancer (8). Moreover, it is the most lethal subtype, being usually diagnosed in advanced stages, thus resulting in a median survival of less than 5 years (9).

The present thesis will exclusively concern epithelial ovarian cancer.

1.2. Epithelial ovarian cancer

1.2.1. Epidemiology and risk factors

Even if EOC represents less than the 3% of the cases of cancer among women in USA (and therefore it does not appear among the ten most frequent cancers, Fig. 1.1), it is the fifth leading cause of cancer-related death among females, and the first cause of death if considering only the gynecological malignancies (Fig. 1.2). In USA, 22,240 new cases are predicted in 2018, and 14,070 patients will die of this cancer (10).

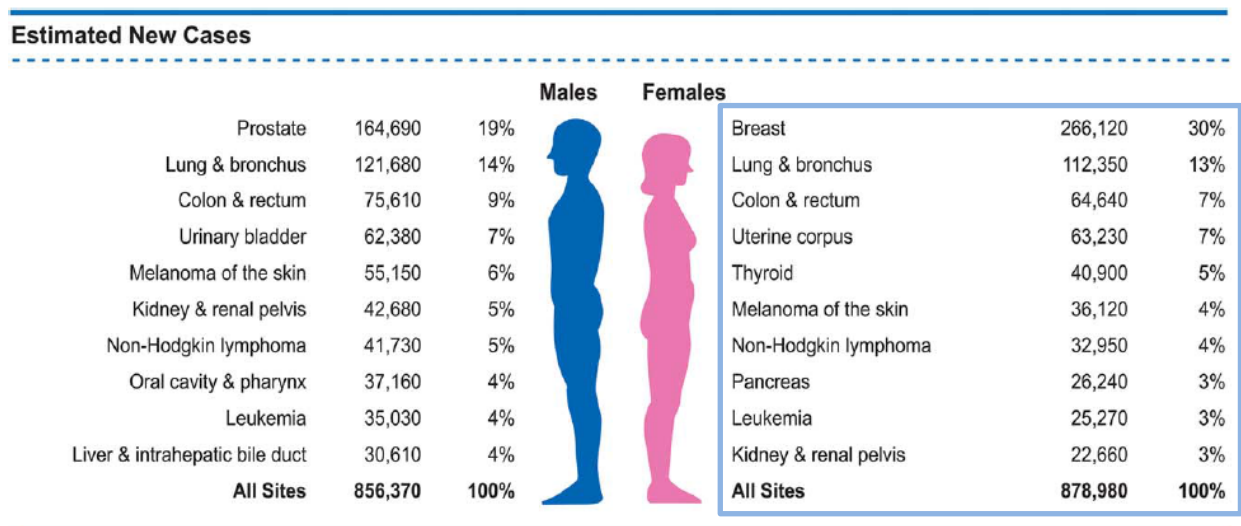


Figure 1.1. Estimated new cases of cancer: ten most frequent types by sex in USA, in 2018 (10).


| Estimated Deaths | | | | | Estimated Deaths | | |
|--------------------------------|----------------|-------------|---|--------------------------------|------------------|-----|--|
| | | | Males | Females | | | |
| Lung & bronchus | 83,550 | 26% |  | Lung & bronchus | 70,500 | 25% | |
| Prostate | 29,430 | 9% | | Breast | 40,920 | 14% | |
| Colon & rectum | 27,390 | 8% | | Colon & rectum | 23,240 | 8% | |
| Pancreas | 23,020 | 7% | | Pancreas | 21,310 | 7% | |
| Liver & intrahepatic bile duct | 20,540 | 6% | | Ovary | 14,070 | 5% | |
| Leukemia | 14,270 | 4% | | Uterine corpus | 11,350 | 4% | |
| Esophagus | 12,850 | 4% | | Leukemia | 10,100 | 4% | |
| Urinary bladder | 12,520 | 4% | | Liver & intrahepatic bile duct | 9,660 | 3% | |
| Non-Hodgkin lymphoma | 11,510 | 4% | | Non-Hodgkin lymphoma | 8,400 | 3% | |
| Kidney & renal pelvis | 10,010 | 3% | | Brain & other nervous system | 7,340 | 3% | |
| All Sites | 323,630 | 100% | All Sites | 286,010 | 100% | | |

Figure 1.2. Ten most frequent causes of cancer-related death by sex in USA, in 2018 (10).

In Italy, 5,200 new cases were estimated in 2016; so, also in Italy EOC does not appear among the first five diagnosed tumor types in women, since it represents only the 2.9% of all cancers. In 2013, 3,302 women died of EOC, making it the fourth cause of cancer-related death in the age range 0-49, and the fifth cause if considering the range 50-69 years (11).

Worldwide, EOC occurs in 240,000 women per year. The incidence is different in highly and poorly industrialized areas: 9.2 per 100,000 people versus 5 per 100,000 people (age-standardized ratio), respectively (12). The median age at diagnosis is 63 years (13), as 2/3 of cases are diagnosed in women over 55 years of age (14). In Italy, the lifetime risk of developing EOC is 1 woman out of 74 (11).

The main risk factors are linked to the number of ovulations (15), including short periods, early age at menarche and late age at menopause, together with nulliparity. On the contrary, late age at menarche, having many pregnancies and breastfeeding, early menopause, a prolonged use of oral contraceptives, short use of intrauterine device, and tubal ligation are protective factors (3, 16-20).

The rationale of the “incessant ovulation” theory is that the monthly injury due to ovulation stimulates cell proliferation in order to repair the wounds in the surface epithelium of the ovary, making mutations and cancerous transformation more likely to occur (21).

Other risk factors are inflammatory conditions, such as endometriosis and pelvic inflammatory disease (15, 22). Indeed, chronic inflammation is a well-known trigger for cancer development (23). This may explain in part the protective effect of tubal ligation, since this contraceptive

intervention does not stop ovulation but can block pro-inflammatory agents, such as talc, vaginal gels and foams, viruses, and menstrual blood and debris, from reaching the ovary (3, 24). Though, whether the perineal use of talc is a cancer-promoting behavior or not, is controversial (25-28).

On the contrary, it has been proposed that acute inflammatory events, *e.g.* mastitis, mumps, or intrauterine device (IUD) use, could raise an immune response against a low-glycosylated form of mucin-1 (MUC-1), which is commonly expressed in cancer and in inflammatory conditions, so stimulating the immune system to recognize cancer precursor lesions. As opposite, chronic inflammation eventually induces immune tolerance (3, 29).

Factors of hormonal nature (postmenopausal hormone replacement treatment based on estrogen only (30), not successful fertility treatments (31, 32), and obesity (33)) are associated to augmented ovarian cancer risk.

Finally, smoking seems to be associated to reduced risk of clear cell and endometrioid carcinoma and to increased risk of mucinous carcinoma; no association with the other histotypes is observed (34).

Genetic predisposition must also be considered. Indeed, women with Lynch syndrome and with germline mutations in breast cancer susceptibility gene (BRCA)-1 and BRCA-2 have an increased lifetime risk of several cancers, including EOC (35), and tend to develop cancer 10 years earlier than the general population (13).

Lynch syndrome is an autosomal dominant disease characterized by germline mutations in mismatch repair genes (*i.e.* MLH1, PMS2, MSH2, MSH6, and EPCAM). Lynch syndrome patients have a lifetime risk for EOC of 6.7% (36). Lynch syndrome is responsible for only the 2% of EOC (37), but the 10% of sporadic EOC are characterized by somatic mutations in mismatch repair genes (38).

BRCA-1 and BRCA-2 are drivers of DNA double strand break repair through homologous recombination (35). Patients with a germline inactivating mutation of BRCA-1 or BRCA-2 have a lifetime risk of EOC of 54 and 23%, respectively (39). BRCA mutations are particularly frequent among Ashkenazi Jews, making this population more prone to develop BRCA-associated cancers (40). Among EOC cases, 13.3% are carriers of germline BRCA mutations, but the proportion is higher if considering only high-grade serous carcinoma (41). Somatic BRCA-1 and -2 mutations and BRCA-1 epigenetic silencing are found in 3.5% (42) and 15% (43) of sporadic EOC, respectively.

For BRCA mutation carriers, a prophylactic bilateral salpingo-oophorectomy is recommended to reduce the risk of EOC (44).

EOC patients carrying BRCA mutations are demonstrated to have a better prognosis (35), and respond better to platinum-based chemotherapy (45). They are also the best candidates to poly ADP-ribose polymerase (PARP) inhibition therapy (8).

In a similar way, mutations in additional genes of the double strand repair pathway (RAD51C, RAD51D, BRIP1) may confer an increased risk of EOC (46).

1.2.2. Staging and grading

Ovarian cancer (epithelial and non-epithelial) is staged according to the International Federation of Gynecology and Obstetrics (FIGO) staging system. The most recent staging system dates back to 2014 (47). FIGO staging parallels the American Joint Committee on Cancer (AJCC) staging system, which uses the TNM score, but is based on information obtained after surgery. When feasible, it also applies to fallopian tube cancer and primary peritoneal cancer.

According to FIGO, the possible stages are: I (A, B, C), II (A, B, C), III (A1i, A1ii, A2, B, C), IV (A, B) (Table 1.1) (48).

| TNM | FIGO | DEFINITION |
|--------------|---------|---|
| Tx | | Primary tumor cannot be assessed |
| T0 | | No evidence of primary tumor |
| T1 | I | Tumor limited to one or both ovaries or fallopian tubes |
| T1a | IA | Tumor limited to one ovary; capsule intact, no tumor on ovarian surface or fallopian tube surface; no malignant cells in ascites or peritoneal washings |
| T1b | IB | Tumor limited to both ovaries or fallopian tubes; capsule intact, no tumor on ovarian or fallopian tube surface; no malignant cells in ascites or peritoneal washings |
| T1c | IC | Tumor limited to one or both ovaries or fallopian tubes with any of the following: surgical spill, capsule ruptured before surgery or tumor on ovarian or fallopian tube surface, malignant cells in ascites or peritoneal washings |
| T2 | II | Tumor involves one or both ovaries or fallopian tubes with pelvic extension or primary peritoneal cancer |
| T2a | IIA | Extension and/or implants on uterus and/or fallopian tubes and or ovaries |
| T2b | IIB | Extension to other pelvic tissues, including bowel within the pelvis |
| T3 and/or N1 | III | Tumor involves one or both ovaries or fallopian tubes or primary peritoneal carcinoma with spread to the peritoneum outside the pelvis and/or metastasis to the retroperitoneal lymph nodes |
| N1 | | Retroperitoneal lymph node metastasis only |
| N1a | IIIA1i | Lymph node metastasis not more than 10 mm in greatest dimension |
| N1b | IIIA1ii | Lymph node metastasis more than 10 mm in greatest dimension |

| | | |
|--------------|-------|---|
| T3a any N | IIIA2 | Microscopic extrapelvic peritoneal involvement with or without retroperitoneal lymph node, including bowel involvement |
| T3b any N | IIIB | Macroscopic extrapelvic peritoneal metastasis, including bowel involvement outside the pelvis with or without retroperitoneal nodes |
| T3c any N | IIIC | Extrapelvic peritoneal metastasis and/or retroperitoneal lymph node metastasis (includes extension of tumor to capsule of liver and spleen without parenchymal involvement of either organ) |
| M1 | IV | Distant metastasis (excludes peritoneal metastasis) |
| M1a | IVA | Pleural effusion with positive cytology |
| M1b | IVB | Parenchymal metastasis and metastasis to extra-abdominal organs (including inguinal lymph nodes and lymph nodes outside the abdominal cavity) |

Table 1.1. AJCC and FIGO stages of ovarian cancer (48)

Apart from the stage, a grade is assigned to ovarian cancer. The grade indicates how abnormal or malignant the cancer cells appear, so it is a measure of their invasiveness and differentiation level.

Grade 1 indicates that the tumor is well differentiated; grade 2 identifies moderately differentiated tumors; poorly differentiated tumors are referred as grade 3.

Grading represents a strong prognostic factor: high-grade tumors have the worst prognosis, while low-grade tumors have the best one (49).

In 2004, Shih and Kurman proposed a new model to classify ovarian cancer into type I and type II tumors, on the basis of their grade and molecular features. Type I tumors are low-grade and include low-grade serous, endometrioid, mucinous and clear cell carcinoma; they are characterized by B-RAF, K-RAS, and phosphatase and tensin homolog (PTEN) mutations and by microsatellite instability. Type II tumors are high-grade (high-grade serous carcinoma and carcinosarcoma), and are frequently mutated in tumor protein 53 (TP53), BRCA-1, BRCA-2, neurofibromin 1 (NF1), and cyclin-dependent kinase 12 (CDK12) (6).

1.2.3. Symptoms, diagnosis, and screening challenges

Even if the five-year survival rate for stage I ovarian cancer is about 90%, the 70% of patients are diagnosed at advanced stage disease (III and IV) and have a five-year survival rate of 30-40% (50).

This is mainly due to the paucity of symptoms, which are often in common with other benign gastrointestinal, urinary, and gynecological conditions, and include abdominal bloating, fatigue, pelvic/abdominal pain or discomfort, back pain, indigestion and loss of appetite, weight loss, constipation or diarrhea, increase in urinary frequency, and postmenopausal vaginal

bleeding (51). These symptoms are often lacking during the early stage of disease because of the anatomical location of the ovaries, and appear only when cancer has grown or disseminated, and ascitic fluid has accumulated in the peritoneum (52).

The diagnostic procedure includes pelvic examination, imaging techniques, such as computed tomography (CT) scan or transvaginal ultrasound, and a complete blood test which can include tumor markers, such as cancer antigen 125 (CA-125) and human epididymis protein 4 (HE4) (53). When an adnexal mass is detected and cancer is suspected, a risk of malignancy index (RMI) should be calculated in order to refer the patient to further assessment by either a general gynecologist or a gynecological oncologist (13). The RMI was firstly proposed by Jacobs *et al.* in 1990 (54), and further evolved over the years to improve its diagnostic value. In 2009, Yamamoto *et al.* (55) compared four different ways to calculate RMI and assessed that the most reliable in discriminating among benign and malignant lesions is:

$$RMI = \text{ultrasound score} \times \text{menopausal score} \times \text{tumor size score} \times \text{CA-125 level.}$$

In this way, if malignant ovarian cancer is suspected, surgery shall be performed by a gynecological oncologist in order to confirm the diagnosis, to classify the tumor from a histopathological point of view, and to assign a FIGO stage. Surgery must include tumor debulking, which is usually accompanied by salpingo-oophorectomy, hysterectomy, lymphadenectomy; omentectomy, and peritoneal washing (56).

Since the diagnosis is often incidental and occurs when the disease is already at an advanced stage and has spread to the peritoneum, resulting in poor prognosis, a screening method for general population to detect early stage EOC is auspicated. EOC is a perfect candidate to screening because it is often a fatal condition and treatment can change the natural history of the disease, if undertaken at an early stage (14, 52). However, the establishment of effective screening procedures has to face major hurdles: first of all, no precancerous lesion has been identified for EOC and it is unclear whether an advanced stage disease is a result of the progression from an early stage or if it directly initiates as a stage III cancer. Several models have been proposed to explain EOC pathogenesis. In fact, molecular evidence suggests that serous carcinoma may originate from the transformed fallopian tube epithelium which is conglobated by ovarian epithelium during ovulation rupture, and that clear-cell and endometrioid carcinomas derive from endometriosis, rather than from the ovarian surface epithelium metaplasia (57). Prophylactic salpingo-oophorectomy in high risk women, indeed, revealed pre-neoplastic lesions in the tubes and not in the ovaries (58).

Secondly, as EOC is characterized by low prevalence, a useful screening test must have both high specificity (99.6%) and high sensitivity (75%) to reach an acceptable positive predictive value (10%), especially because a suspected ovarian cancer invariably results in invasive diagnostic procedures, with associated morbidity (14, 52).

Current screening strategies include transvaginal ultrasonography and the measurement of tumor markers, first of all CA-125.

Transvaginal sonography is better than transabdominal one in revealing details of the ovarian morphology; however, ultrasonography presents some limits. First, it relies upon operator interpretation. Second, in different studies it showed different positive predictive values, which ranged between 1 and 27%. This method would have a lower frequency of false positives in post-menopausal women because the ovary is affected by less physiological changes in this phase of life. Moreover, the number of false positive could decrease by repeating the analysis over the time. However, ultrasonography may lead to unnecessary surgery to remove many benign lesions.

Measurement of serum CA-125 levels is a non-invasive, non-operator dependent and cheaper strategy, but the specificity of the test is low, since CA-125 levels are also elevated in other both benign and malignant conditions. Moreover, CA-125 levels may be in the range of normality in half stage I EOC patients. In order to improve specificity and sensitivity, a panel of tumor markers has been proposed together with CA-125. However, this approach generally resulted in augmented sensitivity but decreased specificity.

A more effective approach is the Risk of Ovarian Cancer (ROC) algorithm, in which CA-125 levels are monitored over the time. The rationale it is based on is that women affected by EOC show a progressive increase of CA-125 values. The result is that ROC has a positive predictive value of 19%, higher of the acceptance threshold.

To sum up, two clinical trial (UKCTOCS and PLCO), designed to evaluate multimodal screening approaches, failed to show a significant decrease in mortality in screened participants compared to non-screened women, but led to unnecessary surgery and to psychological distress due to abnormal test results (59). Hence, several professional organizations do not recommend screening in the general population nowadays; in USA, the National Comprehensive Cancer Network suggests screening every six months only in women at high EOC genetic risk (44), even though the UKFOCCS trial demonstrated no survival benefit also in this cohort (60), and so prophylactic bilateral salpingo-oophorectomy is still the most effective intervention (14).

1.2.4. Therapeutic strategies

The standard of care for EOC consists of debulking surgery followed by adjuvant chemotherapy based on carboplatin plus paclitaxel every three weeks for six cycles (61), and little has changed over the last 20 years (62).

Ovarian cancer is often considered to be chemosensitive, with a response rate higher than 80% after first-line treatment (15). However, about 70% of patients relapse within 12-18 months (63). Patients diagnosed at early stage disease (FIGO I and II) are usually cured with surgery alone (90% cure rate for stage Ia and Ib). Nonetheless, patients with high-risk early stage cancer (Ic and II) often relapse. The ACTION trial has established that the administration of adjuvant chemotherapy improves the 5-year survival rate by 8% in this category of patients (82% vs 74% with surgery alone) (64).

However, the majority of ovarian cancers are diagnosed at advanced stages. For these patients, the cure rate is only 20-25% (64). The gold standard of therapy is primary cytoreductive surgery followed by adjuvant chemotherapy. In these cases, the prognosis is mainly driven by the extent of debulking: patients with no visible masses after surgery have better survival probability than those with residual disease (45). Regarding chemotherapy, in 1996, the superiority of the combination cisplatin/paclitaxel over cisplatin/cyclophosphamide was established (GOG study) (65). Then, cisplatin has been replaced by carboplatin because it causes less non-hematological toxicities (66).

In spite of this, most patients relapse: the progression-free survival is less than two years, and the 5-year survival rate, although improved from the Seventies (64), is still lower than 50% (45% considering all stages, 90% for stage I, 70% for stage II, 39% for stage III, 17% for stage IV) (67). On the other hand, the 20% of advanced stage ovarian cancer patients survive more than 12 years; 12 year after diagnosis, the death risk of EOC patients is similar to general population, and cancer turns to be a chronic disease. This usually happens in patients in whom a status of no residual disease is reached thanks to debulking surgery (62).

Neoadjuvant chemotherapy is suggested only in women with tumors too large to be resected, in order to lower surgery-associated morbidity. In the other cases, it should be avoided because chemotherapy kills the majority of chemosensitive cells and renders the chemoresistant ones invisible to the surgeon, making the goal of “no residual disease” difficult to achieve or, better, it could lead to a false status of “no residual disease” (62). Indeed, it has been reported that the 7-year survival rate among patients referred to be without residual disease after surgery is 74%

if they underwent primary surgery, and 8% if they underwent neoadjuvant chemotherapy followed by interval cytoreduction, probably because they were not really tumor-free (68).

Patients can relapse within 6 months from the completion of therapy: in this case, they are considered platinum-resistant. If patients relapse from 6 to 12 months after the last chemotherapy cycle, they are categorized as partially platinum-sensitive. If the recurrence occurs after 12 months, the disease is platinum-sensitive (13). Platinum-sensitive recurrence is chemo-treated with carboplatin-based second-line regimens (carboplatin is administered alone or, better, in combination with paclitaxel, or gemcitabine, or pegylated liposomal doxorubicin), with a 60% chance of response. The longer the platinum-free interval, the higher is the response rate. Patients with platinum-resistant relapse have the worst prognosis, and they are treated with single agents, such as topotecan, paclitaxel, or pegylated liposomal doxorubicin. For partially platinum-sensitive patients, the consensus is lacking: challenging with a second round of platinum leads to lower response rates in comparison to fully platinum-sensitive patients (25-40%, depending on the duration of the platinum-free interval), together with higher toxicities. An alternative to platinum (which however remains an option) is trabectedin plus pegylated liposomal doxorubicin. Data show that it is possible to revert the resistance towards platinum by extending the platinum-free interval, resorting to different chemotherapeutic agents (45). Often, recurrence is anticipated by an increase in CA-125 levels; however, it has been demonstrated that re-treating patient at the elevation of this marker does not provide a survival advantage compared to treating at symptom appearance, but only leads to higher toxicities (69). Secondary surgery at relapse may be performed for cytoreduction or for palliation; in both cases, it is not curative. The DESKTOP study evidenced that the progression-free survival and the overall survival are prolonged only in patients in whom a complete debulking is achieved. Such patients can be selected thanks to the Arbeitsgemeinschaft Gynaekologische Onkologie (AGO) score, *i.e.* if the ascites is less than 500 mL, if optimal debulking was achieved after primary surgery, and if the performance status at relapse is good (45).

1.2.5. Innovative therapies

In order to improve EOC outcomes, research focused on developing new chemotherapy delivery routes (hyperthermic intraperitoneal chemotherapy, HIPEC), new schedules (dose-dense regimens), and targeted therapies.

Intraperitoneal chemotherapy consists in the delivery of high doses of chemotherapeutics directly to the tumor, in the abdomen, in order to improve efficacy and limit the adverse effects associated to systemic delivery (45). A phase III trial from the Gynecologic Oncology Group (70) compared intravenous paclitaxel/cisplatin to intravenous paclitaxel plus intraperitoneal cisplatin/paclitaxel in optimally debulked stage III patients, and it assessed that the intraperitoneal group had better progression-free survival and overall survival, but at the expense of quality of life: indeed, only 42% of patients completed the six cycles, because of adverse effects. More recently, modified regimens have improved compliance. Indeed, in the OV21/PETROC trial (71), it was demonstrated that advanced stage EOC patients treated with intraperitoneal carboplatin (instead of cisplatin) after neoadjuvant chemotherapy and optimal debulking have a better 9-month progressive disease rate compared to the intravenous delivery, with no increase in toxicity. Further studies have demonstrated that the best outcomes are observed in patients with no visible disease after surgery, as compared to optimally debulked patients, who still have a residual lesion (< 1 cm diameter). Indeed, patients with no residual disease have a 10-year survival rate of 50% if treated intraperitoneally, versus 33% if treated by intravenous chemotherapy. Patients with residual disease have a 5-year survival rate of 45% if treated intraperitoneally, versus 30% if treated with intravenous chemotherapy, but the 10-year survival rate is 18%, regardless the route of delivery (62, 72).

Currently, administration of hyperthermic intraperitoneal chemotherapy (HIPEC) at the time of interval cytoreductive surgery is under evaluation as an alternative to repetitive cycles of intraperitoneal chemotherapy in order to reduce toxicities (73). In a study from van Driel *et al.* (74), it was demonstrated that the addition of HIPEC leads to longer progression-free survival and overall survival than surgery without higher rates of adverse effects. However, the practical implications of similar results are still under discussion, thus HIPEC continues to be an experimental procedure (75).

Dose-dense regimens consist in the administration of lower doses chemotherapeutics weekly instead of the standard schedule of one administration every three weeks. The rationale is that the treatment is more effective if the intervals between administrations are shorter (76). A Japanese study (77) showed that the overall survival is higher in patients who received paclitaxel once a week plus carboplatin once in three weeks, compared to patients who received chemotherapy according to the conventional schedule. On the contrary, these promising results were not supported by GOG262 (78) and MITO-7 (79) studies, which reported much smaller

benefits in terms of progression-free survival using the dose-dense approach instead of the conventional one.

A major effort is now undertaken in the field of precision medicine, in order to develop personalized therapeutic strategies, to mine the cancer at its molecular basis (8).

A number of targeted agents against oncogenic proteins, *i.e.* growth factors, proangiogenic factors and their receptors, signal transducers, and proteins involved in the DNA repair machinery, have been trialed in ovarian cancer patient cohorts.

The most promising molecules are PARP inhibitors. PARP is a family of nuclear enzymes involved in DNA single-strand break repair. Tumor cells from patients with germline or somatic mutations in BRCA-1 or -2 are defective in double-strand break repair and, hence, they are more sensitive to chemotherapeutic agents. These cells rely mostly on single-strand break repair to survive. Therefore, blocking this mechanism in cells that are already defective for double-strand break repair has a cytotoxic effect, due to the phenomenon of synthetic lethality (63).

The SOLO-2 trial results encourage the use of olaparib (a PARP1 inhibitor) as maintenance therapy in patients with platinum-sensitive recurrent ovarian cancer, with germline or somatic mutations in BRCA genes. Indeed, olaparib significantly increases the progression-free survival in this cohort, and causes only limited toxic effects (80).

The ENGOT-OV16/NOVA trial described beneficial effects of a PARP1/2 inhibitor, niraparib, also in patients with platinum-sensitive relapse without BRCA mutations, even though the increase in progression-free survival is not as high as in the BRCA-deficient cohort (81).

Other trials are testing various PARP inhibitors in combination with chemotherapy, in particular with DNA damaging agents, as their effects are expected to be synergistic (63).

Antiangiogenic drugs are agents which target the axis vascular-endothelial growth factor/vascular-endothelial growth factor receptor (VEGF/VEGFR), and include monoclonal antibodies which neutralize VEGF, first of all bevacizumab, and VEGF receptor tyrosine kinase inhibitors, such as cediranib, pazopanib, and sunitinib (82). Angiogenesis is a key pathway in supporting many cancers, including ovarian cancer. It is necessary to deliver oxygen and nutrients when the tumor reaches dimensions such that diffusion is not sufficient to, and it drives ascites formation. Blood vessels formed in this way tend to be abnormal and leaky; blocking this axis leads to vascular normalization, and to a better oxygenation and delivery of chemotherapy. Moreover, it inhibits the formation of malignant ascites (82).

However, drug-resistant clones may emerge; therefore, it is better to combine more antiangiogenic agents that block the pathway at different levels. Nonetheless, this strategy is

accompanied by higher toxicities, including proteinuria, hypertension, and, more importantly, bowel perforation (13, 82), which is one of the main causes of mortality in ovarian cancer patients (83).

Data from several clinical trials testing antiangiogenic drugs in combination with standard chemotherapy regimens and as maintenance therapy highlight that this strategy improves progression-free survival, without affecting overall survival (only ICON6 and ICON7 trial demonstrated a modest increase in the overall survival) (13). As a result of the OCEANS trial (84), the European Medicines Agency (EMA) approved the use of bevacizumab in combination with carboplatin and gemcitabine as first-line therapy in relapsed platinum-sensitive ovarian cancer patients (45).

Up to 70% ovarian cancer overexpress epithelial growth factor receptor (EGFR). EGFR overexpression is linked to chemoresistance and poor prognosis (63). Monoclonal antibodies and tyrosine kinase inhibitors against EGFR exist and they are used in the clinical practice in lung and colorectal cancer. However, clinical trials assessing the efficacy of such agents in improving the prognosis in EOC turned to be unsuccessful (85, 86).

The isoform alpha of folate receptor is expressed in few normal cells, but is overexpressed in epithelial tumors, including EOC. In EOC, it is particularly overexpressed at advanced stages. Folate receptor allows cells to grow even in the presence of low concentrations of this vitamin. All these features make folate receptor a perfect candidate as a druggable target. Vintafolide, a folate conjugated with a vinca alkaloid, has been designed to deliver this agent directly to cells overexpressing folate receptor, and has been studied in the PRECEDENT study, in combination with pegylated liposomal doxorubicin. Vintafolide confers an improvement in progression-free survival, even though modest (5.0 versus 2.7 months) (87).

Farletuzumab is a monoclonal antibody against folate receptor. It has been studied in combination with carboplatin and taxanes or with carboplatin and pegylated liposomal doxorubicin in patients with platinum-sensitive ovarian cancer. These trials highlighted that farletuzumab confers a longer progression-free survival, and the combination with pegylated liposomal doxorubicin is well tolerated (88). More recently, however, another study testing the combination farletuzumab/ carboplatin/taxanes evidenced that the conferred small increase in progression-free survival is not statistically significant (8).

Numerous other agents have been proposed, and are under investigation, including phosphoinositide 3-kinase (PI3K) inhibitors (89), mammalian target of rapamycin (mTOR) inhibitors (90), mitogen-activated protein kinase (MAPK) inhibitors (91), monoclonal antibodies against hepatocyte growth factor (HGF) or its receptor MET, or MET kinase inhibitors (92), or immunotherapy (monoclonal antibodies towards CA-125 to elicit humoral and T-cell responses against tumor (93)). Although promising and effective in preclinical models, all these approaches gave rise to conflicting results in clinical trials and eventually turned to be minimally or not beneficial (8).

Although a great deal of effort at finding a solution to improve the outcome of ovarian cancer patients has been spent, EOC is still a big killer. Understanding the pathogenesis of this heterogeneous disease will help researchers to find an appropriate target that could mine the core of cancer and eventually lead to its cure.

Chapter 2

CANCER STEM CELLS

It has long been supposed that cancer is a disorganized mass of extensively proliferating cells out of the homeostatic control. The tumor mass originally arises from a single transformed cell, but it is often observed that tumors become heterogeneous, as different subclones emerge as a result of the progressive accumulation of mutational events (94). However, in the mid-1990s, pioneering studies shaped a new concept of cancer as a stem cell disease. Indeed, cancer has been described as a malignant tissue organized similarly to its normal counterpart, *i.e.* hierarchically, with cells at different differentiation stages and with different proliferative potential (95). At the apex of this hierarchy, there are a few, long-living, undifferentiated stem cells, which give rise to transit-amplifying progenitors, which finally form the non-proliferative, more (aberrantly) differentiated cancer cells which make up the bulk of the tumor. Within this hierarchy, only cancer stem cells (CSC) are thought to be tumorigenic, unlike differentiated cells, and the progenitors only have a limited proliferative potential (94). This hierarchical model places itself beside a classical (stochastic or clonal evolution) model to explain the observed tumor heterogeneity (Fig. 2.1). According to the stochastic model, tumor heterogeneity is only driven by the subsequent genetic alterations that occur during tumor progression; these mutations give rise to different subclones which undergo the phenomenon of natural selection, through which only the most fit, aggressive, and resistant clones survive and proliferate, eventually perpetuating the process of selection. All cancer cells, in the stochastic model, would have the same tumorigenic potential (94).

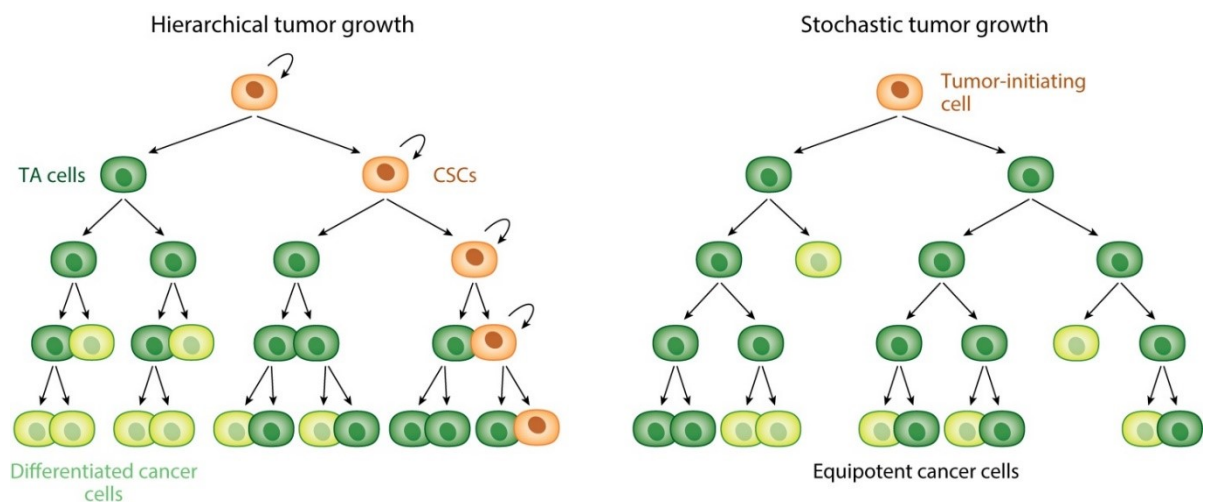


Figure 2.1. Hierarchical and stochastic models of tumor growth in comparison (94).

Nevertheless, these two models are not necessarily mutually exclusive, as tumors may be heterogeneous because of the coexistence of genetically diverse clones, as well as because of genetically identical cells occupying different differentiation levels (96), whose maturation is

driven by epigenetic silencing and activation of particular transcriptional programs (97). Moreover, it may be possible that genetically different clones of cancer cells endowed with stemness can exist in the same tumor, all of them arising from a common ancestor, the cell-of-origin, that is to say, the normal cell that first underwent the oncogenic mutation (95). Similarly, since recent studies evidenced that cancer cells display a certain plasticity degree, differentiated, non-tumorigenic cancer cells may be stochastically hit by genetic mutations or may receive extrinsic signals that make them gain the properties of self-renewal and pluripotency (98).

2.1. History of CSC research

The dissection of the hierarchical organization of hematopoietic system and the development of flow cytometry and fluorescence-activated cell sorting (FACS) techniques boosted CSC research at the end of the Twentieth century (95).

In the mid-Nineties, indeed, the first pieces of evidence supporting the CSC theory were produced in human acute myeloid leukemias (99, 100). These studies demonstrated that not all the leukemic blasts, but only a small subset of leukemic cells characterized by CD34⁺CD38⁻ phenotype, were able to propagate cancer in immunodeficient mice. The surface marker profile used by the Authors to select leukemia stem cells (LSC) mirrors the one that identifies normal hematopoietic stem cells (HSC) (101). LSC also share with HSC the gene expression profile and the differentiation fate, the self-renewal property and the capacity to recapitulate the heterogeneity of the original population (94, 102). Through xenotransplantation assay, LSC were estimated to be very rare (1 in 250,000).

Then, CSC were also identified in many solid tumors, starting from breast cancer (103). The Authors found that the 11-35% of breast cancer cells, characterized by CD44⁺ CD24^{-/low} phenotype, can efficiently recreate the original tumor in non-obese diabetic/ severe combined immunodeficiency (NOD/SCID) mice, since only 100 CD44⁺ CD24^{-/low} cells are sufficient to give rise to a tumor, whereas thousands of cells with different phenotype cannot do it.

In solid tumors, a clear identification of markers for CSC isolation is harder than in blood cancers, mainly because the limited knowledge of the hierarchical organization of the normal tissues from which these cancer originate. For this reason, different studies on the same tumor type often identify CSC by using different combinations of surface markers (95).

CSC research on leukemia and breast cancer paved the way for the flourishing of many studies on other solid tumors, such as:

- brain cancers (*i.e.* glioblastoma multiforme, medulloblastoma, and neuroblastoma), in which CSC were identified by CD133 expression (104), or, otherwise, were Nestin⁺ CD133⁻, or Tbr2⁺ CD133⁻ (105);
- prostate cancer, in which CD44⁺ cells were found to be CSC (106), but also CD133 was proposed as a marker (107);
- melanoma, in which melanosphere were used to enrich the CD20⁺ tumor-propagating fraction (108); alternatively, CD271 (109), or ATP binding cassette subfamily B member 5 (ABCB5) (110) were selected as markers;
- lung cancer, in which both CD133 (111) and aldehyde dehydrogenase 1 (ALDH1) (112) were proposed as markers;
- colorectal carcinoma, in which the CSC markers used were EpCAM/CD44 (113), ALDH (114), Musashi1 (MSI-1)/Leucine-rich repeat-containing G protein-coupled receptor 5 (LGR5) (115), or CD133, CD166, CD44, CD29, CD24, LGR5 (116);
- pancreatic cancer, in which CD44⁺CD24⁺ epithelial surface antigen (ESA)⁺ cells were demonstrated to be endowed with stemness (117); alternatively, CD133⁺ /C-X-C chemokine receptor type 4 (CXCR4)⁺ were identified as CSC.

2.2. CSC features

CSC origin is not clear: they could derive either from normal adult stem cells (having a life-long duration) which can accumulate the long series of genetic hits necessary to carcinogenesis, or from committed progenitors or terminally differentiated cells which undergo tumor transformation causal

of their dedifferentiation and of the acquisition of self-renewal properties (Fig. 2.2), or through both mechanisms (118).

On the basis of the knowledge of HSC and other adult stem cells properties (95), some features have been traditionally ascribed to CSC (119):

- rarity: it is believed that the cell population responsible for tumor outgrowth and propagation has to be tiny;
- self-renewal: in order to be defined as stem, a cell must be able to divide both symmetrically (giving rise to two daughter cells which are either both stem or both non-stem) and asymmetrically (giving a stem and a non-stem cell) under different extrinsic stimuli;
- *in vivo* tumorigenicity and differentiation potential: CSC must be able to give rise to all the cells of the tumor population, and recreate the original phenotypic and functional heterogeneity when transplanted into experimental hosts;

- proliferative quiescence (dormancy): CSC are believed to proliferate more slowly than their differentiated progeny, they can exit the cell cycle and enter again when stimulated;
- longevity: CSC are able to escape senescence by inducing telomerase reverse transcriptase (TERT) (102), therefore they have an extensive proliferative potential which allows them to give rise to tumor relapse years or even decades after the apparent remission;
- chemo- and radio-resistance: CSC are more resistant to treatment than their non-stem counterpart, because of several mechanism, including proliferative quiescence, the ability to extrude exogenous compounds through surface pumps (such as the ABC family), the expression of detoxifying enzymes (such as ALDH), a more intact DNA repair apparatus, and the expression of anti-apoptotic proteins.

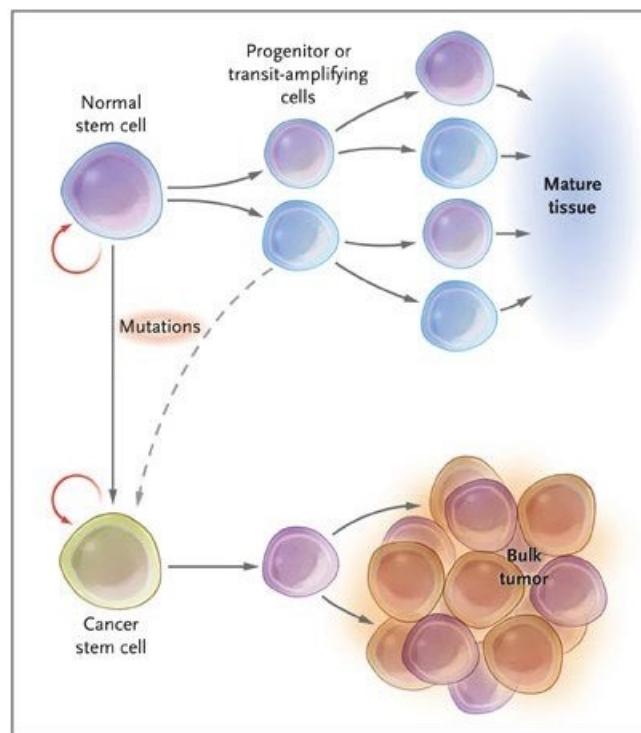


Figure 2.2. Cancer stem cells arise by means of mutations in normal stem cells or progenitor cells (118).

Although these characteristics are worldwide accepted as CSC hallmarks, a definitive demonstration of all of them is often lacking, or only indirect evidence is provided. For example, even though studies on leukemia (99, 100) and solid tumors (103, 104, 110) showed that only a small subset of cancer cells were able to shape a tumor in mice (CSC rarity), some tumors were found to have high percentage of tumorigenic cells (50% in mouse acute lymphoblastic leukemia (120), 25% in human melanoma (121)). The presence of abundant tumorigenic cells does not necessarily mean that the analyzed tumor is not hierarchically

organized and does not follow the CSC paradigm; on the contrary, rarity may be the consequence of an experimental bias deriving from the use of the xenotransplantation assay in murine host, so that only the most robust and aggressive cells can colonize tissues of an organism of a different species, without receiving the most suitable microenvironmental cues (94, 119). Moreover, the CSC content may vary from a patient to another and increase as the disease progresses (98).

Dormancy has never been directly proven in CSC. The ability to retain DNA labels or the lipophilic dye PKH26 (122) has been exploited to enrich the CSC population, finding that the slow-cycling cells display a gene expression profile that makes them *bona fide* CSC, providing in this way indirect evidence. However, Al Hajj *et al.* did not find differences in cell cycle phase distribution between breast CSC and non-CSC (103), and such data are unknown in the majority of CSC (119).

The resistance to chemotherapeutics and radiotherapy is often referred to be linked to the presence of resistant CSC (118). Indeed, *in vitro* treatments result in a selection of cells with a CSC phenotype, and these cells persist after *in vivo* chemotherapy administration: although tumor shrinkage is achieved, the relative amount of CSC is increased in the residual mass (123). This key CSC feature makes them the main responsible for treatment failure and tumor relapse. Therefore, combination regimens including a conventional chemotherapeutic, targeting quickly proliferating cells, and agents that hit specifically CSC, are auspicated to effectively cure many cancers (Fig. 2.3).

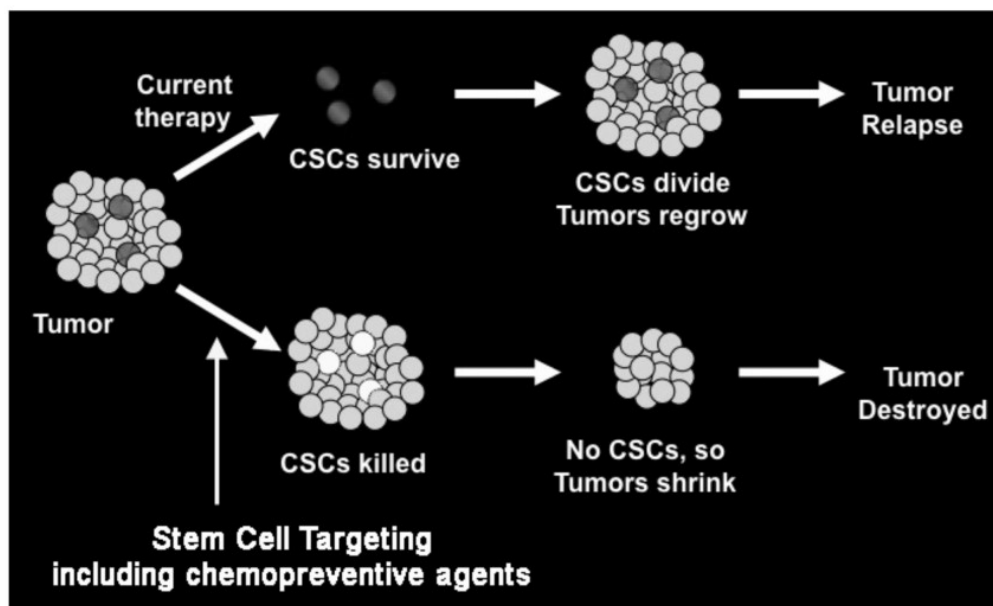


Figure 2.3. Conventional therapies, in spite of initial tumor shrinkage, invariably result in tumor relapse.

The development of therapies directed against CSC may lead to cancer destruction (124).

It has been hypothesized that CSC are able to undergo epithelial-to-mesenchymal transition (EMT) under determined stimuli, in order to acquire motility and colonize distant organs to give rise to metastases (97, 125). Indeed, CSC and EMT have been traditionally interconnected, because EMT transcription factors often co-localize with CSC markers, and *vice versa*, and the key pathways responsible for self-renewal and CSC maintenance are triggers for EMT (97). EMT is a developmental process that takes place during embryogenesis and is also activated during wound healing. As cancer can be considered a disease of pathological wound healing and chronic inflammation, it is usually accompanied by aberrant EMT, which induces in the cells the loss of the apico-basal polarity and of cell-to-cell adhesion, the acquisition of migratory and invasive properties and, therefore, of metastatic potential. At the invasive front, EMT is necessary to induce migration and tumor enlargement in the context of the surrounding healthy tissue. EMT is also necessary to allow the cells to detach from the tumor bulk and enter the blood circulation; circulating tumor cells (CTC) are found to co-express EMT and CSC markers (126). In order to colonize a distant organ, CTC have to extravasate and to find a permissive metastatic niche, all these circumstances making metastasis a non-efficient event; moreover, since the pro-invasive phenotype is acquired to the detriment of the proliferative one (127), detached cells need to undergo the opposite phenomenon of mesenchymal-to-epithelial transition (MET) to give rise to a secondary tumor mass. To be able to seed a new tumor, migrated cells need to be endowed with stemness. Notably, CSC may exist either in an epithelial or a mesenchymal state or may have intermediate characteristics (128). The induction of the EMT program confers CSC resistance to apoptosis (including drug resistance (129)) and the ability to survive in the bloodstream and in the new soil (130).

EMT is induced by soluble factors released by stromal cells, the most important of which are transforming growth factor-beta (TGF- β) and WNT. The result is the induction of transcriptional repressors, like TWIST1, SNAIL, SLUG, ZEB1 and ZEB2, which bind the E-cadherin promoter and recruit some epigenetic modulators, like histone deacetylases (HDAC), which in turn repress the transcription of this epithelial marker. As a result, the cell loses the adherens junctions and modulates Rho GTPases, which reorganize the actin cytoskeleton (97). Beta-catenin, previously bound to E-cadherin, is then free to migrate to the nucleus, where it initiates its transcriptional program, stimulating the expression of its target genes, including pluripotency and self-renewal related genes (131). Therefore, the EMT program can generate stem-like cells from non-stem ones (96).

2.3. Stemness master genes

CSC are characterized by the expression of stemness-related genes, such as Sox2, Oct4, and Nanog (132), two of which (Sox2 and Oct4) are among the four factors used to reprogram fibroblasts into induced pluripotent stem cells by Yamanaka (133).

SRY (sex determining region Y)-box 2, also known as Sox2, is a transcription factor critical for early embryogenesis and for embryonic stem cell pluripotency, as well as for neural stem cell maintenance (134). In mouse embryonic stem cells, leukemia inhibitory factor (LIF) activates Kruppel-like factor 4 (Klf4) through the Janus kinase (JAK)/ signal transducer and activator of transcription 3 (STAT3) pathway and in turn activates Sox2 (135). Sox2 acts as an oncogene, since its amplification promotes the development of squamous cell lung cancer and activates cellular migration and anchorage-independent growth; moreover, Sox2 builds up a stem-like phenotype in cancer cells (136).

Sox2 forms with Oct4 a trimeric complex and they together control the expression of genes involved in embryonic development such as tyrosine-protein kinase YES1, fibroblast growth factor 4 (FGF4), undifferentiated embryonic cell transcription factor 1 (UTF1), F-box protein 15 (Fbx15), and the pluripotency transcription factors ZFP206 and Nanog, as well as Sox2 and Pou5f1 (encoding Oct4) themselves (134, 137).

Oct4 (octamer-binding transcription factor 4), also known as POU5F1 (POU domain, class 5, transcription factor 1), is a homeodomain transcription factor active in embryos during the preimplantation period. Oct-4 expression is associated with an undifferentiated phenotype since its silencing promotes differentiation (138). It has been demonstrated that Oct4 depletion in embryos did not affect totipotency, as the embryos could normally develop; however, its role is critical in maintaining pluripotency (139). Oct4 involvement in tumorigenesis has been proven, since its overexpression in a mouse model causes cutaneous and intestinal dysplasia, by inhibiting cell differentiation in a β -catenin dependent fashion, accompanied by an expansion of the progenitor cells (140).

The homeobox protein Nanog is a transcription factor involved in the maintenance of the pluripotency of embryonic stem cells, by blocking the differentiation program (141). It is also been described as an oncogene, since Nanog-overexpressing NIH3T3 cells have increased proliferative capacity and grow in an anchorage-independent manner (142). Similarly to embryonic stem cells, Nanog is also overexpressed in CSC (143). Nanog expression is transcriptionally induced by Sox2/Oct4 heterodimer (137), by LIF/ STAT3 and zinc finger proteins GLI1 and GLI2, and by hypoxia-inducible factor 2a (HIF2a), and is repressed by p53 (144). Nanog target genes are involved in proliferation and cell cycle progression, maintenance

of self-renewal and undifferentiated state, migration and invasion, and chemoresistance (145). Among Nanog upregulated genes, there are Cyclins D1, D2, D3, and E1, growth differentiation factor-3 (GDF3), cyclin-dependent kinase 1 and 6, DNA methyltransferase 1 (DNMT1), B-cell lymphoma 6 (Bcl6), cyclic AMP-dependent transcription factor (Atf3), focal adhesion kinase (FAK) and ATP binding cassette subfamily B member 1 (ABCB1), whereas it downregulates E-cadherin, forkhead box FOXO1, FOXO3a, FOXJ1, and FOXB1.

2.4. Stemness-promoting signaling pathways

WNT, Hedgehog, and Notch pathways are three developmental signaling cascades shared by normal stem cells and CSC, being the main drivers of self-renewal capacity (Fig. 2.4). Whereas they are tightly regulated in normal stem cells, these pathways are often found constitutively activated in a cancer context (124).

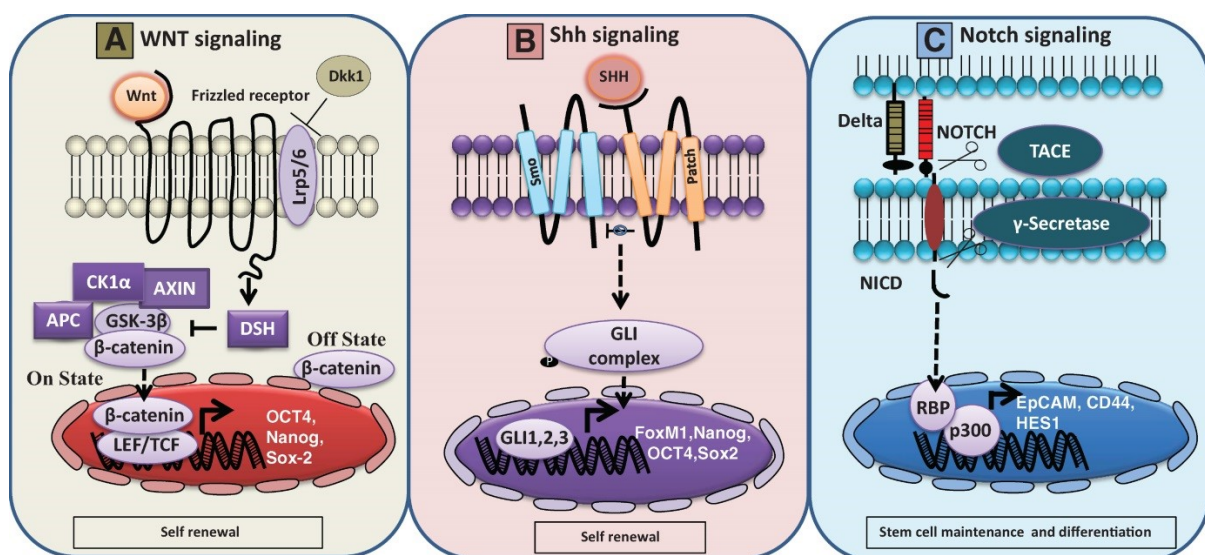


Figure 2.4. Wnt, Hedgehog, and Notch pathways play fundamental roles in CSC maintenance (146).

Wnt proteins are a family of evolutionary conserved secreted morphogens necessary for basic developmental processes, such as cell-fate specification, progenitor-cell proliferation and the control of asymmetric cell division (147). The human genome encompasses 19 WNT-coding genes, which are split into 12 subfamilies. The Wnts are approximately 40 kDa and are modified by a palmitoleate moiety attached to a serine (148). At least three different Wnt pathways exist: the canonical pathway (Fig. 2.4 A), the planar cell polarity (PCP) pathway and the Wnt/Ca²⁺ pathway. In the canonical pathway, Wnt binds to its receptor Frizzled, the β-catenin degradation complex is disrupted, and the stabilized β-catenin is free to enter the nucleus and activate Wnt

target genes by interacting with T-cell factor (TCF) family transcription factors and concomitant recruitment of lymphoid enhancer-binding factor 1 (LEF1). PCP signaling leads to cytoskeleton remodeling and changes in cell motility through the activation of the small GTPases RAS homologue gene-family member A (RHOA) and RAC1, which activate Jun N-terminal kinase (JNK) and RHO-associated coiled-coil-containing protein kinase 1 (ROCK). WNT-Ca²⁺ signaling leads to increase in cytoplasmic free calcium which activates the protein kinase C (PKC) and calcium calmodulin mediated kinase II (CAMKII) and the phosphatase calcineurin. (147). Wnt target genes include stemness-related genes, EMT transcription factors, cell cycle regulators, pro-angiogenic factors, members of Wnt pathway itself and of Notch pathway, and other oncogenes: c-Myc, Cyclin D1, TCF and LEF, c-Jun, urokinase receptor (uPAR), matrix metalloproteinase MMP-7, Axin-2, CD44, Survivin, VEGF, FGF4, FGF9, FGF18, FGF20, MET, Jagged, MSI-1, TERT, LGR5, Gremlin, Nanog, Sox2, Oct4, SNAIL, TWIST, cdc25, Fibronectin, Frizzled-7, Wnt3a, T-box transcription factor (Tbx3), EGFR, cytotoxic T-lymphocyte antigen 4 (CTLA-4), Cyclooxygenase 2 (COX-2) (149).

Wnt pathway over-activation, especially through mutations in a member of the β -catenin degradation complex named adenomatous polyposis coli (APC), triggers malignant transformation of colonic mucosa, EMT, and colorectal cancer progression (124, 150). High nuclear concentrations of β -catenin are often found at the tumor invasive front, where cells become more mobile and CSC reside, and are linked to metastasis and poor prognosis.

CSC from different gastrointestinal cell lines display enhanced expression of Wnt-associated genes (151). Beyond its role in colorectal cancer, Wnt has been demonstrated to be important in CSC maintenance in myeloid leukemia, melanoma, breast, liver, and lung cancer (152).

The Hedgehog (Hh) signaling pathway (Fig. 2.4 B) plays important roles in the control of cell proliferation, tissue homeostasis, stem cell maintenance and development (153). In mammals, three Hh homologs with different biological functions are described: Sonic (Shh), Desert (Dhh), and Indian hedgehog (Ihh). The members of the family are 19 kDa proteins cleaved from a 45 kDa precursor and covalently bound to cholesterol (C-terminus) and to palmitate (N-terminus) (154). In the absence of Hh, the Patched (PTCH) receptor inhibits Smoothened (Smo) activation. GLI proteins are thus phosphorylated by protein kinase A (PKA), casein kinase 1 (CK1), and glycogen synthase kinase 3 beta (GSK3B), and partially degraded. In the presence of Hh, PTCH is internalized, and activated Smo contributes to the dissociation of GLI from the negative regulator suppressor of fused (Sufu). Activated GLI translocates into the nucleus, thus triggering the transcription of Hh target genes (153). Among the latter, there are members of Hh cascade itself (GLI1, PTCH1, PTCH2, Hedgehog interacting

protein HHIP1), of Wnt pathway (Wnt2b and Wnt5a), and of Notch pathway (Jagged2), cell cycle controllers (Cyclin D1 and 2, and Cyclin E), the pro-survival proteins BCL2 and CASP8 and FADD-like apoptosis regulator (CFLAR), Forkhead box FOXC2 FOXM1, FOXF1, FOXL1, PR domain zinc finger protein 1 (PRDM1), Gremlin, Follistatin, N-Myc, stem-cell markers (polycomb complex protein BMI1, LGR5, CD44, and CD133), and EMT markers (SNAIL, SLUG, ZEB1, ZEB2, and TWIST2) (155).

Hh is over-activated in brain tumors, basal cell carcinoma, lung, gastric, pancreatic, and breast cancer (155). Its dysregulation also mediates angiogenesis and metastasis (124). CSC are demonstrated to express high Shh levels in multiple myeloma, pancreatic and breast cancer (117, 156, 157).

The Notch pathway (Fig. 2.4 C) is a conserved intercellular signaling machinery essential for embryonic development (158). The Notch proteins (Notch1-4 in vertebrates) are type 1 transmembrane proteins which act as receptors activated by the Delta (or Delta-like) and Jagged/Serrate families of transmembrane ligands. Ligand binding leads to a proteolytic cleavage mediated by γ -secretase that frees the Notch intracellular domain (NICD) from the membrane. The NICD translocates to the nucleus, where it forms a complex with the DNA binding protein RBPJ (recombination signal binding protein for immunoglobulin kappa J region) and with coactivators, such as Mastermind-like protein 1 (MAML1) and p300 histone acetyltransferase, leading to the transcription of Notch target genes (159). Among Notch target genes, there are hairy/enhancer of split (Hes1, Hes5 and Hes7, Hey1, Hey2 and HeyL), CD25, GATA3, c-Myc, cyclinD1, p21/Waf1, nuclear factor kappa-light-chain-enhancer of activated B cells (NFkB2), A Disintegrin And Metalloproteinase 19 (ADAM19), Notch1 and Notch3 themselves, BCL-2 and E2A and Homeobox protein HoxA5, 9 and 10 (158).

In the normal tissues, Notch pathway controls the balance between self-renewal and differentiation processes (146). In particular, Notch is essential for HSC self-renewal (160) and cooperates with Wnt to block terminal differentiation in the gut epithelium (161).

In addition, Notch signaling plays an important role for the pathogenesis of some human cancers including T-acute lymphoid leukemia, lymphoma, lung, ovarian, pancreatic, brain and breast cancer (124, 146, 150).

It has been demonstrated that Notch promotes CSC survival in glioblastoma, breast, colorectal, and pancreatic cancer (152). Notch3 overexpression is associated with increased MSI-1 levels in colorectal cancer, and its silencing leads to MSI1 downregulation (162). The overexpression of Notch-1 results in increased clonogenicity, migration, invasion in a pancreatic cancer cell line. Moreover, its inhibition causes a reduction in the self-renewal capacity of pancreatic CSC

(146), while the use of γ -secretase inhibitors leads to depletion of CSC in medulloblastoma (163).

2.5. Surface and functional markers for CSC identification

CSC in solid tumors are usually identified and FACS-isolated by exploiting the expression of tissue-specific surface markers; otherwise, strategies exploiting functional properties ascribed to CSC are also employed.

As stated above, since a complete characterization of the cellular hierarchy of most tissues is lacking, the choice of the markers is often based on the documented heterogeneity in the expression pattern of these surface proteins in the context of the bulk population. As a result, a substantial disagreement in different studies about the same tumor type is often found (95).

Nonetheless, the most frequently used surface markers across different tumor types are CD44, CD133, and CD24, whereas the use of others (LGR5, CD166, CD117, CD15, CD20, CXCR4, ESA, EpCAM, CD271) is more restricted to some organs (124, 152, 164, 165).

CD44 is reported to be at least one of CSC markers in many tumors, first of all breast, but also pancreatic, ovarian, colorectal, and head-and-neck cancers. Since CD44⁺ cells are often far to be rare in many tumors, CD44 is usually used in combination with at least another marker (CD24, CD117, or ESA/EpCAM). Interestingly, CD44 is a well-known Wnt target gene. CD44 gene contains 20 exons and is translated both in a standard molecule (CD44s) of 85-90 kDa, coded by 10 standard exons, and also in tissue-specific splice variants, resulting from different combinations of the ten variant exons (CD44v1-10). Beyond being a biomarker, CD44 is a type I transmembrane glycoprotein, receptor for hyaluronan, a component of the extracellular matrix. Thus, it is postulated that CD44⁺ cells are more aggressive and invasive because this molecule facilitates adhesion to the extracellular matrix and migration. Moreover, hyaluronan binding triggers the activation of many signaling cascades, such as MAPK, PI3K, NF κ B, β -catenin, through CD44 intracellular signaling domain and CD44 interaction with other receptors, like EGFR. These signaling cascades translate into the transcription of Nanog, Sox2, ABCB1, and Bcl-xL, thus promoting stemness, chemoresistance, and survival (164, 166).

CD133, also known as Prominin-1, is a widely used biomarker for CSC identification in brain, lung, pancreas, ovarian, liver, prostate, gastric, colorectal, and head-and-neck cancers. CD133 was firstly described in CD34⁺ HSC, as target of the AC133 antibody, and it also expressed in normal adult stem cells. CD133 is a 120 kDa glycosylated pentaspan transmembrane protein, whose biological function is still not well defined. However, CD133⁺ cells in many tumors have been found to be more chemoresistant and radioresistant compared to CD133⁻ cells, with

eventual enrichment upon treatment both *in vitro* and *in vivo*, since they express increased levels of DNA-damage checkpoints and ABC transporters. CD133⁺ cells also express increased levels of Shh, Nestin, BMI1, Nanog, Oct4, and CXCR4, the latter important for the homing in the metastatic niche. Moreover, the activation of MAPK and PI3K pathways, downstream of EGFR and HIF1 α , leads to the expansion of the CD133⁺ population (96, 164).

CD24 is a short glycosylphosphatidylinositol (GPI)-anchored glycoprotein whose expression in normal tissues is restricted to B cells, granulocytes, and stratum corneum. Its role as a CSC marker is highly tissue-specific, since in some cases (breast and prostate) CSC are identified by the lack of CD24 expression, while in others (pancreas and colon) CSC are CD24⁺. In glioblastoma, CD24 is overexpressed as a Shh target gene. CD24 acts as an adhesion molecule, being ligand for P-selectin (167), and seems to be associated to the lipid rafts, where it recruits integrins (168), suggesting a role for CD24 in migration and metastasis (164).

Regarding the functional markers, ALDH activity (measured by ALDEFLUORTM staining), the ability to extrude exogenous compounds through surface pumps (found in the so-called side population, SP), the proliferative quiescence (measured through the ability to retain the lipid-intercalating dye PKH26), and spheroid formation can be enumerated (122, 150, 152, 169, 170). ALDH is a family of intracytoplasmic detoxifying enzymes responsible for the oxidation of aldehydes to carboxylic acids. Within this family, ALDH1A1 characterizes highly tumorigenic cells in lung, prostate, colon, liver, pancreatic, and breast cancer, as well as in leukemia and multiple myeloma. Beyond being a marker, ALDH has a double functional role in CSC maintenance, since it converts retinol into retinoic acid, a compound which controls cell differentiation, and it can contribute to the resistance against those chemotherapeutics which generate toxic aldehydes (164). The most reliable method used to detect ALDH activity (not only its expression as a protein) is by using BODIPY aminoacetaldehyde (BAAA), *i.e.* a fluorochrome linked to an ALDH substrate, known as ALDEFLUORTM (152). However, as ALDH may be induced by the toxic treatments used to enrich the CSC population, ALDEFLUORTM staining should be combined with more stable surface markers (164).

The so-called Side Population (SP) is a small cell subpopulation, characterized by the ability to extrude the fluorescent DNA-binding dye Hoechst 33342 through surface transporters, such as ABCG2 and ABCB1. The same pumps are promiscuous transporters for both hydrophilic and hydrophobic molecules, including a large variety of chemotherapeutics; thus, these cells are inherently chemoresistant. Indeed, SP percentage increases after chemotherapy treatment. Besides being extruders, the ABC transporters also seem to repress cell differentiation, and are down-regulated in transit-amplifying progenitors (150). The SP was first identified in 1996 in

the mouse bone marrow: the Authors found that this population was enriched in HSCs (171). After its discovery, SP cells were then identified in many labile tissues and, finally, in cancers (leukemia, brain, liver, breast, prostate, thyroid, colorectal, and ovarian cancer) (150). SP cells are highly clonogenic and tumorigenic, and overexpress Shh and stemness genes (152). CSC are quiescent from a proliferative point of view. This feature was exploited by Pece *et al.* (122) to isolate stem cells from the mammary gland and CSC from breast cancer, by selecting cells which were able to retain the lipophilic dye PKH26: indeed, the less the cells divide, the less the dye is diluted in daughter cells. The transcriptional and protein expression profile of PKH26^{high} cells was consistent with the one expected from stem cells. Our group used the same strategy to identify stem cells from normal colon epithelium (115). Finally, spheroid-culture conditions can be used to enrich the CSC fraction without requiring a background knowledge on cell surface markers. Indeed, clonogenic cells can extensively survive in such selective conditions (non-adhesion, absence of fetal bovine serum, and presence of growth factors like EGF and bFGF), expand as floating aggregates or sphere-shaped structures, and give rise to secondary and tertiary spheroids when dissociated and replated, whereas non-clonogenic cells die. This assay is a measure of self-renewal capability; tumorspheres have been proven to display CSC features (170).

2.6. CSC metabolism

In the Twenties of the last century, Otto Warburg observed that tumor cells most rely on lactic fermentation to get energy, even in the presence of oxygen. This phenomenon of aerobic glycolysis, also called Warburg effect, allows cancer cells to obtain the ATP necessary for their growth more quickly than oxidative phosphorylation (OXPHOS), even though with a much lower efficiency (2 ATP residues for one molecule of glucose, instead of 36). Cells upregulate glucose transporters to enhance glucose uptake and lactate transporters to extrude this byproduct, while using pyruvate and glutamine as substrates of the tricarboxylic acid (TCA) cycle for the anabolic reactions (172).

In normoxic conditions, normal tissues preferentially activate OXPHOS to metabolize glucose and generate energy; however, normal adult stem cells preferentially rely on glycolysis: indeed, they have fewer mitochondria and produce lower levels of reactive oxygen species (ROS), condition necessary to maintain self-renewal and quiescence (173).

In recent years, in search for new druggable targets, many efforts have been undertaken to describe CSC metabolic traits. Indeed, it seems that, in the context of tumor heterogeneity, CSC display different metabolic properties as compared to the tumor bulk. Nonetheless, whether

CSC are more glycolytic or more oxidative than the tumor mass is still controversial. According to the study model and to the tumor type, CSC have been found to rely preferentially on glycolysis or on OXPHOS, as described in Table 2.1 (174).

| CANCER TYPE | MODEL | CSC ID | METABOLISM | MITOCHONDRIAL TARGETING | YEAR | REF |
|------------------------|-------------------------------------|--|------------|---|------|-------|
| Breast | Cell lines | CD44 ⁺ CD24 ^{low} | ND | Metformin | 2010 | (175) |
| | Cell lines | SP ⁺ sphere-forming cells | ND | Niclosamide | 2013 | (176) |
| | Cell lines | CD44 ⁺ CD24 ^{low} EPCAM ⁺ | Glycolytic | ND | 2013 | (177) |
| Lung | Cell line | SP ⁺ Sphere-forming cells | OXPHOS | ND | 2011 | (178) |
| Glioblastoma | Fresh human tumors, PDX | CD133 ⁺ , Gliomaspheres | OXPHOS | ND | 2012 | (179) |
| Ovary | Cell lines | SP ⁺ cells | ND | Niclosamide | 2012 | (180) |
| | Mouse ovarian surface epithelium | Serial in vivo passaging | Glycolytic | Oligomycin, Antimycin, Rotenone, Metformin | 2014 | (181) |
| | Fresh human samples | CD44 ⁺ CD117 ⁺ cells | OXPHOS | Oligomycin, Antimycin, Rotenone, Metformin | 2014 | (182) |
| Acute myeloid leukemia | Primary cultures from human samples | Quiescent ROS ^{low} cells | OXPHOS | ABT-263 | 2013 | (183) |
| Nasopharynx | Cell lines | Radioresistant sphere-forming cells | Glycolytic | Resveratrol | 2013 | (184) |
| | Cell lines | Radioresistant sphere-forming cells | Glycolytic | FCCP | 2015 | (185) |
| Pancreas | Primary cultures, fresh PDX | CD133 ⁺ cells, Sphere-forming cells | OXPHOS | Metformin, Resveratrol, Rotenone, Menadione | 2015 | (186) |
| Liver | Fresh tumors (mouse/human) | CD133 ⁺ CD49f ⁺ cells | Glycolytic | Paraquat | 2015 | (187) |

Table 2.1. CSC metabolic phenotype identified for several cancer types (ND=not determined; PDX=patient-derived xenografts; FCCP= Carbonyl cyanide p-trifluoromethoxyphenylhydrazone) (174).

This apparent discrepancy may be related to some experimental biases, for example, the use of established cell lines instead of fresh tumor samples or PDX, and the standard culture conditions in media rich in glucose, while the tumor microenvironment is often characterized by nutrient shortage and hypoxia (98).

Reports supporting a CSC glycolytic phenotype hypothesize that CSC are similar to normal stem cells in their metabolic program, where low mitochondrial activity is essential for pluripotency (174). The joining linking between glycolysis and stemness seems to be c-Myc, since it influences glycolysis and mitochondrial biogenesis and it is also necessary for tumorigenic potential of induced pluripotent stem cells (188).

However, a number of studies suggests that CSC are essentially oxidative, since in this way they can have a selective advantage, being more independent from glucose supply. OXPHOS CSC exhibit a higher mitochondrial biogenesis rate (through the overexpression of peroxisome

proliferator-activated receptor gamma coactivator 1-alpha (PGC-1 α), with increased mitochondrial mass and membrane potential, they are resistant to glucose deprivation, they can get energy from the uptake of other molecules, such as fatty acids, glutamine, and the lactate extruded by the tumor bulk, and buffer the higher ROS production due to increased mitochondrial activity by establishing a more powerful antioxidant system (173, 174). CSC differentiation fate may be determined by small changes in ROS levels (189) and by an asymmetric sorting of aged mitochondria in daughter cells with different differentiation fate (190).

Following this line of research, our group demonstrated that ovarian CSC, identified by the coexpression of CD44 and CD117, rely most on OXPHOS for their metabolism (Fig. 2.5), since they upregulate genes related to TCA and electron-transport chain and resist *in vitro* and *in vivo* glucose deprivation. CSC were found to overexpress also genes of the pentose phosphate pathway and of fatty acid oxidation. In addition, CSC display higher mitochondrial but lower total ROS levels compared to the non-stem counterpart, and are sensitive to mitochondrial complex inhibitors, such as oligomycin, antimycin, metformin and rotenone (182).

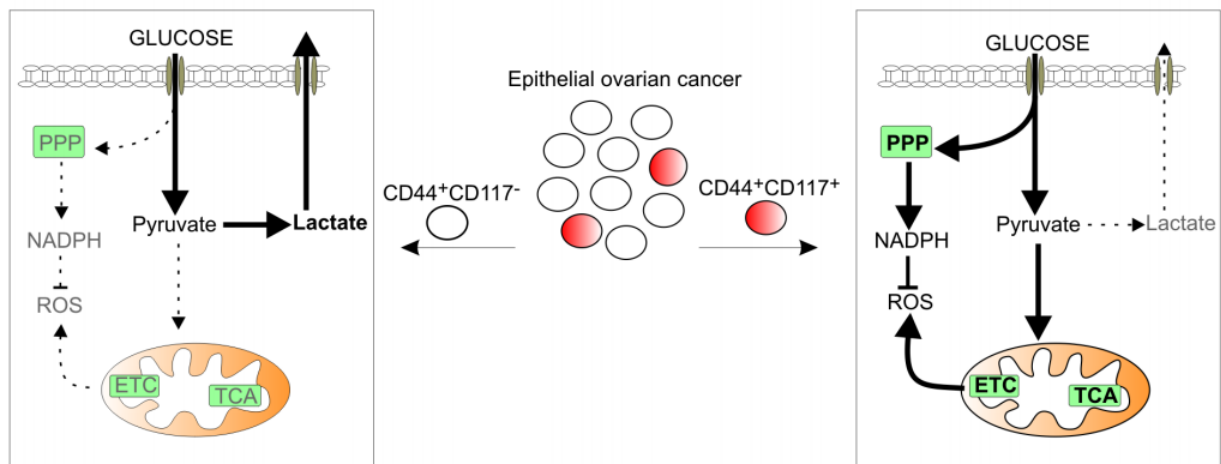


Figure 2.5. Schematic model of the metabolic profile of ovarian CSC and non-CSC (182).

Thus, CSC could be targeted by using molecules directed against mitochondrial complexes and ribosomes, such as the aforementioned oligomycin, antimycin (191), metformin and rotenone, the antibiotics salinomycin (192), azithromycin, doxycycline, tigecycline, and chloramphenicol (193), the anti-helminthic pyrvinium pamoate, niclosamide (176, 180), and closantel, the anti-viral nitazoxanide and the anti-malarial atovaquone (194).

2.7. CSC niche and tumor microenvironment contribution to stemness

Stemness is a cellular intrinsic property as well as a result of extrinsic stimuli and of the CSC cross-talk with the complex network of cells, matrices, vesicles that makes up the tumor microenvironment (96). For example, in a study on breast cancer in which cell lines were used as models, only one subpopulation of cells out of three (stem cell-like, basal-like, and luminal-like cells), *i.e.*, the stem cell-like ones, resulted tumorigenic *in vivo*, whereas in another setting, in which irradiated stromal cells were provided, all the three considered subpopulations were equally tumorigenic (195).

CSC, as their normal adult counterpart, reside in specialized niches, since they need to receive cues from the surrounding cells, in order to activate and maintain their stemness program (self-renewal, proliferation and apoptosis resistance). The CSC niche is well defined only in colorectal cancer, in which CSC reside in the intestinal crypts (196). Moreover, brain CSC seem to depend on a perivascular niche, similarly to normal neural stem cells (197). A perivascular niche has been advanced also for CSC in head and neck cancer (198).

The niche consists of a number of cell types, including tumor-associated fibroblasts (TAF), endothelial cells, pericytes, and immune cells, especially tumor-associated macrophages (TAM) and myeloid-derived suppressor cells (MDSC), as well as non-cellular elements, such as the extracellular matrix and the complex network of growth factors and cytokines (96, 199). Cells of mesenchymal origin, in particular myofibroblasts, secrete prostaglandin E₂, which activates β -catenin signaling in carcinoma cells, and CXCL7 and IL6, which stimulate self-renewal (96). TAF promote EMT and secrete matrix metalloproteinases, also through exosomes. They also produce Wnt, HGF, IGF2 and FGF4 (94). The interaction between CSC and endothelial cells promotes CSC self-renewal and tumorigenicity thanks to the activation of a VEGFA/neuropilin-1 axis and to the production of EGF and nitric oxide, which induce EMT and activate Notch, respectively. Furthermore, endothelial cells secrete the chemokine IL8, and express on their surface Jag1, one of the Notch ligands (94). TAM, in particular the M2 polarized macrophages, are recruited to the tumor by CSF1, CCL2, CCL5, and CXCL12 (96), and support stemness by producing several cytokines, *e.g.* IL6, EGF, and IL10, which cause the expansion of the CSC pool through the activation of STAT3; TGF- β , a potent EMT inducer; the chemokine IL8, which promotes CSC survival and self-renewal by activating several pathways (focal adhesion kinase, Akt, MAPK, Wnt) through the receptor CXCR1/2; TNF- α ; arginase-I (199). MDSC release nitric oxide, which in turn activates Notch and STAT3, promoting stemness; they also produce IL1 receptor antagonist, which sequester IL1 α , thus blocking CSC senescence. Moreover, MDSC isolated from cancer enhance tumor sphere

formation and induce the expression of stemness master genes, whereas cancer cells primed by MDSC resulted to be more tumorigenic and metastatic (199).

CSC are abundant in their niche, and the total number of CSC, at least in tumors at the early stages, is determined by the size of the niche itself. When a CSC divides, its daughter cells compete for the space in the niche: if both can stay in, they will be both CSC, whereas if neither of them can occupy the niche, they will differentiate. If only one can stay, this one will be a CSC, while the other one will differentiate (98). Furthermore, if CSC are depleted as a result of a lineage-specific ablation or of a CSC target therapy, their differentiated progeny can re-enter the niche and acquire stemness properties to reconstitute the CSC pool. Thus, as cancer cells are endowed with plasticity, a therapy intended to deplete CSC must target their niche as well, in order to be effective. As the tumor progresses, tumor cells, including CSC, may acquire further genetic alterations that can finally render them autonomous from the niche. In these cases, CSC become more abundant, spread outside the niche, and their differentiation program is blocked (98).

2.8. CSC as a therapeutic target

Since CSC are resistant to the traditional chemotherapy and radiotherapy, these approaches are expected to have poor success in achieving long-term tumor regression (102). Thus, strategies designed to eradicate CSC are welcome, in order to complement the established cancer therapies which target the quickly proliferating bulk cells.

CSC markers may be targeted by immunotherapy, for example by administering monoclonal antibodies against these molecules, in order to elicit antibody-dependent cell-mediated cytotoxicity (152). Such antibodies may be conjugated to cytotoxic drugs in order to deliver high doses specifically to CSC (98). Some of the limitations are the little knowledge of the functional significance of these markers in the context of CSC, and the unwanted side effects due to the broad expression of some of these proteins in normal tissues, especially in normal adult stem cells (98).

The stemness signaling pathways can be targeted as well, either by synthetic compounds or by natural molecules. For example, nonsteroidal anti-inflammatory drugs (NSAID) interfere with Wnt pathway, since COX2 is a Wnt target gene. Moreover, NSAID can block the production of prostaglandin E2 by myofibroblasts (200). Vitamin A and D compete with β -catenin for TCF interaction. Also new molecules which inhibit elements of the Wnt pathway are in preclinical trials (152). Porcupine inhibitors interfere with the process of Wnt acetylation, necessary for its

secretion (201), and an anti-Frizzled antibody (vantictumab) (202) and a Wnt decoy (ipafricept) (203) are in clinical trial (204).

The Notch pathway can be inhibited either through γ -secretase inhibitors or through neutralizing antibodies directed against DLL4 or Notch (152).

Shh pathway is targeted either by cyclopamine or other Smo antagonists, which entered clinical trials (152).

As mentioned above, OXPHOS CSC may be targeted by hitting mitochondria, by using oligomycin, antimycin (191), metformin and rotenone, the antibiotics salinomycin (192), azithromycin, doxycycline, tigecycline, and chloramphenicol (193), the anti-helminthic pyrvinium pamoate, niclosamide (176, 180), and closantel, the anti-viral nitazoxanide and the anti-malarial atovaquone (194).

ATP-competitive agents can be used to target ABC transporters, thus impairing SP cells (205). Salinomycin also acts as an inhibitor of ABCB1, thus sensitizing CSC to chemotherapeutic drugs, and seems to be also a differentiating agent (152). Curcumin is another natural compound that targets the SP by modulating ABCG2. It also leads to β -catenin cleavage and impairs tumorsphere formation (152). Sulphoraphane targets NF κ B pathway and impairs spheroid formation, ALDH activity, and migratory ability, while inducing apoptosis in CSC (152).

Since the EMT program can lead to CSC generation, and since EMT is mainly driven by epigenetic silencing of epithelial markers (97), histone deacetylase (HDAC) inhibitors, such as *n*-butyrate and pyroxamide (206), can be used to induce the opposite transition. Otherwise, targeting TGF- β signaling can be a promising route, for example through bone morphogenetic protein BMP4 (207).

Another strategy to eliminate CSC is to induce their terminal differentiation in order to make them sensitive to chemotherapy. The most popular differentiation-inducing agents are vitamin A, its analogue retinoid, and *all-trans*-retinoic acid (152, 208-210). *All-trans*-retinoic acid is currently the standard treatment for acute promyelocytic leukemia. Other classes of differentiating agents are epigenetic regulators, such as HDAC inhibitors containing hydroxamate (211), and lysine demethylase LSD1 inhibitors like tranylcypromine (212).

Therapies directed against the CSC niche are needed along with CSC-specific therapies, in order to avoid the re-shaping of a CSC pool from plastic non-CSC. Thus, EGFR and Wnt inhibitors may play a role in blocking the paracrine circuits which sustain CSC (98). Other possibilities are the small molecule RQ-15986, which antagonizes the prostaglandin E2 receptor EP4 (213), or NSC 74859, which inhibits STAT3 transcriptional activity (214), thus blocking the main extrinsic networks intervening in the tumor microenvironment. In order to

stop the recruitment of macrophages in the tumor, anti-CSF1R antibodies (215) and CSF1R tyrosine kinase inhibitors (216) have been developed. It has also been discovered that, besides targeting tumor cells, the chemotherapeutic drug trabectedin causes TAM depletion (217).

Chapter 3

OVARIAN CANCER

STEM CELLS

EOC clinical course, *i.e.* relapse after an initial complete response to chemotherapy together with its heterogeneous histophenotypes, suggests that ovarian cancer is a stem-cell disease (218). However, the limited knowledge about the cell-of-origin and the pathogenesis of this cancer made impossible the exploration in the EOC CSC field starting from markers that identify normal stem cells in the ovary. Thus, researchers relied on general stem cell markers used for the identification of CSC in other carcinomas to delineate ovarian CSC phenotype (219). In Table 3.1, a list of putative ovarian CSC markers used in different studies is reported (218).

| Marker(s) | Endpoint | Model | Ref. |
|------------------------|---|---------------------------|--|
| CD133+ | Increased efficiency | tumorigenic | Cell lines, primary tumor, ascites, xenograft tumor (220, 221) |
| CD44+/MyD88+ | Increased spheroid formation; chemoresistance | tumorigenesis; formation; | Ascites, cell lines (222) |
| CD44+/CD117+ | Increased chemoresistance | tumorigenesis; | Primary tumor, xenograft tumors (223) |
| CD44+/CD24- | Spheroid formation; recapitulate parental tumor | | Cell lines (224) |
| CD44+/CD24+ | Increased tumorigenesis | | Primary tumor, xenograft tumor (225) |
| ALDH1A1+ | Increased pluripotency | tumorigenesis; | Cell lines (226) |
| ALDH1A1+/CD133+ | Increased chemoresistance | tumorigenesis; | Cell lines, primary tumor, xenograft tumor (227) |
| | Increased tumorigenesis; self-renewal | self-renewal | Primary tumor (228) |
| Side population | Increased tumorigenesis | | Cell lines (murine and human), ascites (229) |
| | Increased chemoresistance | tumorigenesis; | Cell lines, ascites, xenograft tumor (230) |
| | Increased chemoresistance; self-renewal | tumorigenesis; | Cell lines, xenograft tumor (231) |
| | Chemoresistance | | Cell lines (232) |

Table 3.1. Putative ovarian CSC markers (218).

In 2005, the first report on ovarian cancer cells endowed with stemness was published (233). Bapat and colleagues derived 19 spontaneously immortalized clones from the ascites of a serous adenocarcinoma patient; one of them was able to grow in soft agar or as floating spheroids and to give rise to tumors when injected subcutaneously or intraperitoneally in nude mice. Another one acquired the same characteristics after 20 passages. All the 19 clones were positive for CD44, EGFR, c-Met, vimentin, CK18, and Slug; the two tumorigenic clones were also positive for c-Kit and its ligand stem cell factor (SCF), and expressed the progenitor markers Nestin, Oct4, and Nanog. Thus, the Authors concluded that these two clones represented the CSC population of those ascites.

As CD133 is one of the most popular CSC markers, Ferrandina *et al.* (234) compared its expression in normal ovary, benign ovarian tumors, ovarian carcinomas and omental metastases, and found that CD133⁺ cell percentage was higher in ovarian carcinomas than in all the other groups. Moreover, FACS-sorted CD133⁺ cells were more clonogenic and had a higher proliferation potential than CD133⁻ cells. Baba *et al.* (220) found that CD133 was heterogeneously expressed in ovarian cancer cell lines and primary samples, with CD133⁺ cells being more chemoresistant, and that only CD133⁺ cells were able to generate both positive and negative daughters, while CD133⁻ cells only gave rise to negative cells. In contrast, Bapat's group re-analyzed the previously obtained 19 clones for CD133 expression and found that the two stem-like clones were CD133⁻ and that the CD133⁺ clones were non-tumorigenic. Interestingly, the CD133⁻ clones were able to differentiate into the endothelial lineage to create blood vessels to support tumor growth (235).

Szotek *et al.* (229) applied the Side Population (SP) strategy to identify CSC in two murine ovarian cancer cell lines. The SP cells were more clonogenic *in vitro* and tumorigenic *in vivo* as compared to non-SP cells, they were arrested in G1 cell cycle phase and resistant to doxorubicin but resulted as sensitive as non-SP cells to Mullerian Inhibiting Substance. Regarding the immunophenotype, the SP from one of the two cell lines was enriched for CD117 (c-Kit). These Authors were also able to detect the SP in 3 human ovarian cancer cell lines and 4 patient ascites. However, these cells did not express c-Kit.

Alvero *et al.* (222) checked the expression of CD44 in chemo-naïve patients and found that all of them were positive, but CD44⁺ cell percentage was higher in ascites and metastases. They also demonstrated CD44⁺ cell tumorigenicity: they could recapitulate the original tumor heterogeneity and could be serially passaged *in vivo*. The Authors found that CD44⁺ cells expressed MyD88 to a higher extent than CD44⁻ cells. These data mean that CD44⁺ cells can establish the pro-inflammatory environment that favors tumor development by secreting the plethora of cytokines induced by NFκB. Subsequently, the same Authors investigated the association between CD44 expression and progression-free survival (236). They found that early-stage EOC expressed CD44 at higher levels than advanced stage disease, suggesting a dilution of CSC in the mass of non-CSC as cancer progresses. Patients with higher CD44 levels had poorer chemotherapy response rate and shorter survival; however, in advanced stage EOC, the number of CD44⁺ cells did not correlate with progression-free survival.

Steg *et al.* (237) measured the percentage of CD44, ALDH1A1, and CD133 in matched samples of primary tumors, tumors collected soon after chemotherapy and after clinical recurrence. They found variable expression in primary tumors; however, after chemotherapy at least one of these

markers resulted enriched. By the way, at the time of relapse the expression levels reverted to the situation observed in primary tumors. This finding support the concept that CSC population may be quite variable among patients and, more importantly, that CSC are the drivers of chemoresistance and relapse (218).

Zhang *et al.* (223) generated spheroids from solid tumors from patients affected by serous adenocarcinomas. These spheroids could be serially passaged *in vitro*, they were more tumorigenic than non-selected parental cells and could be serially passaged also *in vivo*. Moreover, they expressed stemness-associated genes and were more resistant to cisplatin and paclitaxel than spheroid cells cultured in differentiation conditions. Afterwards, the Authors analyzed the spheroids for CD44 and CD117 expression, and found that they were enriched for both markers as compared to the parental cells. Thus, the Authors determined the spheroid-forming capacity and tumorigenicity of FACS-sorted CD44⁺CD117⁺ cells, and found that they could be propagated as spheroids for months and formed tumors at higher efficiency and lower latency than the double negative counterpart. Similarly, Luo *et al.* (238) isolated CD117⁺ cells from 3 out of 14 xenografts and demonstrated that they could give rise to both CD117⁺ and CD117⁻ cells and could be serially transplanted *in vivo*. Moreover, the Authors found CD117 positivity in about 40% of patients; CD117 expression correlated with resistance to chemotherapy. Kusumbe *et al.* (239) analyzed reversibly quiescent cells (*i.e.*, PKH26^{hi} or PKH67^{hi}) from a cell line generated by a patient's ascites. They demonstrated that these cells were endowed with self-renewal, they expressed the stemness-related genes Oct4, Bmi1, Nestin, and Nanog, and they were enriched by chemotherapy treatment but they could generate PKH^{dim} and PKH^{neg} daughters upon treatment removal. Interestingly, the totality of PKH^{hi} cells was also CD44⁺CD117⁺.

Experiments on cell lines are reported in the articles by Ma *et al.* (240) and by Wang *et al.* (241). Ma and colleagues firstly selected the human ovarian cancer cell line SKOV3 with cisplatin and paclitaxel, and then they tested the survived cells for spheroid formation. They found that spheroids were enriched in the expression of Nanog, Oct4, Sox2, Nestin, CD133, CD117, and ABCG2, they were resistant to chemotherapeutics (other than cisplatin and paclitaxel), and they were highly tumorigenic. Transcriptional analysis revealed that differentially regulated genes belonged to some specific pathways, including angiogenesis, extracellular matrix remodeling, cell adhesion, proliferation, and integrin signaling (240). Differently, Wang and colleagues preferred not to use possibly mutagenic agents to select CSC in another human ovarian cancer cell line. Indeed, they propagated OVCAR3 cells as spheroids, and found that spheroid cells were enriched in CD44 expression, and expressed higher levels

of mesenchymal and lower levels of epithelial markers. Moreover, transcriptional analysis showed that spheroids upregulated CSC markers such as CD133, CD117, Sca1, CXCR4, LGR5, SOX2, and ALDH1A1; other differentially regulated genes belonged to EMT, cell adhesion, extracellular matrix remodeling, lipid metabolism, angiogenesis, and to the canonical stemness pathway (241).

Inspired by Zhang's work, our group investigated the role of CD44⁺CD117⁺ cells as CSC in our cohort of EOC ascitic effusions and PDX (182). EOC spheroid formation was associated with an increase in the percentage of CD44⁺CD117⁺ cells and a reduction in the expression of the differentiation marker cytokeratin (CK)-7. Moreover, FACS-sorted CD44⁺CD117⁺ were more tumorigenic than CD44⁺CD117⁻ cells when injected both intraperitoneally and subcutaneously. Additionally, FACS-sorted CD44⁺CD117⁺ cells displayed higher expression of all the stemness and EMT genes examined, and of MRP1, MRP2 and ABCG2 pumps, as well as of ALDH1A. We also found that the percentage of CD44⁺CD117⁺ cells increased following *in vitro* treatment with doxorubicin (182). We further confirmed that the coexpression of CD44 and CD117 was the most reliable CSC marker in our setting. To this aim, we evaluated the expression levels of Nanog, Sox2, and Oct4 in EOC cells FACS-sorted according to the expression of CD133, CD24, ALDH1 or CD44/CD117. CD24 was excluded from the analysis since it was expressed by most tumor cells; CD44⁺CD117⁺ cells significantly overexpressed the stemness genes compared with the negative counterpart, while no differences were detected between CD113⁺ and CD133⁻ or ALDH⁺ and ALDH⁻ cells (242).

As reported above, CSC markers and stemness pathways are attractive therapeutic targets also in EOC. Much effort is needed to decide if the winning strategy is to use CSC targeting therapies in combination with the traditional chemotherapy that hits the tumor bulk or, alternatively, as maintenance therapy after complete clinical response (218).

For instance, hyaluronic acid analogs functionalized with chemotherapeutics have shown efficacy against CD44⁺ cells both *in vitro* and *in vivo* (243).

Imatinib mesylate is a tyrosine kinase inhibitor active against ABL-BCR, PDGFR, and c-Kit. Some efficacy on ovarian cancer cell lines has been demonstrated *in vitro* (244). However, phase II clinical trials testing imatinib mesylate both in recurrent cancer and as a maintenance therapy in patients with complete response did not demonstrate any efficacy (245, 246). Few responses were also associated to the use of imatinib in combination with docetaxel for platinum resistant EOC treatment (247). By the way, it could be possible that these results are affected

by the lack of patient selection and recruitment according to CD117 positivity before the start of the trials (only the 30-40% of EOC express CD117) (248).

It is clear that a consensus for ovarian CSC identification is still lacking (249). It may be possible that the differences in the reported findings are due to the biological materials examined (human and murine cell lines, primary samples or ascites, EOC of different histotypes) (250), and to the methodological approaches applied, including tumor disaggregation techniques (218). It is also possible that each cell population described to be CSC is endowed with a certain degree of stemness, and that some of the stem cell markers are co-expressed by individual cells (*i.e.*, ALDH⁺ cells as a subgroup of CD133⁺ cells characterized by higher tumorigenicity (226)) (249). Additionally, each putative stem cell population might be the “right” CSC for the analyzed cell line or cohort of patients, and the “wrong” one for the cohort analyzed by other Authors. The CSC population may be extremely patient-specific, and it could be very difficult, or even impossible, to find a general CSC that could fit every tumor (218). It is likely that CD133⁺, ALDH⁺, CD44⁺, CD117⁺, and SP cells are none other than progenitors still endowed with a certain degree of tumorigenicity and chemoresistance, and that the true ovarian CSC at the apex of the hierarchy has not been discovered yet (248).

Another level of complexity is related to the high heterogeneity linked to EOC. It could be possible that each EOC histotype is generated by a specific CSC (249); alternatively, a common CSC not yet identified and characterized by multipotency might exist (218, 251).

Chapter 4

SCF/c-KIT AXIS

Stem cell factor (SCF), or c-Kit ligand (KL), is a protein encoded by a gene made up of nine exons, mapping on human chromosome 12. Six alternative transcripts have been described in *Homo sapiens*, 4 of which are translated into protein; however, two splice variants, which differ in exon 6 presence, are mainly expressed: a 248 amino acid isoform (SCF²⁴⁸) includes exon 6, which contains a proteolytic cleavage site, giving rise to SCF¹⁶⁵, a 18 kDa soluble cytokine (sSCF), and a shorter, 220 amino acid isoform (SCF²²⁰), lacking exon 6, which remains membrane-bound (mSCF) (Fig. 4.1 A) (252).

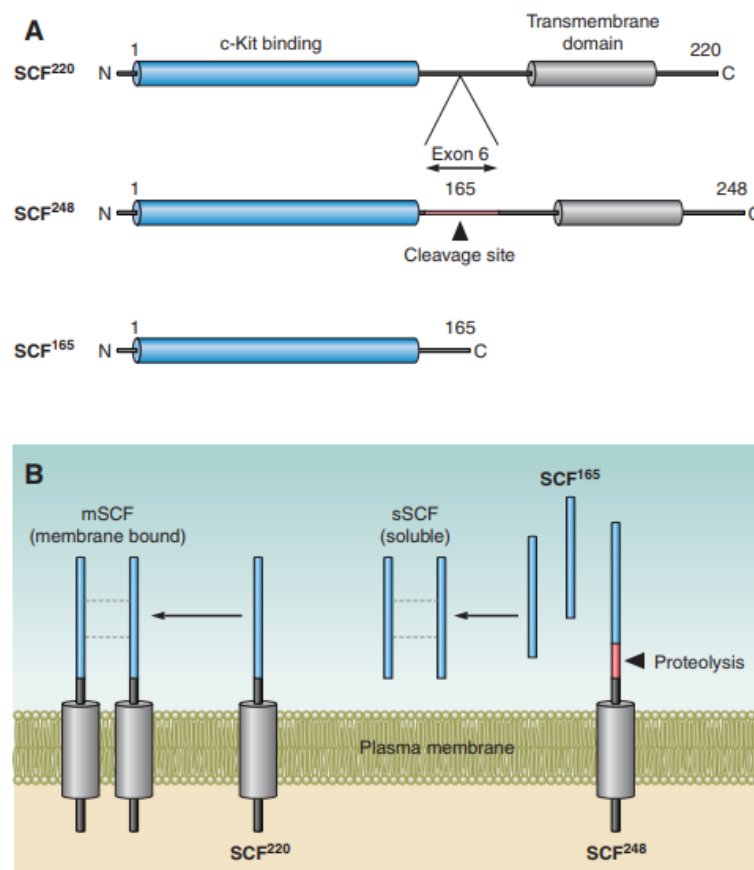


Figure 4.1. Schematic representation of SCF splicing isoforms (A) and protein processing into mSCF and sSCF homodimers (B) (252).

Both isoforms are translated into a transmembrane protein, with an N-terminal extracellular domain, a transmembrane domain and a C-terminal cytoplasmic tail; the longer isoform, however, includes a juxtamembrane proteolytic cleavage site, recognized by proteases such as MMP-9, chymase-1, ADAM17, and ADAM33. When cleaved, SCF is shed in the extracellular space and forms non-covalently bound, *N*-glycosylated homodimers of two four-helix bundles (253). Since the shorter isoform cannot be trimmed, it remains cell-associated, generating the 31 kDa mSCF. The latter also forms homodimers (Fig. 4.1 B) (252).

Both isoforms are biologically active, but with some differences. Obviously, while sSCF transmits long-range signals, mSCF requires cell-to-cell interaction. Moreover, only mSCF is able to induce proliferation through phospholipase C gamma (PLC γ) (254).

SCF expression is widespread detected in mouse embryos, being mainly observed in the yolk sac, liver, bone, gonads, and in the skin precursors (255), consistently with SCF/c-Kit role in hematopoiesis, melanogenesis, and gametogenesis. Indeed, the pleiotropic functions of this axis are suggested by the observation that loss-of-function mutations in either SCF or c-Kit cause anemia, piebaldism, and sterility (256). In human adult healthy tissues, SCF is mainly expressed by myoepithelial, smooth muscle, fibromuscular stromal and endothelial cells; its expression is often complementary to c-Kit distribution (257).

The SCF receptor c-Kit was discovered in 1987 as the cellular homolog of the viral oncogene v-Kit of the Hardy-Zuckerman 4 feline sarcoma virus (258). It is a monomeric tyrosine kinase receptor, encoded by a 21 exon gene mapping on human chromosome 4. C-Kit, together with PDGFR, M-CSFR, and FLT-3/FLT-2, belongs to the class III subfamily of receptor tyrosine kinases (RTK). It has a glycosylated extracellular N-terminus for ligand binding, made up of 5 immunoglobulin-like domains, a transmembrane domain, and, in the intracellular face, a juxtamembrane region followed by a tyrosine kinase domain split by an 80 amino acid long kinase insert sequence into an ATP-binding part and a phosphotransferase part, and a C-terminus tail. Postmeiotic germ cells express a truncated form of c-Kit, which only consists of the C-terminal tail and the part of the kinase domain closer to the C-terminus. Truncated c-Kit lacks kinase activity, but still takes part in signaling by acting as a scaffold protein (Fig. 4.2) (252).

Additionally, c-Kit undergoes alternative splicing: two splice variants only differ in the presence/absence of a serine in the kinase insert region, while the most important variants differ for a sequence of four amino acids (glycine-asparagine-asparagine-lysine, GNNK) in the extracellular domain, close to the plasma membrane (Fig. 4.2). The GNNK⁺ and GNNK⁻ isoforms are coexpressed in many tissues, but the GNNK⁻ is usually predominant. The two isoforms exert different transforming activity. Indeed, it has been demonstrated that the GNNK⁻ isoform (differently from the GNNK⁺) induces in NIH3T3 cells loss of contact inhibition, anchorage-independent growth and tumorigenicity in mice, although the affinity for SCF is identical. Nonetheless, SCF induces a more rapid and strong GNNK⁻ c-Kit phosphorylation and subsequent degradation, whereas GNNK⁺ activation is long-lasting (259). The GNNK⁻ isoform leads to a stronger ERK activation (260); in contrast, Akt activation seems to be more dependent on cellular context, since in NIH3T3 Akt phosphorylation is similar in cells expressing either

splice form, while in the Ba/F3 cell line a stronger Akt phosphorylation is induced in cells expressing the GNNK⁻ splice variant (261).

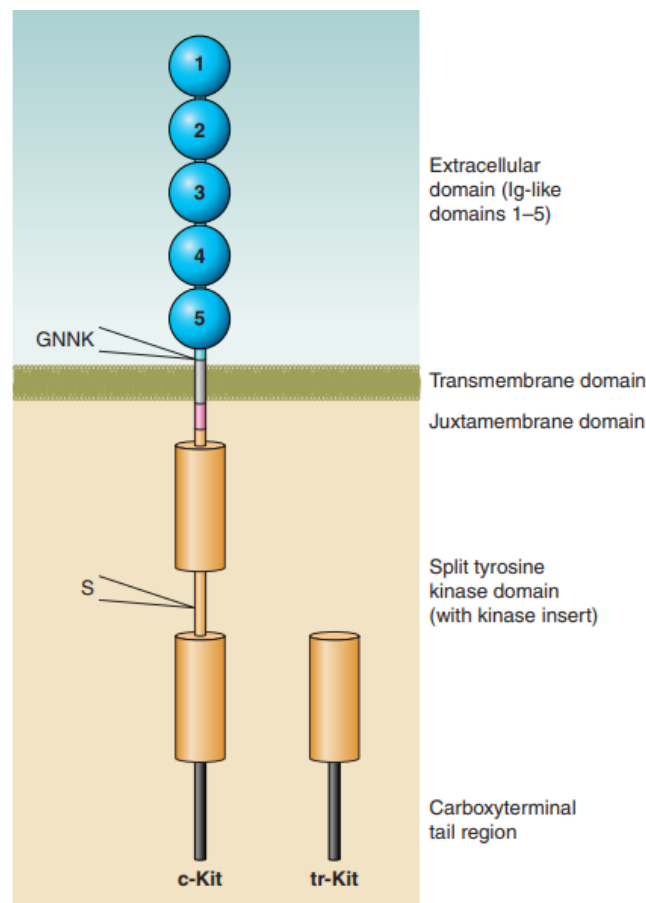


Figure 4.2. Schematic representation of the c-Kit structural domains (252).

In addition, there are 9 sites that can be *N*-glycosylated in the N-terminus of the receptor. Thus, even though the amino acidic backbone molecular weight is 110 kDa, the mature protein is between 140 and 160 kDa, depending on the glycosylation levels (262).

In the steady state, the receptor is kept inactive by the steric interaction between the juxtamembrane and the kinase domain. Upon SCF dimer binding, c-Kit becomes active very rapidly: in a few minutes, SCF simultaneously binds to the first three immunoglobulin-like domains of two c-Kit monomers, inducing a conformational change that brings the fourth and fifth immunoglobulin-like domains in close proximity. The homotypic interaction between these domains renders the receptor dimer more stable, allowing for more efficient trans-phosphorylation. The juxtamembrane domain is released from its inhibitory configuration as a result of the phosphorylation of two tyrosine residues, Tyr-568 and Tyr-570, thus enabling kinase domain catalytic function. Consequently, eight tyrosines in the intracellular portion of

the receptor (Tyr-568, -570, 703, -721, -730, -823, -900, and -936) can be phosphorylated, out of which seven provide the docking sites for adaptors or signal transduction molecules containing Src homology 2 domains (SH2) or phosphotyrosine binding domains (PTB) (263). The main pathways activated by c-Kit are PI3K/Akt, MAPK (ERK1/2, ERK5, p38, and JNK), Jak/STAT, Src family kinases, PLC γ and PLD, depending on the phosphotyrosine (pTyr) involved. However, these pathways are not isolated entities, but rather they belong to a finely integrated circuit where pTyr-activated signaling cascades are interconnected leading to different downstream effects, as depicted in Fig. 4.3 (253).

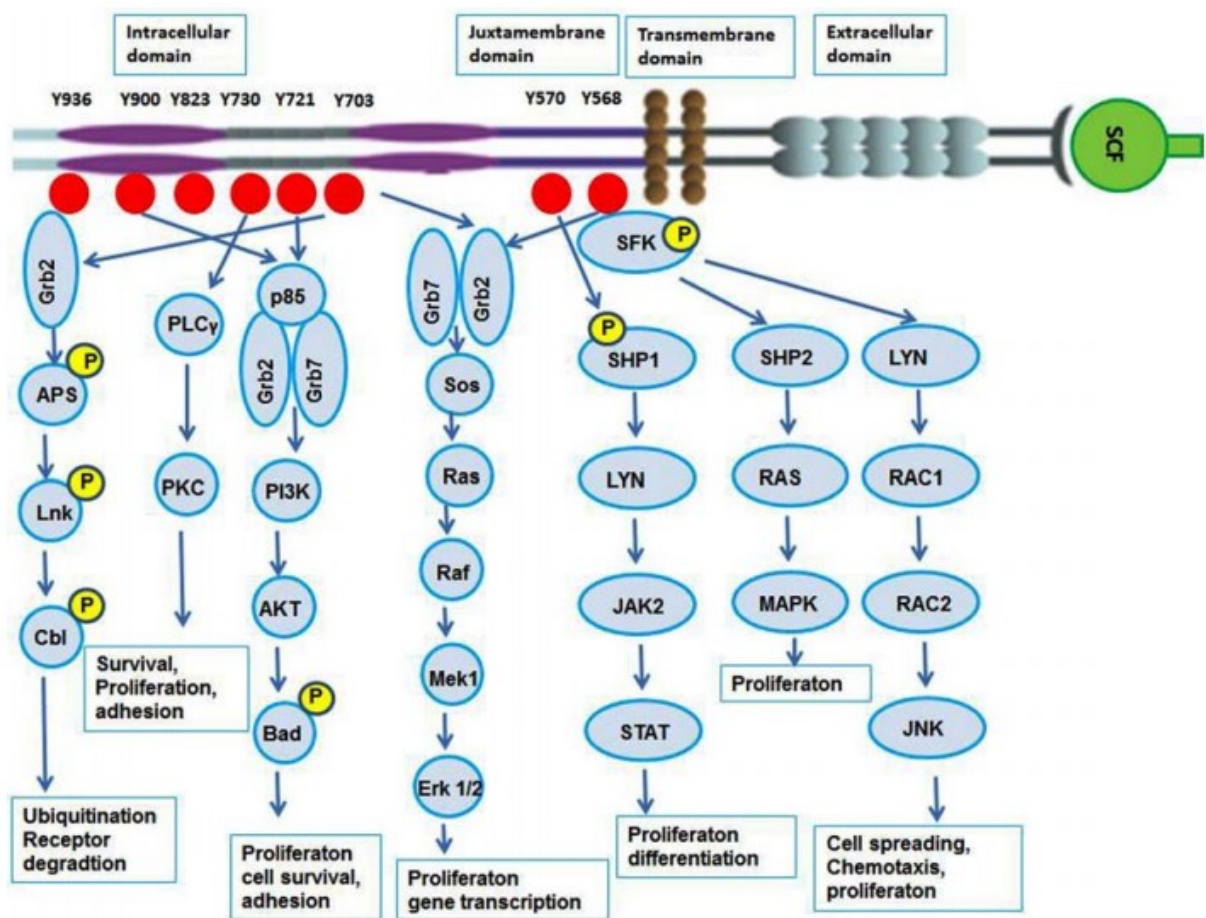


Figure 4.3. C-Kit tyrosine phosphorylation sites and related signaling pathways and effects (253).

PI3K/Akt is one of the major c-Kit activated pathways, responsible for mediating proliferation, migration and resistance to apoptosis (252, 253).

Src family kinases play different roles depending on the cellular context and, thus, on the specific kinase involved. Broadly, this family contributes to the activation of other pathways, including MAPK and PI3K/Akt, inducing proliferation, migration, and survival.

The MAPK pathways are important for the proliferative responses and survival. In particular, ERK1/2 pathway can be alternatively activated by Ras/Raf or by PI3K.

Activated Jak phosphorylates STAT, which induces cell proliferation and differentiation.

Even though PLC γ plays a minor role in c-Kit signaling, cell proliferation induction by mSCF needs to pass through PLC γ pathway. In contrast, while sSCF fails to activate PLC γ , it can activate PLD through PI3K (252, 253).

Since c-Kit activity, similarly to other RTK, promotes cell proliferation, survival, and migration as downstream effects, it needs to be tightly regulated in order to avoid oncogenic transformation. There are three main mechanisms of c-Kit shut down: internalization, inactivation of the catalytic domain by serine phosphorylation, and tyrosine dephosphorylation. SCF-induced phosphorylation provides the docking sites for the E3 ubiquitin ligase c-Cbl or for suppressor of cytokine signal SOCS6, thus leading to receptor lysine monoubiquitination and internalization in clathrin-coated vesicles followed by receptor-ligand lysosomal or proteasomal degradation. A different way of c-Kit modulation is the negative feedback loop consisting in the PKC-mediated phosphorylation of Ser-741 and Ser-746 in the kinase insert region. Finally, phosphate groups can be removed by SHP1 protein phosphatase (252).

C-Kit signaling is crucial in hematopoiesis, melanogenesis, and gametogenesis. Specifically, c-Kit synergizes with other cytokine and growth factor receptors, namely erythropoietin, GM-CSF, IL7, and IL3 receptors, for the regulation of self-renewal, proliferation, and differentiation of HSC and the committed progenitors of erythropoiesis, megakaryopoiesis, lymphopoiesis, as well as for mast cell development (264, 265). Indeed, c-Kit is detected on HSC and early progenitors, and the expression is lost during differentiation. On the contrary, c-Kit expression is maintained in mature mast and dendritic cells (266). C-Kit is also crucial in mediating the haptotactic migration of melanocytes from the neural crest to the skin during embryogenesis (267). C-Kit is also involved in folliculogenesis, oogenesis and spermatogenesis, since it mediates proliferation and migration of germ cells and has a protective role against apoptosis (268). In the gastrointestinal tract, c-Kit is expressed in the interstitial cells of Cajal, which govern gut motility (269). C-Kit also plays a role in the nervous system development and wound repair, by promoting the migration of neuronal stem cells (270).

C-Kit is a well-known proto-oncogene as it is implicated in several human neoplasias, including small cell lung carcinoma, melanoma, testicular carcinoma, mast cell leukemia, acute myeloid

leukemia, and gastrointestinal stromal tumor (GIST) (271). Indeed, c-Kit overactivation or gain-of-function mutations in the tissues where the receptor is physiologically expressed cause their malignant transformation. The majority of the oncogenic mutations fall in the kinase domain and in the juxtamembrane domain; as a result, the receptor is constitutively activated, also in the absence of the ligand, and this phenomenon supports aberrant proliferation (252). GIST derives from the interstitial cell of Cajal. Almost all GIST are c-Kit⁺, and in 80% of cases the receptor is mutated, frequently in the juxtamembrane domain. Moreover, this tumor often produces the ligand SCF. In this context, competition of imatinib mesylate with the ATP-binding pocket of c-Kit nullifies the constitutive signaling of the receptor (272). Imatinib more efficiently inhibits c-Kit in its inactive state, thus, the emergence of secondary activating mutations in the kinase domain often makes the cells imatinib-resistant. To overcome the primary and secondary imatinib resistance, novel drugs have been developed, including dasatinib and nilotinib. Whether it is better to use more selective inhibitors, in order to reduce side effects, or multi-kinase inhibitors, such as sorafenib, to hit multiple targets also downstream to the receptor, in order to improve effectiveness, is still debated (273).

The existence of a putative autocrine/paracrine SCF/c-Kit circuit promoting cancer stemness has been advanced. Fatrai and colleagues (274) demonstrated that differentiated colon tumor cells produce SCF, which interacts in a paracrine manner with c-Kit-expressing CSC-enriched colonospheres, thus stimulating their clonogenicity and tumorigenic potential; the SCF/c-Kit axis inhibition through imatinib, the selective inhibitor ISCK03, or an anti-SCF neutralizing antibody resulted in decreased clonogenic and tumorigenic potential, together with decreased CSC-associated marker expression. Similarly, it has been demonstrated that SCF is produced by non-small cell lung cancer stem cells, and induces their own proliferation and eventual self-renewal, which were inhibited by SCF-neutralizing antibodies or by imatinib. Importantly, SCF/c-Kit axis inhibition prevented CSC enrichment due to cisplatin treatment (275). Also Lewis lung carcinoma pneumospheres were found to express higher SCF levels than their differentiated counterpart; SCF silencing by short hairpin RNA (shRNA) decreased sphere formation efficiency and the expression of stemness- and EMT-related genes, and resulted in reduced *in vivo* tumorigenicity (276).

Chau *et al.* (244) showed that c-Kit is not just a marker of ovarian CSC, but it can also determine their stem phenotype. Indeed, both c-Kit and SCF were overexpressed in tumorspheres from SKOV3 and HEYA8 ovarian cell lines and, similarly to the work in Lewis lung carcinoma, the use of small interfering RNA (siRNA) against c-Kit reduced the sphere-forming efficiency, the expression of stem cell markers, chemotherapy resistance, and the tumorigenic capacity of

CSC. Imatinib exerted similar effects. The Authors also investigated the molecular mechanism underlying c-Kit-promoted stemness and chemoresistance, and demonstrated the activation of β -catenin and then ABCG2 downstream of c-Kit.

The hypoxic tumor microenvironment has been demonstrated to be a trigger for c-Kit and SCF expression. Indeed, hypoxia promotes c-Kit expression (244, 274), which in turn induces the expression of SCF as a positive feedback loop by stabilizing HIF1 α as shown also in normoxyc conditions. As a consequence, HIF1 α -induced SCF can cooperate with HIF1 α -induced VEGF by binding their respective receptors on endothelial cells, thus promoting angiogenesis (277).

Chapter 5

AUTOPHAGY IN CANCER AND CANCER STEM CELLS

Autophagy is a highly conserved catabolic pathway, characterized by the lysosomal degradation of cell self-components, which guarantees the turnover of long-living proteins and organelles, the quality control by destroying damaged organelles and unfolded proteins, and the supply of building blocks such as amino acids, lipids, and sugars for anabolic processes and metabolic intermediates in the case of nutrient shortage (278). Three main types of autophagy are known: 1) macroautophagy consists in the sequestration of cytoplasmic areas in autophagosomes prior to delivery to the lysosomes; 2) microautophagy, in which the material doomed to degradation is directly engulfed by lysosomes through membrane invagination, and 3) chaperone-mediated autophagy, in which substrates are bound by chaperone proteins such as Hsc70, which is recognized by a lysosome membrane receptor (lysosomal-associated membrane protein 2A, LAMP-2A) for translocation into the lumen (279). Macroautophagy, or just autophagy, is the most extensively studied process, and I will refer to it hereafter. It can involve random substrates or can be selectively addressed to specific targets, or even organelles (279); in particular, if mitochondria are the target, it will be referred to as mitophagy, or pexophagy if it is directed against peroxisomes; xenophagy is the name of autophagy when it degrades intracellular bacteria (280).

Autophagy was first observed in the late Fifties by Clark (281) and Novikoff (282), and subsequently described by others (283, 284), through morphological analyses. Indeed, these Authors observed intracellular membrane vesicles surrounding semi-digested mitochondria and endoplasmic reticuli (ER) and containing lysosomal hydrolases. By the way, the extensive molecular characterization of the entire process was deconvoluted only in the Nineties by Takeshige *et al.* (285), who took advantage of yeast mutants and identified the autophagy-related genes (ATG). Later, ATG homologs were identified in mammals (286). Autophagy consists of five key stages, orchestrated by 4 ATG complexes: initiation, elongation, closure, maturation, and degradation (278). The autophagic process, with the five stages and mammalian complexes, is represented in Fig. 5.1 (287).

The initiation phase takes place at the pre-autophagosomal structure (PAS) in yeast, and near the ER in mammals, and it is characterized by the phagophore formation. The phagophore (previously named “isolation membrane”) origin is not clear, but compelling evidence suggests that it derives from the ER membrane, even though a contribution from the trans-Golgi network, endosomes, nuclear envelope, and plasma membrane cannot be excluded (280). In mammals, the initiation is triggered by the ULK1/2-mATG13-FIP200-ATG101 complex. ULK1 and 2 (Unc51-like kinase) are two homologs of yeast Atg1, and are the only kinases involved in the process.

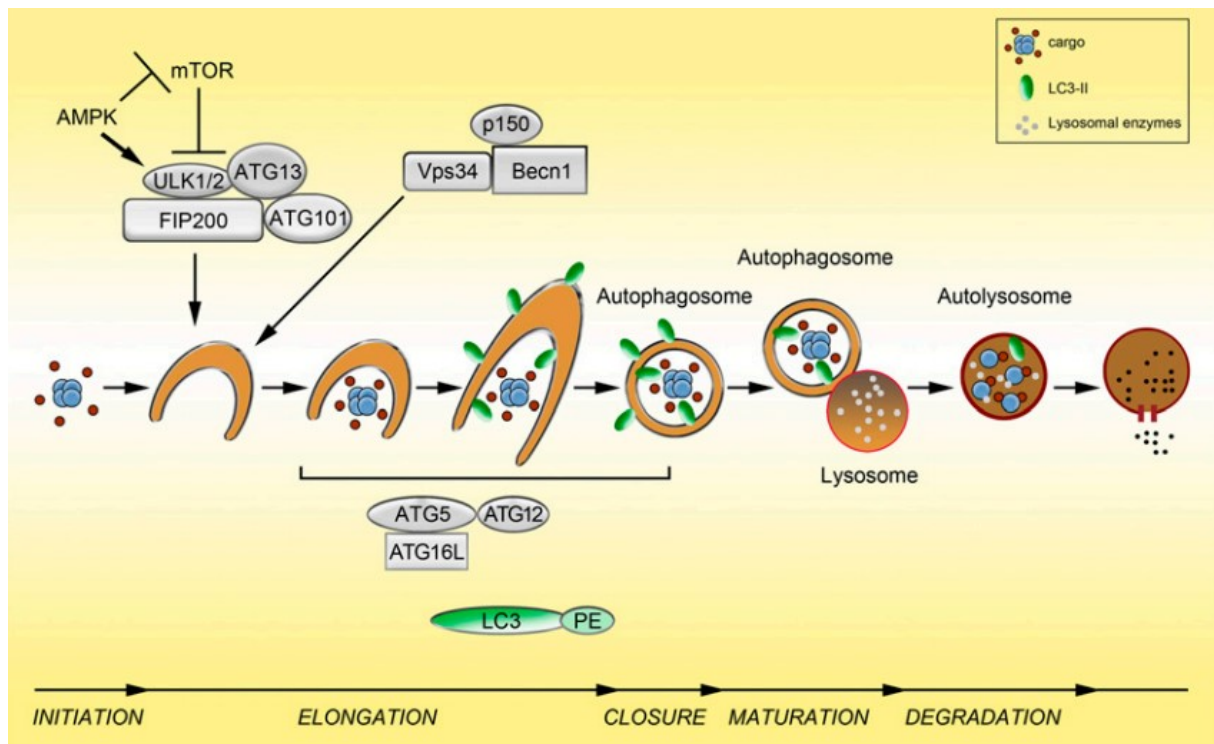


Figure 5.1. The stages of autophagy (287).

The complex is constitutively formed but it is kept inactive by ULK and mATG13 phosphorylation, mediated by mTORC1, protein kinase A (PKA), and AMP-activated protein kinase (AMPK), which act as nutrient and energy sensors (280). When nutrient and ATP levels are high or growth factors like insulin are bound to their receptors, the autophagy machinery is inhibited; on the contrary, in case of energy shortage, the complex is activated and a second complex can work (278). In mammals, the second complex involves a class III PI3K, named vesicular protein sorting 34 (Vps34), ATG14L, Vps15, and Beclin1 (280). Vps34 generates phosphatidylinositol-triphosphate (PI3P), essential for phagophore elongation and recruitment of the other complexes. Several regulatory proteins are associated with this complex, among which UV Radiation Resistance Associated (UVRAG), Bax-interacting factor 1 (BIF1), Autophagy And Beclin 1 Regulator (AMBRA) (autophagy-promoting), Rubicon and BCL2 (autophagy-inhibiting). Notably, BCL2 plays a role in determining cell viability both in apoptosis and in autophagy. Indeed, in case of nutrient abundance, Beclin1 is kept inactive by binding to BCL2; the interaction is disrupted in starvation by JNK-mediated phosphorylation of BCL2 (279).

The elongation is then carried on by two ubiquitin-like systems. The first one catalyzes the ATG5-ATG12 conjugation, important for inducing the curvature of the extending phagophore by placing itself on the outer surface of the structure and dissociating from it immediately before

the closure stage (280). ATG12 is activated by the E1 enzyme ATG7, transferred to the E2 enzyme ATG10 and finally linked to ATG5. ATG12-ATG5 dimerizes and finally forms a complex with two ATG16L molecules. The complex promotes the lipidation of microtubule-associated protein 1 light chain 3 (LC3, homolog of ATG8) by the second ubiquitin-like system. LC3 is synthesized as a cytosolic protein, proLC3, which is proteolytically cleaved by ATG4 to generate LC3-I. LC3-I C-terminus is activated by ATG7, transferred to the E2 enzyme ATG3, and finally linked to a phosphatidylethanolamine (PE) to give rise to LC3-II. LC3-II is inserted into both the internal and external surface of the phagophore, where it plays a critical role in the tethering and hemifusion of membranes for elongation and in cargo selection. Indeed, LC3-II binds the adaptor protein p62/SQSTM1, bringing poly-ubiquitinated protein aggregates in the lumen of the forming autophagosome (279). The closure step, through which the phagophore terminal parts fuse to give rise to a closed, double-membrane vesicle, is not well characterized from a molecular point of view. Probably, it involves some ATG8 mammalian homologs different from LC3 such as gamma-aminobutyric acid receptor-associated protein GABARAP, GABARAPL1, and GABARAPL2/GATE16 (288). The maturation step consists in the fusion of the autophagosome with endosomes to generate amphisomes or the fusion with lysosomes to give rise to autolysosomes (288). In the amphisome, the pH in the lumen of the vesicle lowers in order to prepare to the fusion with lysosomes, where acid hydrolases degrade the vesicle content (279). Finally, lysosomal permeases allow the release of the degradation products into the cytosol (278).

The gold standard for autophagy detection is transmission electron microscopy (TEM), which allows for directly observing the autophagosome presence in the complex cellular context (288). However, more rapid and easily available assays are often used to monitor autophagy levels and changes. The most used autophagy marker is LC3-II, usually detected by Western blot. LC3-I lipidation gives rise to a bigger protein which, however, has a higher electrophoretic mobility than LC3-I: LC3-I is detected as a band at 16-18 kDa, while LC3-II is found at 14-16 kDa. LC3-II levels are increased in comparison to LC3-I when autophagy is induced; however, an increase in LC3-II band intensity should be interpreted cautiously, since it could be a result of blocking of the later autophagy stages, rather than induction. As autophagy is a dynamic process, the autophagic flux, rather than a static measurement, should be determined to exclude a block of the pathway in any point. The autophagic flux is defined as the passage of the degradation substrates through the entire autophagic system, from initiation to degradation. To evaluate the autophagic flux, the rate of substrate breakdown should be measured over time.

Alternatively, autophagy can be perturbed by using inhibitors of the late stages of the process, such as bafilomycin A1 (which inhibits the V-ATPase), chloroquine (CQ) and NH₄Cl (which raises the lysosomal pH), or protease inhibitors (which inhibit lysosome-mediated proteolysis). If LC3-II accumulates in this setting, a block in the autophagic machinery can be excluded. A transcriptional regulation of proLC3 mRNA should also be excluded. LC3-II levels may be extremely tissue-dependent; moreover, LC3-II levels vary in a limited dynamic range (289). Additionally, LC3 is not an autophagy-specific marker, as it can also associate to other membrane compartments, including secretory vesicles and endosomes. Thus, this marker should always be accompanied by the evaluation of a more suitable marker or by a different assay. Another marker used to evaluate the autophagic flux is p62/SQSTM1. P62 is actively degraded as a result of autolysosome formation; thus, if the autophagic flux is occurring, low p62 levels are associated to enhanced autophagy, and autophagy blockade results in p62 accumulation. In some aspects, p62 is a better marker than LC3 in following the autophagic flux. Indeed, it shows high magnitude changes following autophagy induction or inhibition, and these changes are more durable than LC3-II variations, which are particularly rapid. A set of commercial kits for flow cytometry detection of autophagosomes, including CYTO-ID[®] Autophagy detection kit (290), deserves a final mention, since they have been developed to allow a high throughput analysis (288).

Autophagy is a housekeeping process necessary for cellular homeostasis. Interest is growing in this field since it is emerging that autophagy deregulation is involved in many pathological conditions, including neurodegeneration and cancer (278). In neurons, autophagy activation hinders the accumulation of misfolded proteins such as mutant huntingtin in Huntington disease, tau in Alzheimer disease, and α -synuclein in Parkinson disease, thus preventing cell death.

In cancer, autophagy role is controversial. Indeed, in the early phases of tumorigenesis, autophagy seems to have an anti-tumoral effect, by eliminating damaged organelles, including old mitochondria, *i.e.* the place where the majority of reactive oxygen species (ROS) are produced. Impaired autophagy may result in increased ROS levels and DNA damage, delayed onset of senescence, and death from necrosis in apoptosis-incompetent cells, with eventual inflammation and creation of a tumor-promoting environment (287). Moreover, p62 accumulation in autophagy-deficient cells induces NF κ B nuclear translocation, thus exacerbating the inflammatory response, and it binds and inhibits the direct inhibitor of nuclear factor-erythroid 2 p45-related factor 2 (NRF2), named Kelch-like ECH associated protein 1

(KEAP1). Consequently, NRF2 can transcriptionally activate an antioxidant defense. In this way, increased ROS levels trigger DNA damage, but the induction of an antioxidant program enable cell survival (291). Experimental evidence of autophagy tumor suppression is provided, since beclin1 heterozygous mutant mice are more prone to spontaneously develop lymphomas and lung and liver cancers, without undergoing loss of heterozygosity, suggesting that cancer cells cannot survive in the complete absence of this protein, while liver-specific ATG5 and ATG7 deletion results in benign hepatomas only, suggesting a role of these proteins in malignant evolution. Monoallelic loss of Beclin1 has been reported in 40-75% of human prostate, breast, and ovarian cancer (292).

On the other hand, autophagy has a tumor-promoting role in already established tumors. Indeed, tumor microenvironment conditions, characterized by starvation, growth factor deprivation, and hypoxia, all induce autophagy as a survival mechanism. Also resistance to chemo- and radiotherapy and target agents can be mediated by autophagy, since it allows the removal of damaged cell components (287). It has been demonstrated that, while normal cells usually have low levels of basal autophagy, cancer cell lines have higher basal levels also in non-stressful conditions. For instance, oncogenic RAS-expressing tumor cells are autophagy-addicted, since autophagy provides intermediates for all their metabolic demands (291), and autophagy inhibition abrogates their tumorigenicity (292). These findings raised the interest in inhibiting autophagy for cancer therapy. The antimalarial drug hydroxychloroquine (HCQ), a chloroquine derivative, is investigated in several clinical trials in a variety of human cancers in combination with classical chemotherapy or proteasome inhibitors (291). While it is demonstrating efficacy and synergism with other drugs, whether the effect is due to autophagy inhibition or to different mechanisms involving lysosomes is still unclear (293).

Regarding the autophagy dependence in CSC, controversial findings are reported in literature (294, 295). Several papers support the idea of highly autophagic CSC. Chatterjee *et al.* (296) observed that ATG5, ATG12, and LC3B were overexpressed in dormant breast cancer stem cells. Inhibition of autophagy by 3-methyladenine (3-MA) reversed the dormant phenotype. Similarly, Filippi-Chiela *et al.* (297) found that 3-MA reduced sphere formation and the percentage of CD133⁺ and Oct4⁺ cells in glioma. Gong *et al.* (298) showed that expression of Beclin1 was increased in mammospheres and was crucial for CSC tumorigenesis in nude mice. Moreover, basal and starvation-induced autophagy flux was higher in ALDH1⁺ cells. Cufi *et al.* (299) demonstrated that CQ treatment or LC3 and ATG12 knockdown reduced the CD44⁺CD24^{-/low} population and vimentin expression in breast cancer. Zhu *et al.* (300) studied

the role of HIF1 α and autophagy in the conversion of non-stem pancreatic cancer cells to CSC, reporting that hypoxia induced HIF1 α , LC3-II and Beclin1 and enhanced stem-like properties in non-CSC. Bellodi *et al.* (301) showed that imatinib mesylate resistance in chronic myeloid leukemia was due to autophagy induction mediated by imatinib itself. CQ treatment or ATG5/ATG7 silencing increased cell death induced by imatinib and resulted in near complete eradication of CSC. Ojha *et al.* (302) reported that SP cells from bladder cancer cells were characterized by high autophagic flux; autophagy inhibition potentiated the effects of chemotherapeutic drugs against these cells. Galavotti *et al.* (303) found that the autophagy proteins DRAM1 and p62 regulated cell migration and invasion in glioblastoma stem cells. On the contrary, Jiang *et al.* (304) showed that an oncolytic virus used to treat glioma induced cell death in CSC through excessive autophagy, demonstrated by the accumulation of ATG5, LC3, and autophagic vacuoles. Moreover, Zhao *et al.* (305) observed that glioma stem cells exhibited lower autophagic activity compared with neural stem cells. A higher autophagy level was induced by differentiation; conversely, autophagy inhibition impaired the differentiation program. Similar results were reported by Zhuang *et al.* (306), who found that rapamycin, an autophagy inducer, caused differentiation in glioma stem cells and subsequential sensitization to X-ray irradiation. Torin-1, an autophagy inducer similar to rapamycin, was reported to inhibit colon CSC migration, invasion, and colony formation, *in vitro*, as well as tumor growth and angiogenesis *in vivo*, without affecting normal colon stem cells (307).

Another level of complexity was brought by Sharif *et al.* (308), who demonstrated that both inhibition of the autophagy machinery, through ATG7 or ATG12 knockdown, and induction, through rapamycin, starvation, or Tat-Beclin1, caused loss of pluripotency in the NT2/D1 model by inducing either differentiation or senescence, thus suggesting that a tight control of autophagy levels is necessary to ensure the maintenance of stemness features, and that any perturbation, either in a positive or negative way, is detrimental to CSC homeostasis.

Taken together, all these works suggest that, since autophagy is highly activated to maintain stemness in some normal stem cells, but is lower in others (309), something similar may happen also in CSC, *i.e.* autophagy role could be extremely context-dependent.

Chapter 6

CASEIN KINASE 1 AND TUMORIGENESIS

Casein kinases are a group of evolutionarily conserved serine/threonine kinases ubiquitously expressed in eukaryotes. This group is divided into two families, due to the high homology level in the catalytic domain: casein kinase 1 (CK1) and casein kinase 2 (CK2).

Seven CK1 genes have been identified in mammals: CK1 α , β , γ 1, γ 2, γ 3, δ , and ϵ . CK1 β was only found in bovines. Furthermore, several splice variants have been described. The seven CK1 isoforms display a high homology in their catalytic domain: for example, the highly related CK1 δ and ϵ are 98% identical in their kinase domain, but they differ in the regulatory N-terminal and C-terminal domain. A schematic drawing of human isoforms is depicted in Fig. 6.1 (310).

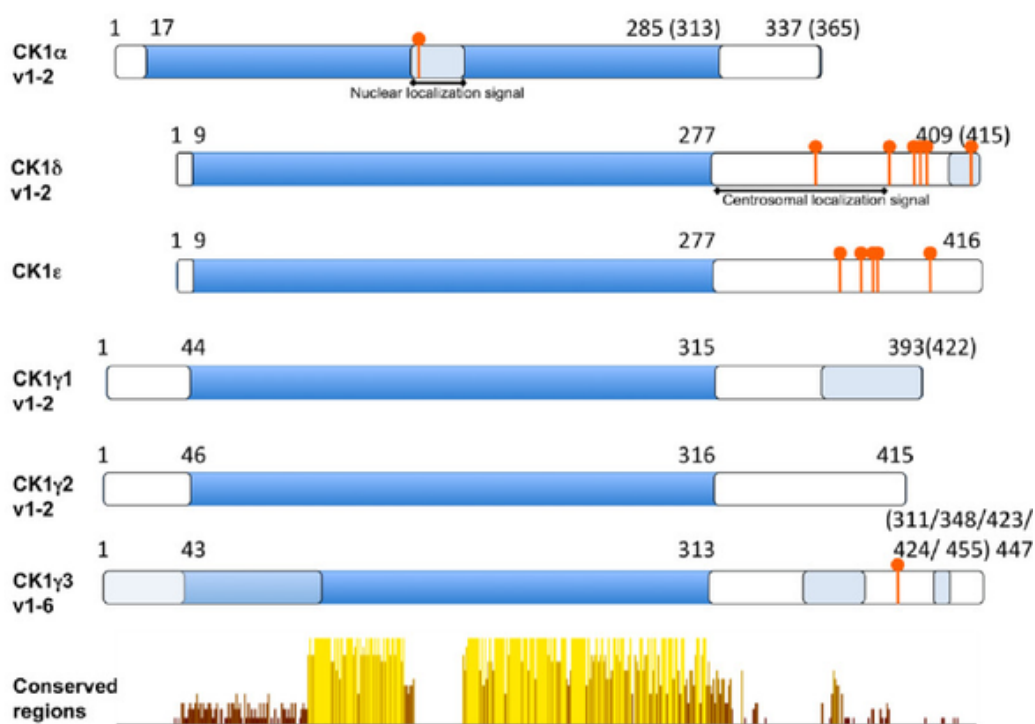


Figure 6.1. Scheme of human CK1 isoforms. In dark blue, the kinase domain, in light blue the variable regions of the splice variants. As red spots, the phosphorylation sites. The yellow bars show the conserved regions (310).

CK2 is usually found as a tetramer, made up of two catalytic (the 42 kDa α and/or the 38 kDa α' , encoded by two different genes) and two regulatory (the 28 kDa β) subunits, important to determine substrate specificity and protein stability (311). More than 300 substrates, involved in many physiological processes, have been described. In cancer, CK2 has an anti-apoptotic and pro-survival function, thus making it a promising druggable target (312).

CK1 are monomeric, constitutively active, co-factor independent kinases, which can only use ATP as phosphate donor. This does not implicate that their activity is not regulated. Indeed, treatment with insulin, topoisomerase inhibitors, γ -irradiation, and viral transformation induce

CK1 expression; the subcellular compartmentalization is fundamental to determine the interaction between enzyme and substrate; CK1 δ dimerization has been shown to inhibit its activity; different ATP-dependent RNA helicases (DDX) act as allosteric activators of CK1 α , γ , δ , and ϵ . Importantly, the C-terminus of CK1 δ and ϵ includes many inhibitory autophosphorylation sites. These modifications are reversible, since phosphatases activated downstream of signaling pathways can remove the phosphates and activate the enzyme; moreover, part of the C-terminus can be cleaved, thus leading to activation (313). CK1 recognize a consensus sequence for phosphorylation: S/T(P)-(X)₁₋₂-S/T, *i.e.* they need a preceding phosphorylation of serine/threonine residues N-terminal of the target site. However, if the phospho-serine/threonine is substituted by an acidic amino acid, the sequence can still be efficiently phosphorylated by CK1, without the intervention of a priming kinase. Moreover, an additional non-canonical motif (SLS) has been discovered to be recognized by CK1 (313). The substrates targeted by the different CK1 are involved in a plethora of cellular functions, including cell cycle progression, chromosome segregation, apoptosis, DNA repair, circadian rhythm, ribosome biogenesis, vesicle trafficking, Wnt, Shh, and Hippo pathways (310, 314). CK1 δ and ϵ play an important role in determining the duration of the circadian rhythm, by phosphorylating the three Period (PER) proteins, thus causing their degradation. If PER are complexed with Cryptochrome (CRY), the complex PER/CRY/CK1 translocates into the nucleus, where it represses the transcriptional activity of BMAL1/CLOCK. PER hypophosphorylation due to mutations in CK1 ϵ leads to shortening of the circadian rhythm, while the CK1 ϵ hyperactivity due to a polymorphism at an autophosphorylation site results in elongation of the circadian rhythm (313).

CK1 α , γ , δ , and ϵ exert both positive and negative effects on the Wnt pathway depending on the phosphorylated substrate. Although CK1 δ/ϵ and CK1 γ mainly have a positive role and CK1 α a negative role, a study in *Drosophila* also reveals a negative role for CK1 ϵ and a positive role for CK1 α (315). It was shown that CK1 δ/ϵ positively regulate Wnt signaling by phosphorylating Dvl on multiple sites. CK1 α , instead, negatively regulates Wnt signaling since it phosphorylates β -catenin at Ser45, which belongs to the non-canonical SLS motif, thus priming GSK3 β to phosphorylate Thr41, Ser37, and Ser33, hence leading to its ubiquitination and proteasomal degradation. APC is also a target of CK1 ϵ and CK1 δ and its phosphorylation enhances its binding affinity for β -catenin, facilitating its degradation. Axin is also a target, but the biological significance is unknown. In response to Wnt, the co-receptor LRP5/6 is phosphorylated by GSK3 β and by CK1 α , δ , ϵ , and γ ; phospho-LRP5/6 recruits the destruction complex by binding axin, leading to inhibition of β -catenin phosphorylation and degradation

(316). CK1 ϵ positively regulates Wnt signaling also by phosphorylating TCF3: phospho-TCF3 binds β -catenin thus protecting it from destruction (313). At the nuclear level, CK1 δ negatively regulates the pathway by phosphorylating LEF1, thus disrupting the transcription factor complex (310).

One of the most important targets of the different CK1 isoforms is p53. The N-terminus of p53 can be efficiently phosphorylated at multiple sites by CK1 α , δ , and ϵ (317), leading to its stabilization by weakening the interaction with its inhibitor mouse double minute 2 (MDM2). Moreover, CK1 δ and ϵ phosphorylate MDM2, thus exacerbating the activating effect on p53. In addition, activated p53 induce the transcription of CK1 δ , thus establishing a positive feedback loop (313).

CK1 activity leads to anti-apoptotic effects, in many different ways. Indeed, CK1 α mediates the resistance to TRAIL (tumor necrosis factor related apoptosis inducing ligand) by phosphorylating members of the death-inducing signaling complex (DISC). CK1 α , δ , and ϵ and CK2 phosphorylate the pro-apoptotic protein BID, thus reducing its caspase 8-mediated cleavage. Additionally, CK1 α interacts with retinoid X receptor (RXR), thus interfering with the apoptosis process induced by retinoids.

Among the CK1 isoforms, CK1 δ has been shown to be implicated in cell cycle progression and mitotic spindle dynamics. Indeed, it is associated to microtubules and phosphorylates α , β , and γ tubulin, as well as microtubule associated proteins (MAP), and other regulatory proteins (tau and stathmin) in response to genotoxic stress, thus preventing genome instability. It is also associated to the centrosomes and to the kinetochores, thus controlling the proper chromosome segregation and cytokinesis (313). Indeed, CK1 δ/ϵ inhibitor IC261 induces centrosome amplification, ring-shaped centrosome formation, and multipolar mitosis; as a result, cells expressing wild type p53 are arrested in the G2/M phase, while p53-knockout cells pass over the checkpoint control and undergo duplication without division, developing micronuclei. Eventually, all of them die by apoptosis due to mitosis failure (318, 319). However, these findings are likely biased by the fact that IC261 has multiple off-target effects besides inhibiting CK1 δ/ϵ ; for example, it acts as a spindle poison (320), and this may explain why IC261 effects are similar to that of the spindle inhibitor nocodazole (318). However, more selective CK1 δ inhibitors similarly suppressed proliferation of colon cancer cell lines, by blocking cells in G2/M phase (321), and CK1 δ/ϵ potent and selective inhibitors, such as SR-3029, displayed significant anti-proliferative properties on a melanoma cell line (320).

In addition to CK1 δ role in microtubule dynamics, this enzyme has been shown to exert an effect on cell cycle progression also by interacting and regulating (and being regulated by)

proteins of the checkpoints. Indeed, CK1 δ expression increases as cell cycle progresses from G1/S to G2/M phase, in order to efficiently phosphorylate and lead to proteasomal degradation the tyrosine kinase Wee1, which is a negative regulator of Cdk1-cyclin B1, the checkpoint that controls the mitotic entry. CK1 δ/ϵ inhibitors (SR-653234 and SR-1277) are able to stabilize Wee1; as a result, the mitotic entry is delayed and cells accumulate in S and G2/M phases. CK1 δ and ϵ specific depletion by siRNA confirmed that the effect on Wee1 is exerted by CK1 δ (322). Moreover, CK1 δ is phosphorylated at its regulatory C-terminal domain by the checkpoint kinase Chk1. The latter is induced in response to DNA damage, and, by inhibiting CK1 δ , Chk1 arrests cell cycle to allow DNA repair or cell death (314).

CK1 involvement in the regulation of cell cycle progression and DNA-damage response, apoptosis, Wnt pathway, and p53 stabilization, sets the rationale for CK1 investigation in the field of cancer. Indeed, deregulation of CK1 isoforms might favor tumorigenesis by affecting multiple cellular functions. However, CK1 mutations seem to be rare in The Cancer Genome Atlas (TCGA) set of cancers. Additionally, the detected mutations do not accumulate in hotspots. Nonetheless, copy number variations are more frequently found, even though are still rare events. For example, in ovarian cancer, CK1 δ gene (CSNK1D) is amplified in about 4% of the cases reported and is much more rarely deleted, while point mutations are not recorded (Fig. 6.2) (310).

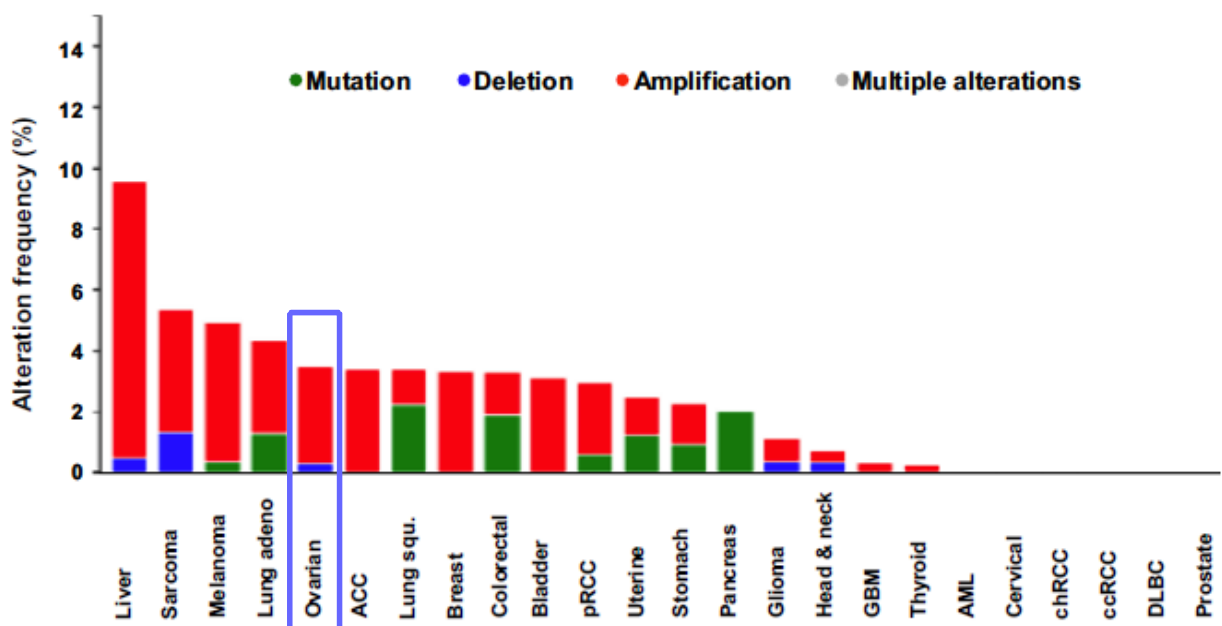


Figure 6.2. Mutational analysis of CSNK1D in 24 tumor types performed using the cBioPortal for Cancer Genomics accessing the TCGA datasets (310).

Expression of CK1 α is variable: high in cancers of the brain and prostate, in lymphoma and leukemia, lower in bladder cancer, lung cancer and melanoma. The case of melanoma is emblematic as CK1 α expression decreases as tumor progresses. In renal cancer, an enhanced CK1 γ 3 activity has been described, while in adenoid cystic carcinoma of the salivary gland and in pancreas ductal adenocarcinoma a high expression of CK1 ϵ was found (310, 313). In colorectal cancer, patients with higher CK1 ϵ expression have a prolonged survival (321); CK1 δ is overexpressed in cells of hyperplastic B cell follicles and B cell lymphomas in p53-deficient mice (323), as well as in human choriocarcinoma (319) and in pancreas ductal adenocarcinoma (310, 313, 324). In breast cancer, the situation is similar to that observed in melanoma: CK1 δ is strongly expressed in low grade carcinomas and is reduced in less differentiated cancers (313). Mutations in the CK1 ϵ gene were found in breast cancer; in colon adenoma, R324H mutations in the CK1 δ gene correlated with a high oncogenic potential (310). Forced expression of a dominant-negative mutant CK1 δ impairs SV40-induced transformation of mammary cells (320).

To sum up, CK1 α seems to act as a tumor suppressor, whereas CK1 δ and ϵ are either pro- or anti-tumorigenic depending on the cell context (310). Due to the different contribution of the CK1 isoforms in tumors, the development of CK1 δ and ϵ specific inhibitors to be used in the clinical practice is under investigation. The first ATP-competitive inhibitor developed was CKI-7, which is specific for CK1 in a micromolar range but does not have isoform selectivity and does not pass the plasma membrane. Later on, the more cell permeable and potent inhibitors IC261, D4476, and (R)-DRF053 were developed, but displayed some limitations, as they have either off-target effects or showed limited anti-proliferative activity in cell-based assays. As a result of a high throughput screening, SR-653234 and its analog SR-1277 were identified as highly selective CK1 δ/ϵ inhibitors, but were characterized by poor solubility and pharmacokinetic properties. Starting from the backbone of these molecules, Bibian *et al.* (320) developed several analogs and characterized them in order to individuate the best ones for CK1 δ/ϵ specificity, potency, anti-proliferative effect in cell-based assays, and pharmacokinetic properties for *in vivo* applications, and focused their attention on SR-2890 and SR-3029. Rosenberg *et al.* (325) tested SR-3029 on a highly CK1 δ -expressing breast cancer cell line *in vitro* and in a xenograft model generated from this line *in vivo*, and found that SR-3029 treatment impaired the colony-forming capacity, triggered apoptosis *in vitro* and provoked tumor growth inhibition or even regression *in vivo*. However, in order to dissect if the observed effects can be ascribed to CK1 δ or CK1 ϵ inhibition, it is still necessary to compare the specific CK1 δ and CK1 ϵ knockdown by selective siRNA or shRNA (320). Thus, while waiting for the

development of molecules that selectively inhibit either CK1 δ or CK1 ϵ (a hard task, since the two isoforms are almost identical in their kinase domain and, overall, highly homologous), the genetic silencing is still the only way to study the roles of these kinases.

The present thesis work will focus specifically on the CK1 family, and in particular on CK1 δ .

Chapter 7

AIM OF THE THESIS

The present thesis is the result of my three year-PhD work in Prof. Amadori's lab. During these years, I investigated multiple aspects of EOC biology: autophagic regulation of CSC, microenvironment contribution to CSC maintenance, and CK1 δ pro-tumorigenic role.

EOC is the fifth leading cause of cancer-related death among females, and the first cause of death if considering only the gynecological malignancies (10). This lethality is mainly due to the lack of specific symptoms and of an effective screening program; as a result, EOC is usually diagnosed at advanced stages (52). EOC is often considered chemosensitive, with a response rate higher than 80% after first-line treatment. However, about 70% of patients relapse within 18 months (63). The cause of this frequent relapse rate after an apparent treatment success could be ascribed to a tiny subpopulation of cancer cells, named cancer stem cells (95). Our group (182) and others (223, 233) demonstrated that EOC CSC can be identified by the coexpression of CD44 and CD117. It has been hypothesized that CSC are responsible for tumor establishment, outgrowth, therapy resistance, and metastasis. Thus, a successful treatment should include a target agent for CSC eradication (96).

Recent studies have revealed metabolic reprogramming as a new hallmark of cancer (326). Among the catabolic pathways, autophagy is a process of lysosomal degradation of self-components, whose role in cancer depends on tumor stage. Indeed, in the early stages of tumorigenesis, it has an anti-cancer effect by preventing the accumulation of defective organelles, while, as tumor progresses, it seems to be a survival mechanism that counteracts the damage induced by chemotherapy or nutrient starvation (287). In the last decade, autophagy has also been identified as a survival mechanism potentially exploited by CSC. Indeed, high autophagy levels have been detected in CSC from solid and hematologic malignancies (295). Here, we decided to evaluate autophagy activation and the effects of its perturbation in CSC from EOC ascites and PDX.

The CSC marker CD117, or c-Kit, is a tyrosine kinase receptor, whose ligand is stem cell factor (SCF). SCF exists both as a soluble cytokine and as a transmembrane protein (327), and it is produced mainly by fibroblasts and endothelial cells (257). The SCF/c-Kit axis plays a key role in hematopoiesis and melanogenesis (252). Moreover, SCF and c-Kit have been demonstrated to play a role in cancer, in particular in GIST, where imatinib (Bcr-Abl, PDGFR and c-Kit inhibitor) is a therapeutic option (253). Since stemness is a cellular intrinsic property as well as

a result of extrinsic stimuli from the tumor microenvironment (197), we decided to investigate SCF production in primary samples of EOC ascites, and its effect on CD117⁺ cells.

Besides CSC, EOC cancer cells are also sustained by pro-tumorigenic protein activation. Casein kinase 1 is a family of evolutionary conserved serine/threonine kinases involved in many cellular functions. We focused on CK1 δ because its amplification rate in ovarian cancer is about 4% (310). Moreover, CK1 δ inhibition in a variety of tumor cell lines of different origin induced cell cycle arrest and apoptosis (318), and its silencing or inhibition slowed breast cancer growth *in vivo* (325). Thus, we evaluated the effects of CK1 δ knockdown on OVCAR3 and IGROV1 cell lines both *in vitro* and *in vivo*.

Chapter 8

MATERIALS AND

METHODS

8.1. EOC primary samples, cell lines, and *in vitro* culture

This study was approved by the Institutional Ethics Committee for patient studies, according to the Declaration of Helsinki. After obtaining written informed consent, 51 patients diagnosed with EOC entered this study; all the patients had received chemotherapy prior to sampling.

Cells were isolated from ascitic effusions of EOC-bearing patients by centrifugation (1,300 rpm, 6 minutes), as reported elsewhere (182), whereas the liquid phase was stored at -80°C for subsequent enzyme-linked immunosorbent assay (ELISA). After red blood cell osmotic lysis, cells were maintained in RPMI-1640 medium (Euroclone, Milan, Italy), supplemented with 10% fetal bovine serum (FBS; GIBCO, Thermo Fisher Scientific, Waltham, MA), 1% Penicillin/Streptomycin (Lonza, Basel, Switzerland), 1% sodium pyruvate (Lonza), and 1% Ultraglutamine (Lonza). Cells were cultured at 37°C, 5% CO₂, and harvested at confluence using trypsin-EDTA (GIBCO).

OVCAR3 and IGROV1 ovarian cancer cell lines, embryonic kidney HEK293T cells, and human B-lymphoma RAJI cells were purchased from ATCC (Manassas, VA). Acute myeloblastic leukemia KASUMI1 cells were kindly provided by Dr Francesco Piazza, (Venetian Institute of Molecular Medicine VIMM, Padova, Italy). OVCAR3 and IGROV1 cells were cultured in the same conditions as primary samples. HEK293T were cultured in DMEM medium (Euroclone) supplemented as described before. RAJI cells were cultured in suspension in RPMI-1640 medium supplemented as described before. KASUMI1 cells were cultured in suspension in RPMI-1640 medium, supplemented with 20% FBS, 1% Penicillin/Streptomycin, 1% sodium pyruvate, and 1% Ultraglutamine.

For spheroid culture, cells from primary samples or PDX were seeded in poly-2-hydroxyethyl methacrylate (PhEMA, Sigma Aldrich, St Louis, MO)-coated, non-tissue culture treated six-well plates (Corning, New York, NY), at the density of 5×10^4 cells/well (242) in serum-free DMEM/F12 medium (GIBCO) supplemented with 1% Penicillin/Streptomycin, 1% Ultraglutamine, bovine serum albumin (BSA, 4 mg/mL; Sigma Aldrich), bFGF (20 ng/mL; Peprotech, Rocky Hill, NJ), EGF (20 ng/mL; Peprotech), insulin (5 µg/mL, Sigma Aldrich), heparin (0.625 U.I/mL, PharmaTex, Milan, Italy), and B27 (GIBCO). Medium was replaced every 7 days, and after 2 weeks cells were harvested for subsequent analysis.

Pictures of OVCAR3 cells and of spheroids were taken with a Leica DM IL LED microscope (Wetzlar, Germany). Spheroid diameter was measured using ImageJ software (328).

8.2. Lentiviral vector production and cell transduction

For CK1 δ gene (CSNK1 δ) knockdown, MISSION[®] TRC shRNA bacterial glycerol stocks transformed with plasmids encoding short hairpin RNA (shRNA) targeting human CSNK1 δ (sh599, sh1552) or a scramble sequence (shCTRL) as a control were purchased from Sigma-Aldrich.

Cells expressing the firefly luciferase (Fluc) gene were generated to perform *in vivo* imaging. The plasmid (pHR'EF-Fluc-WSIN) was kindly provided by Dr. Takeya Sato (University of Toronto, Canada).

For membrane-associated SCF overexpression, pLenti-C-mGFP-P2A-Puro plasmid encoding GFP-tagged human KIT ligand, transcript variant “a”, as well as the empty vector, were purchased from OriGene Technologies (Rockville, MD). One Shot[™] Stbl3[™] chemically competent *E. coli* (Invitrogen, Thermo Fisher Scientific) were transformed by heat shock and chloramphenicol-selected (Sigma Aldrich).

Bacteria were cultured in LB broth (Sigma Aldrich), and plasmids were purified by Plasmid Maxi Kit (Qiagen, Hilden, Germany), as per manufacturer's instructions.

Lentiviral vector stocks were generated by a transient three-plasmid vector packaging system. Briefly, HEK293T cells were co-transfected with VSV-G construct (pHCMV-G, kindly provided by Prof. Volker Erfle, Institut für Molekulare Virologie, Neuherberg, Germany), pCMVR8.74 (Addgene plasmid #22036, gift from Didier Trono, École Polytechnique Fédérale de Lausanne, Lausanne, Switzerland), and the plasmid of interest. Lentiviral particles were obtained by ultra-centrifugation of cell supernatants (24,000 rpm for 2 hours).

For CSNK1 δ knockdown in OVCAR3 and IGROV1 cells, concentrated virus-containing supernatant was incubated with target cells, previously seeded into six-well plates at 1.5×10^5 cells/well. After overnight incubation, the supernatant was replaced with complete medium. After 48h, cells were puromycin-selected (1 μ g/mL, Sigma Aldrich).

For Fluc expression, shCTRL, sh599, and sh1552 OVCAR3 cells were transduced as described above. To determine bioluminescence intensity, 5×10^5 cells were seeded in black 96-well microplates (Perkin Elmer, Waltham, MA), incubated with D-luciferin (150 ng/mL, Perkin Elmer) or PBS alone as negative control, and subjected to bioluminescence analysis with IVIS Imaging System (Xenogen Corporation, Alameda, CA).

For SCF overexpression, RAJI cells were subjected to spinoculation: briefly, 1,000,000 cells were seeded in 24-well plates with concentrated vector-containing supernatant, centrifuged at 2,400 rpm for 2 hours, and incubated overnight. Then, the supernatant was replaced with

complete medium. After 48h, cells were puromycin-selected. Empty vector-transduced RAJI cells were named CTRL-RAJI; RAJI cells expressing membrane SCF were named SCF-RAJI.

8.3. PDX generation and *in vivo* experiments

Non-Obese Diabetic/Severe combined immunodeficiency (NOD/SCID) and NOD/SCID gamma (NSG) mice were obtained from internal breeding. Procedures involving animals and their care were performed according to institutional guidelines that comply with national and international laws and policies (EEC Council Directive 86/609, OJ L358, 12 December 1987). PDX were generated by injecting NOD/SCID mice intraperitoneally (i.p.) with 10^6 tumor cells derived from ascitic effusions of EOC-bearing patients.

For autophagy project *in vivo* experiments, 5×10^5 PDX cells were injected s.c. in 200 μ l of Matrigel® (Corning) in both dorsolateral flanks of NSG mice. When tumors reached 100 mm³ volume, mice were randomized in four groups, and treated i.p. with chloroquine (100 mg/kg every 2 days), carboplatin (50 mg/Kg weekly), both drugs, or with equal saline amounts as a control. Tumor size was measured using a caliper. Mice were sacrificed when the tumors of the control group reached a volume of 600–800 mm³. Tumors were harvested, smashed on a 100 μ m cell strainer, and after red blood cell lysis cells were collected for subsequent flow cytometry analysis.

For CK1 δ project *in vivo* experiments, 1×10^6 OVCAR3 and IGROV1 cells transfected with different constructs (shCTRL, sh599, sh1552) were injected subcutaneously (s.c.) in 200 μ l of Matrigel® in both dorso-lateral flanks of NSG mice, and the growth rate of the tumors was monitored by caliper measurements. Mice were sacrificed when the tumors of the shCTRL group reached 600-800 mm³ volume. Tumors were snap-frozen in liquid nitrogen and homogenized with a T18 basic Ultra-Turrax® disperser (Ika, Staufen im Breisgau, Germany) in RIPA buffer.

For lung colonization assay, 1×10^6 shCTRL, sh599, and sh1552 Fluc-OVCAR3 cells were injected into the tail vein of NOD/SCID mice. At 2 and 24 hours after cell injection, mice received 200 μ L of D-luciferin (15 mg/mL) i.p. for 8 minutes. Then, mice were sacrificed and lungs harvested and subjected to bioluminescence analysis with IVIS Imaging System, as previously described (162).

8.4. Extreme limiting dilution assay (ELDA)

To determine the frequency of spheroid-forming cells, EOC primary cells or PDX cells were counted and plated at different concentrations in 96-well flat-bottom ultra-low attachment PhEMA-coated plates (Corning) in a total volume of 0.1 ml of serum-free DMEM/F12 medium supplemented with 1% Penicillin/Streptomycin, 1% Ultraglutamine, BSA, (4 mg/mL), bFGF (20 ng/mL), EGF (20 ng/mL), insulin (5 µg/mL), heparin (0.625 U.I/mL), and B27. Fifteen replicate wells were set up for each cell concentration. After a week of incubation, the wells were scored for spheroid formation; the frequency of spheroid-forming precursors in each population was calculated by ELDA web tool (329). Data are expressed as the number of spheroid-forming cells/10³ cells.

8.5. Flow cytometry analysis and FACS-sorting

Cells were labeled with the anti-human antibodies listed in Table 8.1.

| Antibody | Fluorochrome | Dilution | Staining | Brand |
|---|--------------|----------|---------------|---|
| CD45 | FITC | 1:10 | Membrane | Miltenyi Biotec (Bergish Gladbach, Germany) |
| CD44 | PE-Cy7 | 1:1,000 | Membrane | Abcam (Cambridge, UK) |
| CD117 (non-activating AC126 clone) | PE | 1:10 | Membrane | Miltenyi Biotec |
| CD14 | APC | 1:20 | Membrane | Biolegend (San Diego, CA) |
| CD90 | PE | 1:200 | Membrane | BD Bioscience (Franklin Lakes, NJ) |
| CD3 | PerCP | 1:20 | Membrane | Miltenyi Biotec |
| CD19 | FITC | 1:10 | Membrane | Biolegend |
| Ki67 | FITC | 1:10 | Intracellular | BD Bioscience |
| Phospho Akt | Unconjugated | 1:100 | Intracellular | Cell Signaling Technology (Boston, MD) |
| SCF | Unconjugated | 1:50 | Intracellular | Thermo Fisher Scientific |

Table 8.1. Anti-human antibodies used for flow cytometry applications.

Live/Dead (1:600; Molecular Probes, Thermo Fisher Scientific) labelling was used to discriminate living cells. After adding the antibodies, the cells were incubated for 30 minutes at 4°C.

For intracellular staining, cells were fixed with 4% paraformaldehyde (PFA) (Sigma-Aldrich), followed by permeabilization with Triton X-100 0.1% (Sigma-Aldrich) and blocking with a

PBS/5% BSA solution. The secondary antibodies (Alexa Fluor, 1:500, Invitrogen, Thermo Fisher Scientific) were added for 30 minutes at 4°C.

All the flow cytometry analyses were performed using a FACS LSRII (BD Bioscience, Franklin Lakes, NJ); data were collected from at least 1×10^5 cells/sample and elaborated with FlowJo software (TreeStar, Ashland, OR).

FACS-sorting was performed with a MoFlo Astrios cell sorter (Beckman Coulter, Brea, CA). The purity of the sorted population always exceeded 90%.

For the identification of the ascitic populations, the following gating strategies were used:

- viable cells were identified as Live/Dead negative cells;
- CD45-positive cells identify cells of lympho-myeloid origin;
- among CD45⁺ cells, tumor-associated macrophages (TAM), T-, and B-lymphocytes were selected as CD14⁺, CD3⁺, and CD19⁺, respectively;
- among CD45⁻ cells, tumor-associated fibroblasts (TAF), CSC and noCSC were selected as CD90⁺, CD44⁺CD117⁺, and CD44⁺CD117⁻, respectively;
- among each cell population, the percentage of SCF⁺ cells was reported.

For intracellular autophagosome staining, EOC and PDX cells were first labeled with CD44 and CD117 antibodies. Then, cells were incubated for 30 minutes at room temperature with Cyto-ID reagent (1:2,000; Cyto-ID[®] Autophagy detection kit, Enzo Life Sciences, Lörrach, Germany). Prior to analysis, cells were resuspended in Cyto-ID assay buffer. Signal mean fluorescence intensity (MFI) = $MFI_{\text{stained cells}} - MFI_{\text{unstained control}}$.

For combination index (C.I.) analysis, cells from EOC primary samples or PDX were treated with different doses of chloroquine (10, 20, and 50 μM) and carboplatin (10, 20, and 50 $\mu\text{g/mL}$) and their combination; after 72 h cell viability was evaluated by Annexin-V-FLUOS/Propidium Iodide staining (1:50, Roche, Basel, Switzerland) and data were subjected to automatic calculation of C.I. using CompuSyn software (330). $CI < 1$, $CI = 1$, and $CI > 1$ indicate synergism, additivity, and antagonism, respectively.

For *ex vivo* analysis of tumors harvested at the end of the autophagy *in vivo* experiment, cells were Live/Dead stained and labeled with CD44, CD117, and Ki67 antibodies. Ki67 positivity was recorded within the CD44⁺CD117⁺ population.

For SCF-induced pAkt determination, KASUMI1 cells were either treated with human recombinant SCF (hrSCF, 50 ng/mL) for 5 minutes, or cocultured with CTRL-RAJI or SCF-RAJI cells for 5 minutes in 50 μL of medium in round bottom 96-well plates. For cocultures, a 10:1 RAJI:KASUMI1 ratio was chosen. Before stimulation, KASUMI1 cells were pretreated or not with imatinib (30 μM , Sigma Aldrich) for 1h 30 min at 37 °C. Cells were then fixed in

cold methanol 100%, permeabilized with Triton X-100 0.1%, blocked with FcR blocking reagent (1:5, Miltenyi Biotec). Cells were then stained with anti-phospho Akt antibody (1:33 for coculture experiment), followed by Alexa Fluor 546 goat anti-rabbit secondary antibody. P-Akt Signal MFI was recorded within the GFP-negative population.

For apoptosis assays, sh599, sh1552, and shCTRL OVCAR3 and IGROV1 cells treated for 72h with different doses of carboplatin were incubated for 15 minutes at room temperature with Annexin-V-FLUOS (1:50, Roche).

8.6. Western blotting (WB)

Cells were lysed with RIPA buffer supplemented with protease and phosphatase inhibitors. Protein concentration was determined by using the bicinchoninic acid (BCA) assay (Quantum Micro Protein, Euroclone). Equal protein amounts were loaded on NuPAGE™ 4-12% Bis-Tris protein precast polyacrylamide gels (Invitrogen, Thermo Fisher Scientific) in denaturing and reducing conditions. Proteins were then transferred onto nitrocellulose membranes (Perkin Elmer). Membranes were saturated with 5% non-fat milk in TBS-Tween 20 buffer, and hybridized with primary antibodies overnight at 4 °C. Primary antibodies were diluted either in 5% milk or in 5% BSA in TBS-Tween 20 buffer, depending on manufacturer's instructions. The primary antibodies used are listed in Table 8.2.

| Antibody | Species | Dilution | Brand |
|-------------------------------|---------|----------|---------------------------|
| LC3B | Rabbit | 1:1,000 | Cell Signaling Technology |
| p62 | Rabbit | 1:1,000 | Genetex (San Antonio, TX) |
| SCF | Rabbit | 1:1,000 | Peprtech |
| phospho c-Kit (Tyr719) | Rabbit | 1:1,000 | Cell Signaling Technology |
| c-Kit | Mouse | 1:1,000 | Cell Signaling Technology |
| phospho Akt (Ser473) | Rabbit | 1:2,000 | Cell Signaling Technology |
| pan Akt | Rabbit | 1:1,000 | Cell Signaling Technology |
| CK1δ | Mouse | 1:5,000 | Abcam |
| p21 Waf1/Cip1 | Rabbit | 1:1,000 | Cell Signaling Technology |
| α-tubulin | Mouse | 1:4,000 | Sigma Aldrich |
| β-actin | Mouse | 1:1,000 | Abcam |

Table 8.2. Primary antibodies used for WB applications.

Secondary horseradish peroxidase (HRP)-conjugated anti-rabbit or anti-mouse antibodies (Perkin Elmer), diluted 1:5,000 in 1% milk in TBS-Tween 20 buffer, were added for 1h at room temperature. Finally, the chemiluminescence signal was detected with Western Lightning® Plus-ECL (Perkin Elmer) on a ChemiDoc™ XRS Imaging System (Bio-Rad, Hercules, CA),

and band densitometry was analyzed by Quantity One[®] software (Bio-Rad). Signal intensity was normalized either to α -tubulin or β -actin housekeeping proteins.

8.7. RNA extraction, reverse transcription, and quantitative RT-PCR

Total RNA was extracted following the TRIzol method (Ambion, Thermo Fisher Scientific) according to manufacturer's instruction, as previously described (162). cDNA was synthesized from 1 μ g of total RNA using the High capacity RNA-to-cDNA kit (Applied Biosystems, Thermo Fisher Scientific), then it was mixed with the gene-specific primers and Platinum[™] SYBR[™] Green qPCR SuperMix-UDG (Invitrogen, Thermo Fisher Scientific); each sample was run in duplicate. The PCR step was performed on ABI PRISM[®] 7900HT Sequence Detection System (Applied Biosystems, Thermo Fisher Scientific). Results were analyzed using the comparative $\Delta\Delta$ Ct method; $\Delta\Delta$ Ct values were utilized to calculate the fold change = $2^{-\Delta\Delta$ Ct}. Data were expressed as the fold difference in gene expression (normalized to the housekeeping β 2-microglobulin gene) relative to a reference sample, as indicated in the figure legends. Primer sequences are listed in Table 8.3.

| Gene Name | Forward | Reverse |
|---------------------------------|------------------------------|------------------------------|
| β2micro | 5'-TCTCTCTTTCTGGCCTGGAG-3' | 5'-TCTCTGCTGGATGACGTGAG-3' |
| NANOG | 5'-CCAAAGGATGAAGTGCAAGC-3' | 5'-CAAGTTGGGTGGTCCAAGT-3' |
| SOX2 | 5'-CCGCGTCAAGAGGCCCATGAA-3' | 5'-CCCGCTTCTCGGTCTCGGACAA-3' |
| OCT4 | 5'-TGGCGTGGAGACTTTGCA-3' | 5'-GGTCCCTCTGAGTTGCTTC-3' |
| CD117 | 5'-GGATTCCCAGAGCCACAAT-3' | 5'-GGCAGTACAGAAGCAGAGCA-3' |
| LC3 | 5'-AGACCTTCAAGCAGCGCCG-3' | 5'-ACACTGACAATTTTCATCCCG-3' |
| SCF 248 | 5'-CCATTGATGCCTTCAAGGAC-3' | 5'-TGGCCTTCCTATTACTGCTACT-3' |
| SCF 220 | 5'-CTGAGAAAGGGAAGGCCAA-3' | 5'-GGCTCCAAAAGCAAAGGCCAA-3' |
| IL1β | 5'-TGAAAGCTCTCCACCTCCAG-3' | 5'-GCCCAAGGCCACAGGTATTT-3' |
| TNF | 5'-GGACCTCTCTAATCAGCC-3' | 5'-GGGTTTGCTACAACATGGGC-3' |
| CCL22 | 5'-GAAACACTTCTACTGGACCTCA-3' | 5'-AATCATCTTCACCCAGGGCA-3' |
| IL10 | 5'-TGCTGGAGGACTTTAAGGGT-3' | 5'-CGCCTTGATGTCTGGGTCTT-3' |
| CSNK1D | 5'-GCCCTAGTTATCGTAACAG-3' | 5'-CGCCAATAAAGAGTCTGTCA-3' |

Table 8.3. Primers used for qRT-PCR. All the oligonucleotides were purchased from Sigma Aldrich.

8.8. PBMC purification, monocyte isolation, and macrophage differentiation and polarization

Peripheral blood mononuclear cells (PBMC) were isolated by density gradient centrifugation on Ficoll-Paque (GE Healthcare, Chicago, IL) from healthy donor buffy coats. Monocytes were purified from PBMC using Pan Monocyte Isolation Kit on LS Separation columns (Miltenyi-

Biotech). Monocytes were cultured at a density of 1×10^6 cells/mL for 7 days in FBS-coated dishes in RPMI-1640 medium supplemented with 20% FBS, in the presence of granulocyte-macrophage colony-stimulating factor (GM-CSF, 100 ng/mL, Peprotech) for differentiation into M0 macrophages. Subsequently, M0 macrophages were stimulated with LPS (100 ng/mL; Sigma Aldrich) and IFN γ (20 ng/mL; Peprotech) for M1 polarization, and with IL4 (20 ng/mL; Peprotech) and IL13 (20 ng/mL; Peprotech) for M2 polarization, in RPMI-1640 medium supplemented with 5% FBS, as reported elsewhere (331). After 24 h and 48 h, the conditioned medium was collected, 50-fold concentrated with Amicon[®] Ultra-15 centrifugal filter units (Merck Millipore, Sigma Aldrich) and stored at -80°C for subsequent ELISA analysis, while cells were harvested for flow cytometry, Western blot and RNA extraction. M1 and M2 polarization was confirmed by qRT-PCR analysis of M1 (IL1 β and TNF) (332) and M2 (CCL22 and IL10) marker (333) expression.

8.9. Enzyme-linked immunosorbent assay (ELISA)

Ex vivo ascitic liquid phases, concentrated conditioned media from M0, M1, and M2 polarized macrophages and FACS-separated CD44⁺CD117⁺ (CSC), CD44⁺CD117⁻ (noCSC), CD90⁺ (TAF), CD14⁺ (TAM), CD3⁺ (T cells), and CD19⁺ (B cells) ascitic cell population supernatants were tested for soluble SCF production with a Human SCF Quantikine[®] ELISA Kit (R&D, Minneapolis, MN), according to manufacturer's instructions. For all the different cell subtypes, cells were plated at a concentration of 1×10^6 cells/mL and medium was collected after 24 h of culture.

8.10. Proliferation assay

shCTRL, sh599, and sh1552 OVCAR3 and IGROV1 cells were plated in triplicate in four 24-well plates at 5,000 cells/well. Cells were fixed with 4% PFA after overnight culture (day 0) and after 1, 2, and 3 days, and crystal violet-stained (Sigma Aldrich), as reported elsewhere (334). Crystal violet was solubilized in 1% sodium dodecyl sulfate (SDS), and the absorbance was measured at 595 nm using the plate reader Victor[™] X4 (Perkin Elmer). The absorbance values were normalized on the corresponding day 0.

8.11. *In vitro* migration assays

shCTRL, sh599, and sh1552 OVCAR3 and IGROV1 cell migratory capacity was determined *in vitro* both by wound healing and by transwell migration assays, as previously described (335).

For wound healing assay, confluent cells were scratched with a p200 pipet tip. Wells were washed to remove detached cells, and medium was replaced with serum-free RPMI-1640, to exclude proliferation related effects. At time 0 and after 24 and 48 h, pictures of the wounded area were taken with Leica DM IL LED microscope. The distance between scratch edges was quantified using ImageJ software.

For transwell migration assay, 5×10^4 cells resuspended in 200 μ L of RPMI-1640 supplemented with 0.2% FBS were seeded into 8 μ m pore cell culture insert (migration chambers, Falcon, Corning) in 24-well plates. Wells were filled with 800 μ L of RPMI-1640 medium containing 20% FBS, and cells were incubated at 37°C. After 18 hours, cells that had not crossed the membrane were removed with a cotton swab, and inserts were fixed with 4% PFA. Cells on the bottom of the membrane were stained with crystal violet. Images of five fields per insert were taken with a Leica DM IL LED microscope and the area covered by migrated cells was quantified using ImageJ software.

8.12. Statistical analysis

Data from replicate experiments were shown as mean values \pm Standard Deviation (SD). Comparisons between groups were done by the two-tail Student's t-test and Mann-Whitney test, as appropriate. Association between CD44⁺CD117⁺ percentage and EOC tumor histotype, stage, or grade was assessed by χ^2 test. Association between SCF concentration and EOC tumor histotype, stage, or grade was assessed by Kruskal-Wallis test or Mann-Whitney test, as appropriate. Statistical analyses were performed by using the Sigmaplot software (Systat Software, San Jose, CA).

Chapter 9

RESULTS

According to the experimental pathway followed during my PhD course, the results are divided into three major parts:

- 1) Autophagy inhibition reduces chemoresistance and tumorigenic potential of ovarian CSC;
- 2) SCF is abundant in EOC ascites, it is produced by fibroblasts and macrophages, and it activates the downstream pathway in CD117⁺ cells;
- 3) CK1 δ plays a role in the regulation of cell proliferation, response to chemotherapy and migration in ovarian cancer cells.

Fifty-one ascitic effusions from EOC bearing patients with different histotypes (serous, mucinous, endometrioid, and clear cell/undifferentiated carcinoma), staging (advanced stages 3A, 3B, 3C, and 4) and grading (G1, G3, and G4) were collected and analyzed for both the autophagy and the SCF studies. Forty ascitic effusions were analyzed by flow cytometry to evaluate the CSC content using CD44 and CD117 as stemness markers. We found that the percentage of CD44⁺CD117⁺ cells ranged between 0.62 and 12.6%, with no significant association with tumor histotype, stage, or grade. Sample features are summarized in Table 9.1. The liquid phases of thirty-two ascitic effusions were analyzed for SCF content (see paragraph 9.2.1).

For CK1 δ , experiments were performed on two EOC cell lines, OVCAR3 and IGROV1.

| | N (% of total) | %CSC (range) | P value |
|-----------------------------|----------------|-----------------------|---------|
| Histotype | | | NS |
| Serous | 36 (90) | 2.05±2.0 (0.62-12.6) | |
| Mucinous | 1 (2.5) | 1.18 (-) | |
| Clear cell/undifferentiated | 3 (7.5) | 2.5±1.01 (1.5-3.50) | |
| Stage | | | NS |
| 3A | 1 (2.5) | 2.69 (-) | |
| 3B | 4 (10) | 1.29±1.6 (1.28- 4.24) | |
| 3C | 24 (60) | 1.59±0.5 (0.62- 2.50) | |
| 4 | 11 (27.5) | 2.8±3.3 (0.8-12.6) | |
| Grade | | | NS |
| G1 | 3 (7.5) | 2.05±1.2 (1.44- 3.53) | |
| G3 | 37 (92.5) | 2.05±1.2 (1.44- 3.53) | |
| Total | 40 (100) | | |

Table 9.1. Clinical characteristics of EOC-bearing patients and association with the percentage of CSC (NS=not significant, χ^2 test).

9.1. Autophagy inhibition reduces chemoresistance and tumorigenic potential of ovarian CSC

9.1.1. Ovarian CD44⁺CD117⁺ CSC display higher basal autophagy compared to bulk tumor cells

Autophagy is invariably associated with conversion of LC3-I to LC3-II by lipidation. We analyzed by Western blotting the LC3-II/LC3-I ratio in FACS-sorted CD44⁺CD117⁺ (CSC) and CD44⁺CD117⁻ (non-CSC) cells. To evaluate the autophagic flux, we took advantage of the autophagy inhibitor bafilomycin A1 (BafA1). As shown in Figure 9.1 A, CSC presented a more active basal autophagy compared to non-CSC, as represented by the significantly higher *ex vivo* levels of LC3-II in basal conditions. Treatment with BafA1 induced in both populations an increase in LC3-II, thus demonstrating that the autophagic flux was present and excluding that the higher LC3-II levels were due to a block of the pathway in the CD44⁺CD117⁺ fraction. However, the autophagic flux (calculated as LC3-II ratio between BafA1-treated and untreated cells) did not show any significant difference in the two cell subsets (Fig. 9.1 B).

Real-Time PCR did not highlight any difference in LC3 mRNA between CSC and non-CSC, indicating that the higher protein levels of LC3-II were not due to gene upregulation in CSC but rather to enhanced autophagic activity (Fig. 9.1 C).

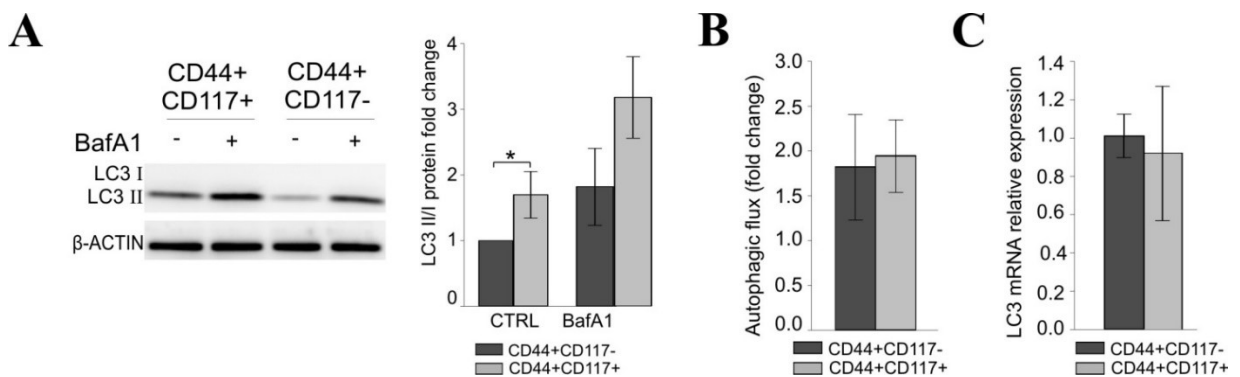


Figure 9.1. WB analysis of LC3-II/LC3-I ratio in FACS-sorted CD44⁺CD117⁺ and CD44⁺CD117⁻ cells either treated with 100 nM BafA1 for 2h or left untreated. Signals were normalized to actin. The graph on the right shows mean expression ratios \pm S.D. (n=4). *P<0.05 (A). The autophagic flux calculated dividing LC3-II normalized signal intensity of BafA1-treated cells by the signal intensity of untreated cells for each cell subpopulation. The bars represent mean \pm S.D. (n=4) (B). qRT-PCR analysis of LC3 mRNA expression in each cell subpopulation. Mean relative expression values in CD44⁺CD117⁺ cells compared to CD44⁺CD117⁻ cells (\pm S.D., n=4) are shown (C).

The different basal autophagy activation between CSC and non-CSC was confirmed by protein level analysis of p62/SQSTM1. When autophagy was inhibited, p62 levels increased, making it a useful marker for the autophagic flux. Results indicated that CSC presented significantly lower levels of p62 compared to the non-CSC counterpart, *i.e* a higher autophagic activity (Fig. 9.2).

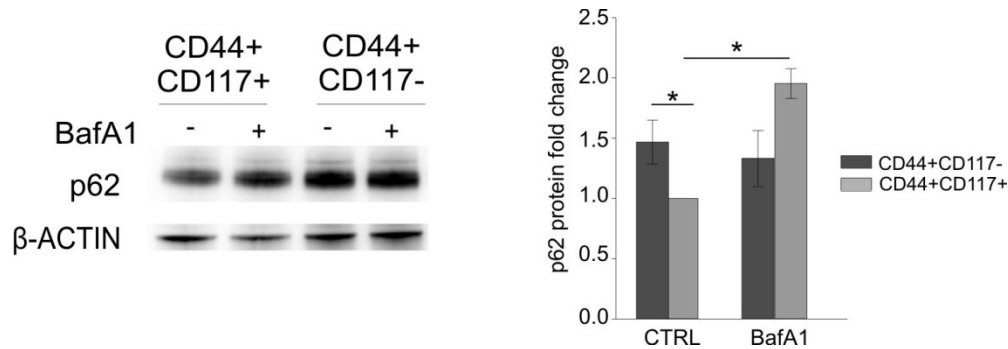


Figure 9.2. WB analysis of p62 protein expression in FACS-sorted CSC and non-CSC either treated with BafA1 or left untreated. Signals were normalized to actin. The graph on the right represents mean expression ratios \pm S.D. (n=4). *P<0.05.

Autophagic activity was also analyzed by intracellular autophagosome staining by Cyto-ID[®] autophagy detection kit and quantified by flow cytometry. The obtained results confirmed a significantly higher autophagic activity in CSC (Fig. 9.3).

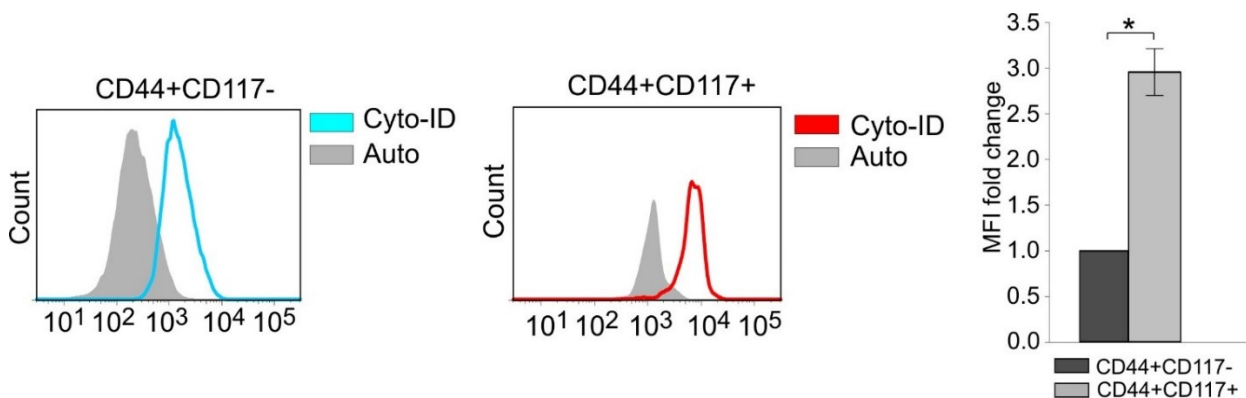


Figure 9.3. Flow cytometry analysis of autophagic activity in CSC and non-CSC. Cells were labeled with anti-CD44, anti-CD117 antibodies and Cyto-ID[®] Autophagy detection kit. One representative experiment is shown (left panel). The graph represents the mean fluorescence intensity (MFI) \pm S.D. (n=7) (right panel). *P<0.05. Auto = unstained cells; Cyto-ID = stained cells.

We next took advantage of a spheroid-formation assay as a model to further study the autophagic flux in ovarian CSC-enriched population. Cancer cells obtained from primary EOC

samples and PDX were cultured for two weeks in spheroid-forming conditions. The enrichment in CSC was measured by evaluating the mRNA expression levels of CD117 in cells maintained in normal (adhesion) and in stem cell culture conditions (spheroids) (Fig. 9.4).

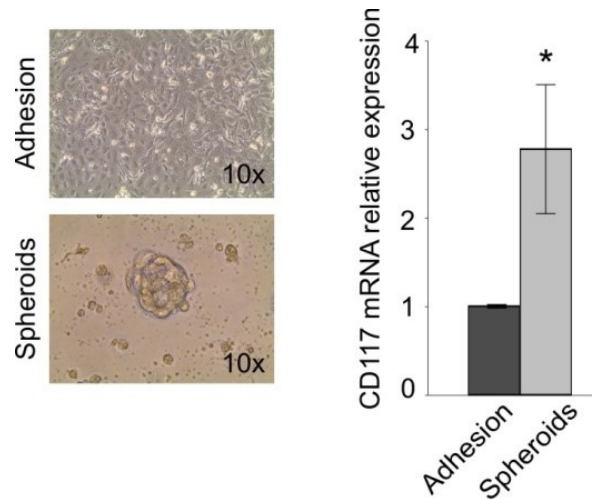


Figure 9.4. EOC primary and PDX cells were analyzed by qRT-PCR for the expression of CD117. On the left, a representative picture of a sample in adherent and spheroid conditions. On the right, the bars represent the mean relative expression values (\pm S.D., $n=4$) in samples cultured in spheroid-forming conditions compared to the same samples cultured in adherent conditions. * $P<0.05$.

All cell cultures were treated with BafA1, and LC3-II protein levels compared to the corresponding untreated samples were assessed. As demonstrated in FACS-sorted CSC, also the CSC-enriched spheroids presented higher basal autophagy compared to the adherent counterpart (Fig. 9.5 A). The autophagic flux, instead, was again comparable in adherent cells and spheroids (Fig. 9.5 B).

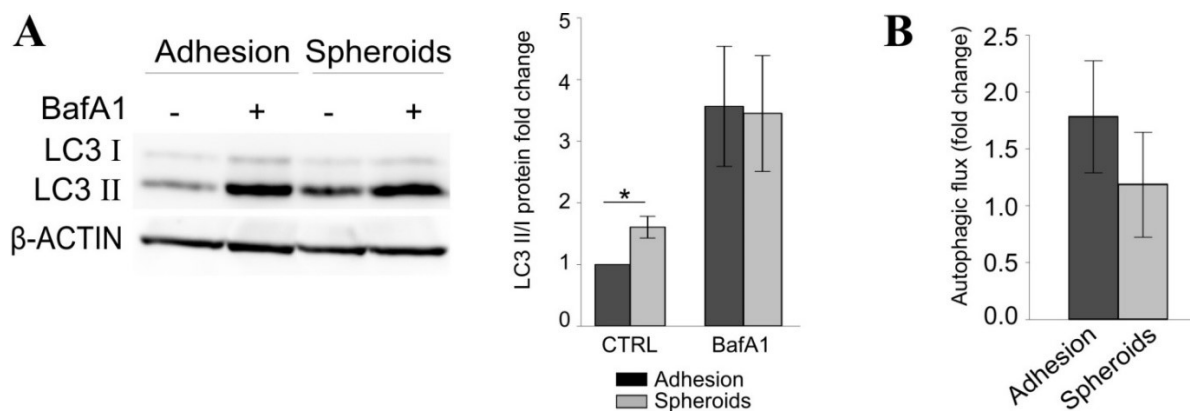


Figure 9.5. WB analysis of LC3-II/LC3-I ratio in adherent cells vs spheroids either treated with BafA1 or left untreated. Signals were normalized to actin. The graph shows mean expression ratios \pm

Figure 9.5. (continued) S.D. (n=4). *P<0.05 (A). Autophagic flux was calculated as in Fig. 9.1 B. The bars represent the mean \pm S.D. (n=4).

Altogether, these experiments indicate that both *ex vivo* derived and PDX-derived ovarian CSC show a prominent autophagic activity, compared to the non-CSC counterpart.

9.1.2. Inhibition of autophagy affects canonical CSC properties

The interconnection between autophagy and maintenance of the CSC phenotype was further investigated by culturing EOC cells in CSC-enriched spheroid culture for two weeks. The cells were then treated with different concentrations of the autophagy inhibitor chloroquine for 72h. In parallel, chloroquine treatment was performed on the same samples cultured in adherent conditions. Interestingly, spheroids were more sensitive to chloroquine treatment, in terms of cell viability reduction, than the adherent counterpart (Fig. 9.6), suggesting that autophagy might be particularly important for the maintenance of ovarian CSC viability.

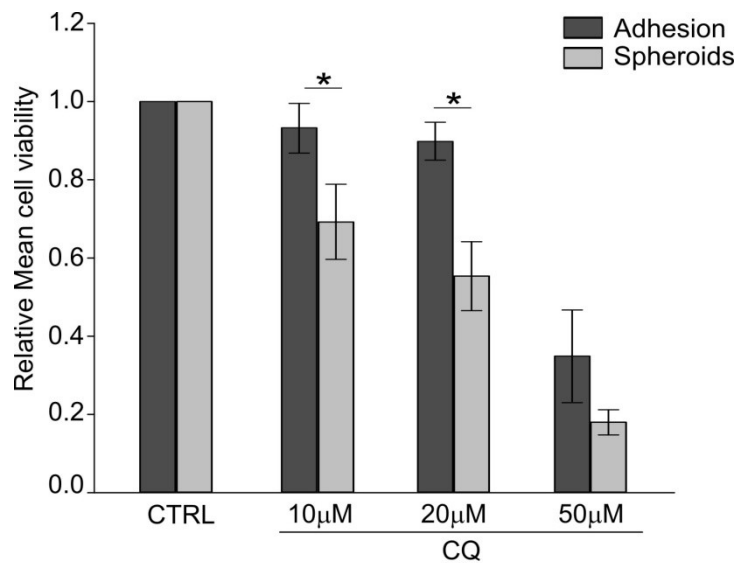


Figure 9.6. Cell viability analysis by Live/Dead staining of EOC cells cultured either in adherent or spheroid-forming conditions for 2 weeks and then treated with chloroquine (CQ, 10, 20 or 50 μM) for 72h. The graph represents the mean cell viability \pm S.D (n=3) normalized to the untreated cells (CTRL) for each culture condition. *P<0.05.

In another set of experiments, CQ was added at the beginning of culture in stemness conditions, and spheroid generation was evaluated 1 week later. In this experimental setting, we observed a dose-dependent cell viability reduction (Fig. 9.7) as well as a decrease in the mean diameter of the obtained spheroids (Fig. 9.8).

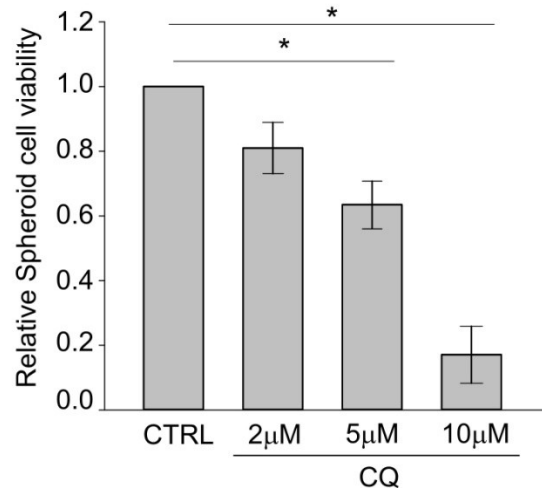


Figure 9.7. Cell viability analysis by Live/Dead staining of EOC cells maintained for 1 week in spheroid-culture conditions in the presence of CQ (2, 5 or 10 µM). The bars represent the mean ± S.D. (n=3) normalized to the untreated cells (CTRL). *P<0.05.

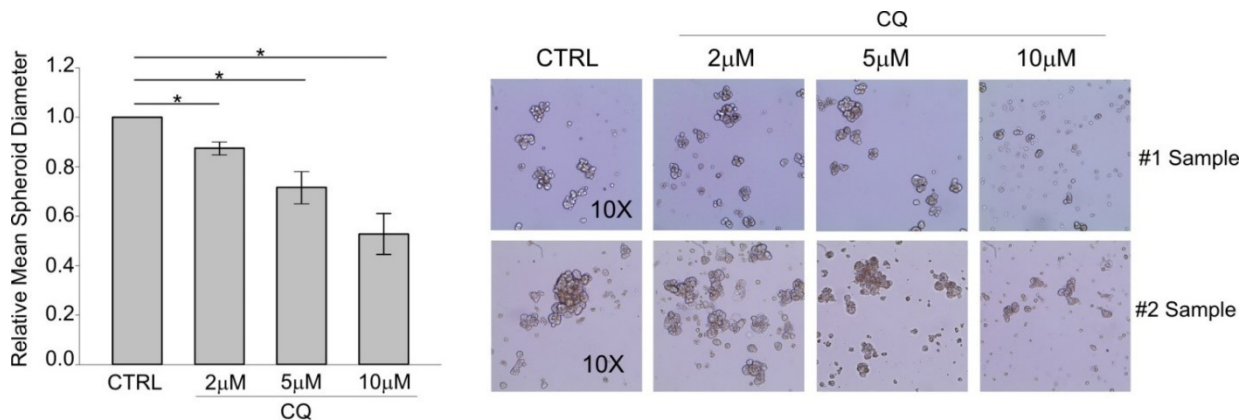


Figure 9.8. Spheroid diameter of EOC cells cultured in the presence (CQ) or absence of chloroquine (CTRL). The bars represent the mean ± S.D. (n=3) of treated cells normalized to the untreated ones. *P<0.05. On the right, representative pictures of spheroids from two EOC samples.

Altogether, these results show that autophagy blockade severely impairs one of the canonical CSC properties, *i.e.* the ability to form spheroids.

9.1.3. Autophagy blockade reduces CSC ability to resist *in vitro* and *in vivo* chemotherapy treatment

An important limit to conventional therapy is CSC ability to resist chemotherapeutic treatment. It has been demonstrated that autophagy is induced in ovarian cancer cell lines in response to platinum treatment as a survival mechanism, resulting in a sensitization of the cells to the treatment when autophagy is inhibited (336). Thus, we evaluated carboplatin (CPT)-mediated autophagy activation by Cyto-ID® staining in primary EOC and PDX samples. As shown in

Fig. 9.9, 72h carboplatin treatment induced a significant increase in mean fluorescent intensity (MFI) in CD44⁺CD117⁺ cells compared to the CD44⁺CD117⁻ counterpart.

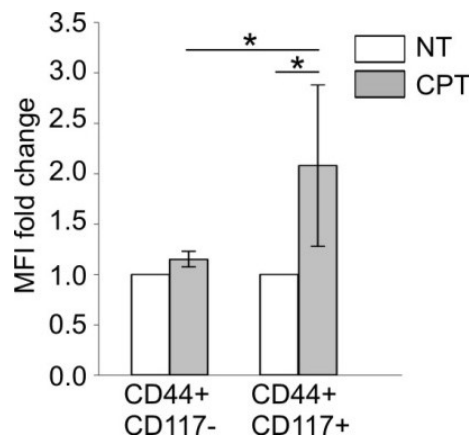


Figure 9.9. Flow cytometry analysis of autophagic activity in CSC and non-CSC by Cyto-ID[®] Autophagy detection kit. Cells were either treated *in vitro* with CPT (20 µg/mL) for 72h or left untreated. Data are expressed as MFI ± S.D. (n=3) *P<0.05.

This result justifies the use of an autophagy-targeting drug, such as chloroquine, to specifically sensitize CSC cells to this chemotherapeutic agent. First of all, we determined the CPT-CQ combination index (C.I.) in primary and PDX samples. As reported in Table 9.2, the results indicate a synergistic effect of the two drugs when CQ (20 µM) was combined with 20 µg/ml CPT (C.I.= 0.85).

| Carboplatin (µg/ml) | Chloroquine (µM) | Fractional Inhibition | CI |
|---------------------|------------------|-----------------------|------|
| 10 | | 0.17 | |
| 20 | | 0.11 | |
| 50 | | 0.4 | |
| | 10 | 0.22 | |
| | 20 | 0.46 | |
| | 50 | 0.65 | |
| 10 | 10 | 0.26 | 1.17 |
| 10 | 20 | 0.44 | 0.67 |
| 10 | 50 | 0.58 | 0.52 |
| 20 | 10 | 0.45 | 0.98 |
| 20 | 20 | 0.52 | 0.85 |
| 20 | 50 | 0.72 | 0.45 |
| 50 | 10 | 0.66 | 1.05 |
| 50 | 20 | 0.69 | 0.99 |
| 50 | 50 | 0.8 | 0.62 |

Table 9.2. C.I. analysis of CPT and CQ treatment. Data collected from three EOC samples were subjected to automated calculation of C.I. using the software CompuSyn. CI<1, CI=1, and CI>1 indicate synergism, additivity, and antagonism, respectively.

Therefore, we next addressed the role of autophagy in stress conditions by evaluating the effect of CPT, alone and in combination with CQ, on the spheroid-forming ability of tumor cells from EOC patients. To this end, EOC cells were pulsed for 72h with CPT, CQ, or the combination of the two; subsequently, equal numbers of live cells were plated in spheroid-forming conditions according to the Extreme Limiting Dilution Assay (ELDA) protocol. As shown in Fig. 9.10 A, pre-treatment of tumor cells with CQ or with CPT alone did not cause any significant change in the spheroid-forming ratio, compared to untreated cells. On the contrary, pre-treatment for 72h with a combination of CPT and CQ caused a significant decrease in the number of spheroid-forming cells. Additionally, the mean spheroid diameter was lower in samples pre-treated with CQ or CPT alone or the combination of the two (Fig. 9.10 B).

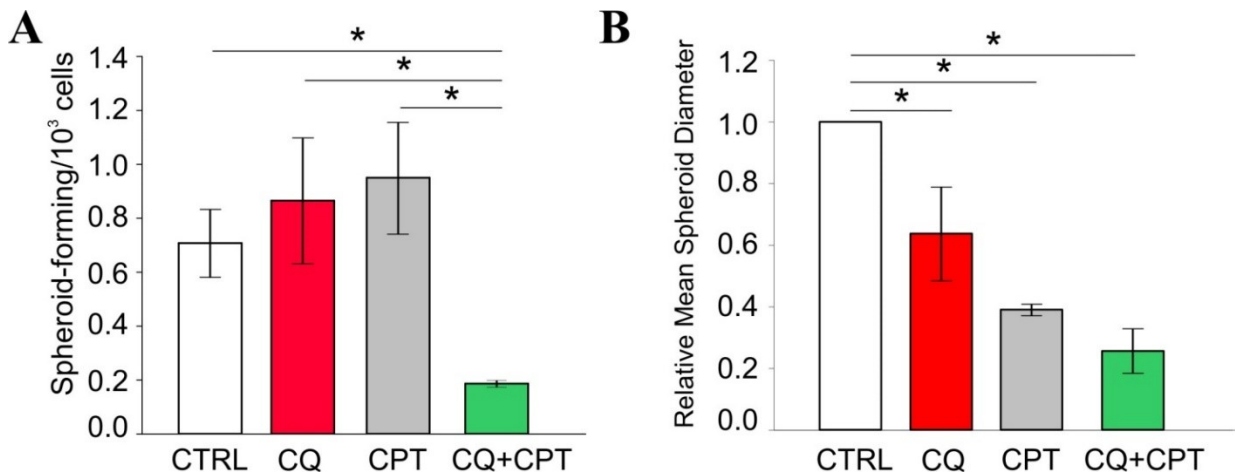


Figure 9.10. ELDA performed on EOC cells cultured *in vitro* for 72h under normal culture conditions in the presence of CQ (20 μ M), CPT (20 μ g/ml) or the combination of the two drugs. Data are expressed as mean \pm S.D. (n=3), *P<0.05 (A). Spheroid diameter following the different treatment regimens described in A. The mean spheroid diameter (\pm S.D.) (n=3) normalized to the untreated cells (CTRL) is plotted in the graph. *P<0.05 (B).

Altogether, these data suggest that autophagy is a mechanism exploited by ovarian CSC to survive CPT treatment.

Finally, to evaluate the effect of autophagy inhibition on the CSC tumorigenic potential, PDX cells were injected subcutaneously (s.c.) into NSG mice. Treatments were performed according to different therapeutic regimens: saline solution (as a control), CQ, CPT or a combination of the two. Single CPT and CQ treatments significantly slowed tumor growth, compared to control. Strikingly, combination treatment had a synergistic effect inducing an even more pronounced tumor growth reduction (Fig. 9.11).

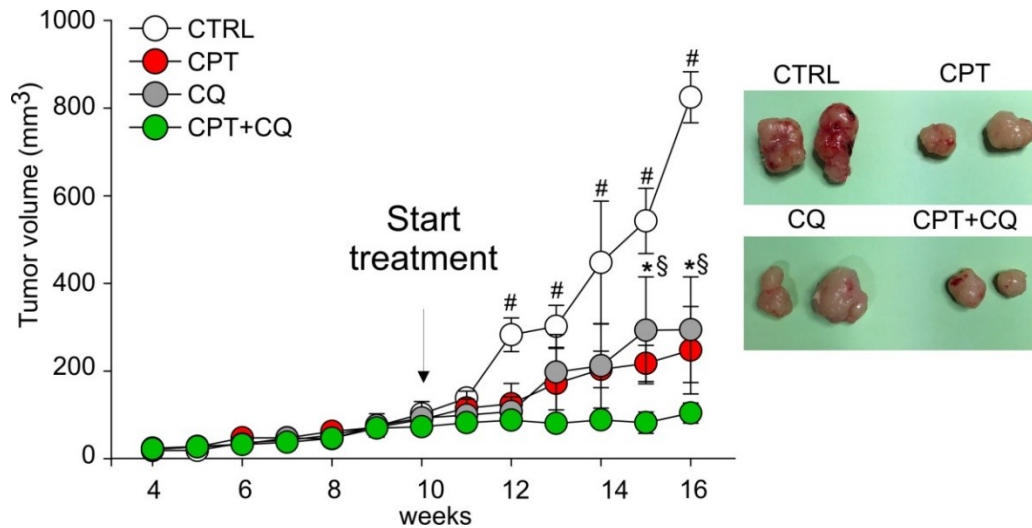


Figure 9.11. Tumor growth curves in NSG mice treated with saline solution (CTRL), CPT (50 mg/Kg, weekly), CQ (100 mg/Kg, every 2 days) or the combination of the two, after s.c. injection of EOC cells. Data are mean values \pm S.D. (n=6/experimental group). $P < 0.05$. * CPT+CQ vs CQ alone; § CPT+CQ vs CPT alone; # CPT+CQ vs CTRL. On the right, representative pictures of tumors at the end of the experiment.

Ex vivo analysis further demonstrated that autophagy can represent a survival mechanism adopted by CSC to resist chemotherapy treatment. Indeed, the percentage of CD44⁺CD117⁺ cells was significantly lower in tumor harvested from mice that received the combination treatment compared to CTRL or single-treated mice (Fig. 9.12 A). Moreover, *ex vivo* Ki67 analysis within the CD44⁺CD117⁺ compartment demonstrated that CSC proliferation was not affected by autophagy blockade (Fig. 9.12 B), suggesting that the observed reduction in CSC number is likely ascribed to an impaired survival.

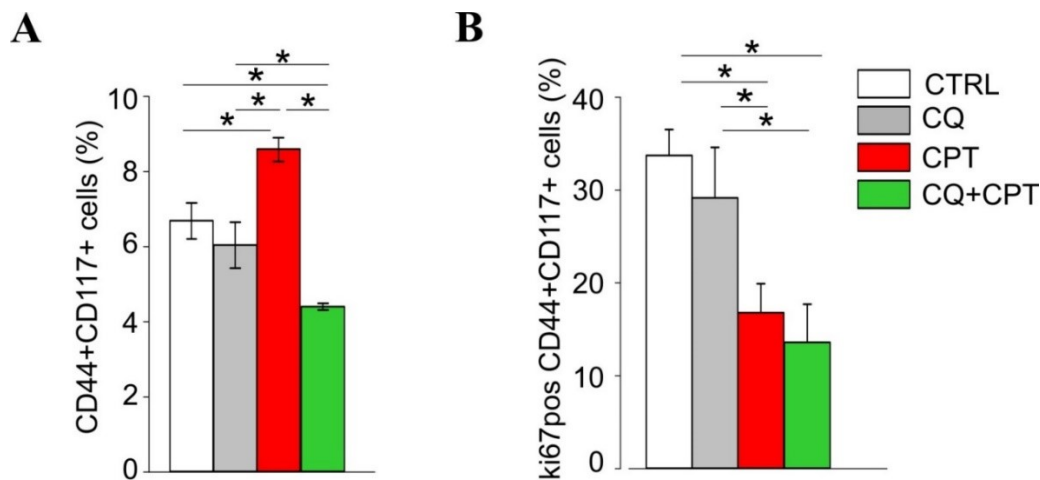


Figure 9.12. *Ex vivo* flow cytometry analysis of CD44/CD117 co-expression (A) and Ki67 (B) in tumors harvested from mice treated with saline solution (CTRL), CPT, CQ or the combination of the two drugs (CPT+ CQ). Data are expressed as mean \pm S.D. (n=4/experimental group). * $P < 0.05$

9.2. SCF is abundant in EOC ascites, it is produced by fibroblasts and macrophages, and it activates the downstream pathway in CD117⁺ cells

9.2.1. SCF soluble form is produced by tumor-associated fibroblasts and macrophages

Ovarian CSC are characterized by the expression of the SCF receptor CD117, also known as c-Kit. Thus, we wondered whether a c-Kit/SCF circuit could be actively involved in promoting CSC survival and expansion in EOC patients. Therefore, we first assessed the presence of soluble SCF in ascitic effusions from EOC patients. As shown in Fig. 9.13, ELISA analysis of 32 ascitic effusion samples revealed detectable amounts of SCF in all the samples tested ($1,306.8 \pm 460.5$ pg/mL; range 161.83-2,374.88 pg/mL). No association between tumor histology, grading or stage and ascitic fluid SCF content was observed (Table 9.3).

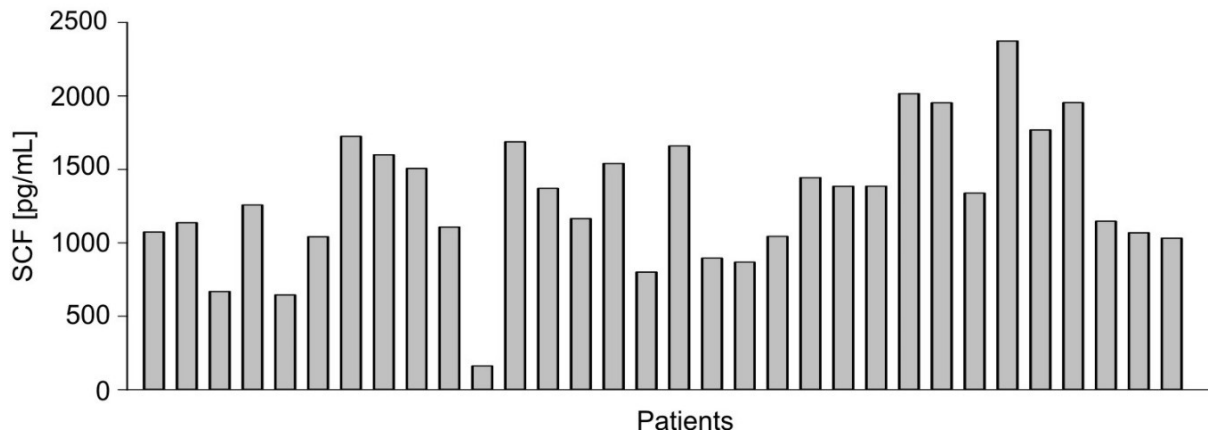


Figure 9.13. ELISA analysis of SCF levels in ascitic effusions collected from EOC patients (n=32).

| | N (% of total) | SCF pg/mL [median \pm SD] (range) | P value |
|------------------|----------------|-------------------------------------|--------------------|
| Histotype | | | 0.083 [§] |
| endometrioid* | 1 (3.13) | 1953.5 (-) | |
| serous tubal* | 2 (6.25) | 1153.1 \pm 499.1 (800.2-1506.05) | |
| undifferentiated | 6 (18.75) | 1105.1 \pm 249.4 (668.3-1444.0) | |
| serous papillary | 13 (40.62) | 1599.2 \pm 442.2 (868.5-2374.9) | |
| serous | 6 (18.75) | 1102.7 \pm 353.6 (645.5-1687.7) | |
| N.A. | 4 (12.5) | | |
| Stage | | | 0.161 [#] |
| 3 | 17 (53.12) | 1385.7 \pm 441.3 (645.5-2374.9) | |
| 4 | 9 (28.13) | 1107.7 \pm 354.8 (668.3-1768.9) | |
| N.A. | 6 (18.75) | | |
| Grade | | | 0.192 [#] |
| G1* | 1 (3.13) | 1338.4 (-) | |
| G3 | 19 (59.37) | 1371 \pm 455.2 (645.5-2374.9) | |
| G4 | 6 (18.75) | 1105 \pm 249.4 (668.3-1444.0) | |
| N.A. | 6 (18.75) | | |
| Total | 32 (100) | | |

Table 9.3. (continued) SCF concentration in EOC patient ascites and association with histotype, stage and grade (N.A.= not available; * not used for statistical analysis; §Kruskal-Wallis test; #Mann-Whitney test).

It is known that SCF is produced by a variety of cells in physiological contexts, mainly by fibroblasts and endothelial cells (257). Moreover, it has been reported that SCF is produced also by tumor cells, either differentiated (274) or progenitor cells (275). We thus wondered whether ovarian tumor cells could also be responsible for its secretion, as observed in other tumors, and whether SCF production could be a distinctive feature of the CSC subset. However, when *ex vivo* FACS-sorted CD44⁺CD117⁺ and CD44⁺CD117⁻ cells from EOC ascitic effusion samples were cultured *in vitro* for 24h, SCF could not be detected in culture supernatants of either population (Fig. 9.14 A). Nonetheless, SCF positivity was recorded by flow cytometry in either cell populations, which accounted for $6.1 \pm 3.1\%$ and $1.2 \pm 0.4\%$ in CD44⁺CD117⁺ and CD44⁺CD117⁻ cells, respectively (Fig. 9.14 B), thus suggesting that CSC and non-CSC could produce only the membrane-associated, non-cleavable form of SCF. The production of small, not detectable amounts of soluble SCF could be an alternative explanation.

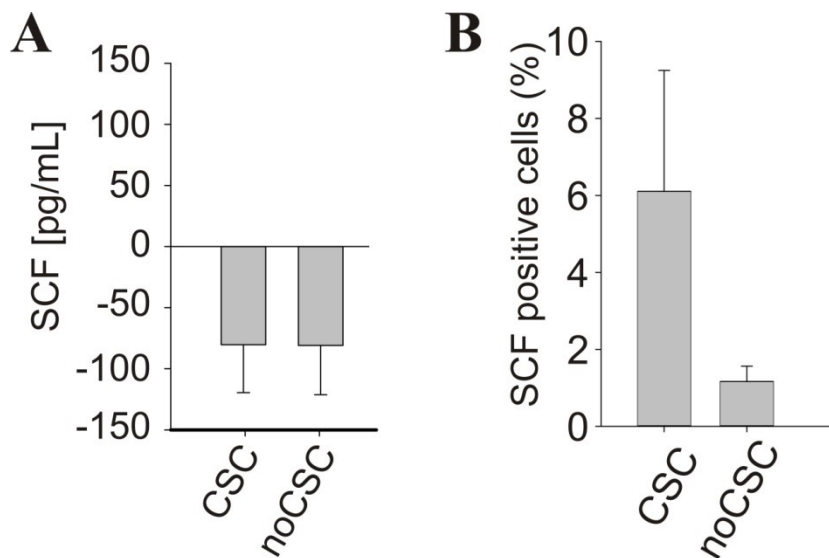


Figure 9.14. ELISA analysis of SCF production in conditioned media of CD44⁺CD117⁺ (CSC) and CD44⁺CD117⁻ (noCSC) cells sorted by FACS from primary samples of EOC ascitic effusions. The bars represent the mean \pm S.D. (n=4) (A). Flow cytometry analysis of SCF expression in CD44⁺CD117⁺ and CD44⁺CD117⁻ cells. The bars represent the mean \pm S.D. (n=4) (B).

Since EOC ascitic effusions not only include tumor cells, but also tumor-associated fibroblasts (TAF) and cells of myeloid (tumor-associated macrophages (TAM)) and lymphoid (tumor infiltrating lymphocytes (TIL), *i.e.* T and B cells) origin, we evaluated SCF secretion in the

supernatant of these cell populations. Detectable SCF amounts were found in the supernatants of *in vitro* cultured TAF and TAM from EOC samples (78.52 ± 62.21 pg/mL and 42.90 ± 5.29 pg/mL, respectively), whereas no SCF release by tumor-associated T and B cells was observed (Fig. 9.15).

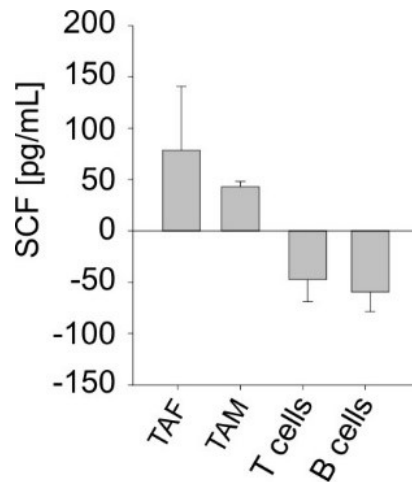


Figure 9.15. ELISA analysis of SCF levels measured in conditioned media of TAF, TAM, T cells and B cells sorted by FACS from primary samples of EOC ascitic effusions. Data are expressed as mean \pm SD (n=4).

Flow cytometry analysis further demonstrated SCF expression by TAF and TAM ($26.8 \pm 9.9\%$ and $91.3 \pm 0.78\%$, respectively), whereas SCF expression was almost absent in tumor-infiltrating T and B cells (Fig. 9.16).

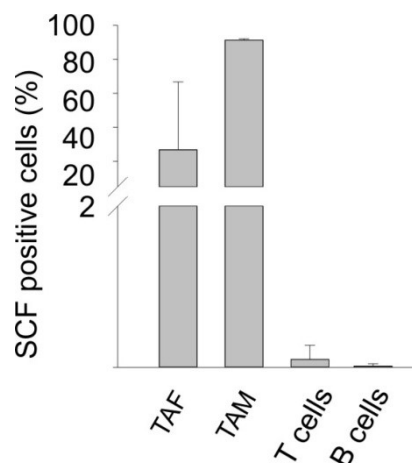


Figure 9.16. Flow cytometry analysis of SCF expression in TAF, TAM, T cells and B cells sorted from EOC ascitic effusions. The bars represent the mean \pm SD (n=4).

Quantitative RT-PCR analysis confirmed that FACS-sorted CD44⁺CD117⁺ and CD44⁺CD117⁻ cells expressed the mRNA for membrane-associated SCF isoform (SCF 220) at higher levels as compared to TIL, clearly almost negative for both SCF isoforms. On the other hand, both CSC and non-CSC expressed levels of the mRNA coding for the soluble isoform (SCF 248) comparable to TIL. Instead, TAF and TAM expressed both the SCF 220 and the SCF 248 isoforms (Fig. 9.17).

In conclusion, high levels of SCF were detected in the ascitic effusions from EOC-bearing patients. Among the several cell populations found in the ascitic fluid, only TAM and TAF released soluble SCF in the supernatant, whereas most likely cancer cells did not produce the cleavable SCF isoform, irrespective of their CSC or non-CSC status. However, akin to TAM and TAF, cancer cells were positive for membrane-associated SCF isoform, while TIL resulted completely negative for either isoform.

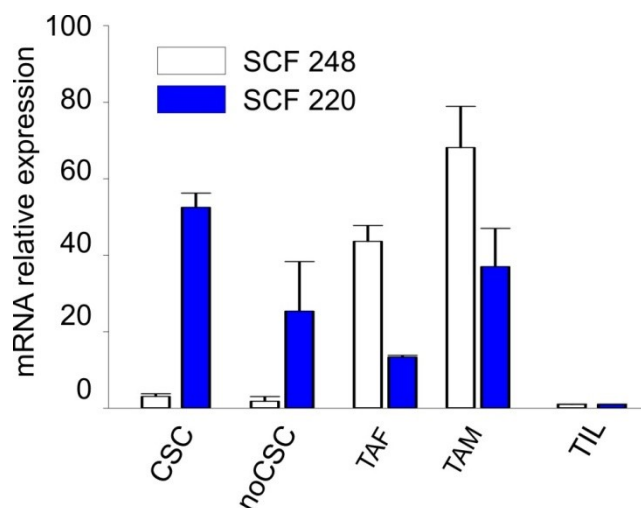


Figure 9.17. qRT-PCR analysis of SCF 248 and SCF 220 isoforms in CSC, noCSC, TAF, and TAM sorted by FACS from EOC ascitic effusions; data are normalized to SCF expression in TIL. The bars represent the mean \pm S.D. (n=4).

9.2.2. Monocyte-to-macrophage differentiation induces SCF expression, irrespective of M1 or M2 polarization.

Since SCF production by fibroblasts is firmly established (257, 337), we decided to focus our attention on macrophages. Indeed, TAM represent a topic of intense research as they orchestrate several tumor-promoting processes, including cytokine secretion and immune escape (338). Macrophages fall into two different functional populations, namely M1 and M2, characterized by an inflammatory or immunosuppressive phenotype, respectively, even though macrophages with intermediate features also exist (199).

We thus wondered whether SCF expression could be a preferential property of M1 or M2 populations. For this purpose, circulating monocytes from healthy donors were isolated by using magnetic beads, they were differentiated into macrophages (M0) by adding GM-CSF for one week, and then cultured in the presence of LPS and IFN- γ in order to obtain M1 polarization (as confirmed by TNF and IL1 β expression; Fig. 9.18), or IL4 and IL13 for M2 polarization (as confirmed by IL10 and CCL22 expression; Fig. 9.18) for 24h and 48h.

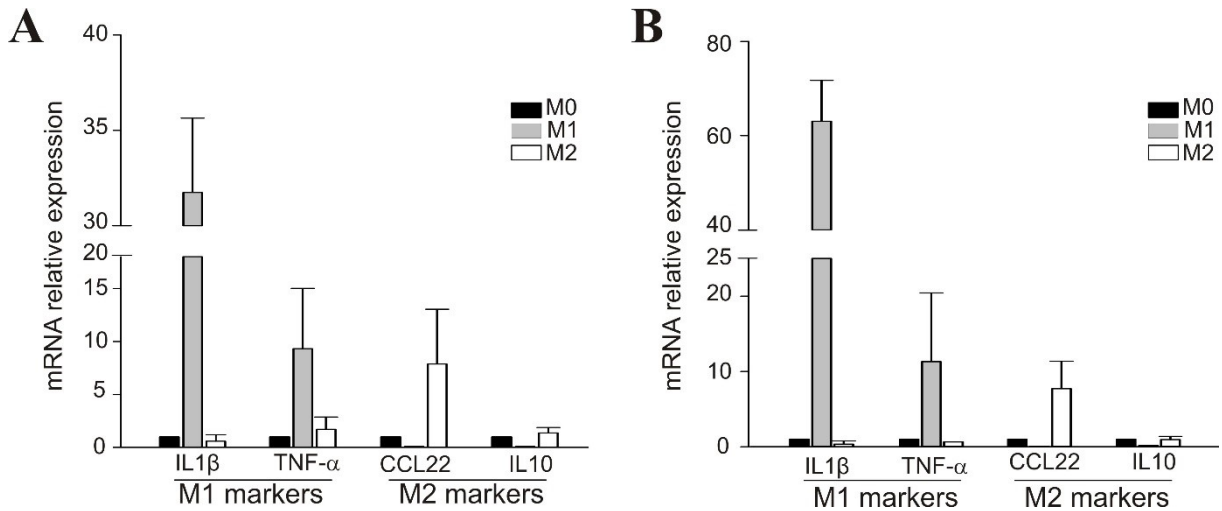


Figure 9.18. qRT-PCR analysis of M1 (IL-1 β and TNF) and M2 (IL10 and CCL22) markers in *in vitro* differentiated (M0), M1 and M2 macrophages after 24h (A) and 48h (B) from polarization. Data are normalized to the corresponding M0. The bars represent the mean \pm S.D. (n=3).

SCF expression was assessed by qRT-PCR (Fig. 9.19), Western blotting (Fig. 9.20) and flow cytometry (Fig. 9.21). Even though qRT-PCR analysis highlighted a downregulation of both SCF isoform mRNA level after 24h of polarization in M1 macrophages (partially recovered after 48h, concerning SCF 220 isoform), all macrophage populations expressed SCF protein, while monocytes were completely negative (Fig. 9.21). WB analysis and quantification did not show any difference in SCF protein expression among the different populations (Fig. 9.20), but the technique did not allow the discrimination of the two isoforms.

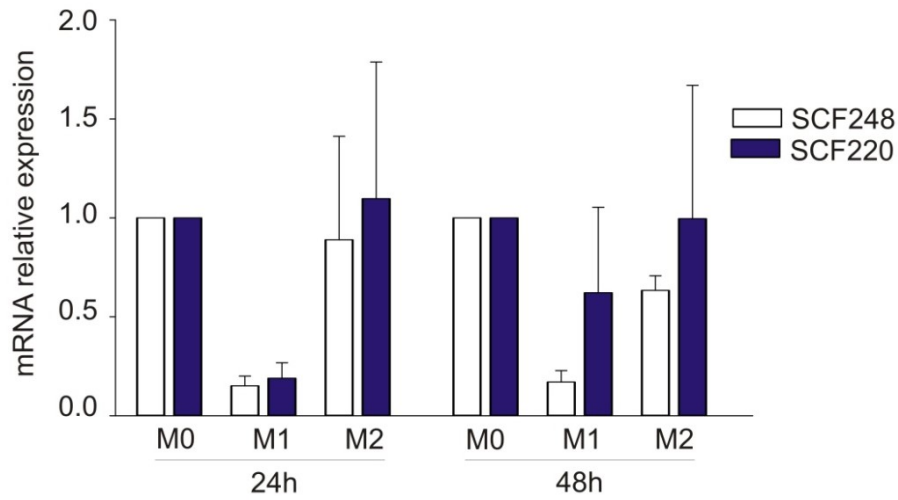


Figure 9.19. qRT-PCR analysis of SCF 248 and SCF 220 in *in vitro* differentiated (M0), M1 and M2 macrophages after 24h (A) and 48h (B) from polarization. Data are normalized to the corresponding M0. The bars represent the mean \pm S.D. (n=3).

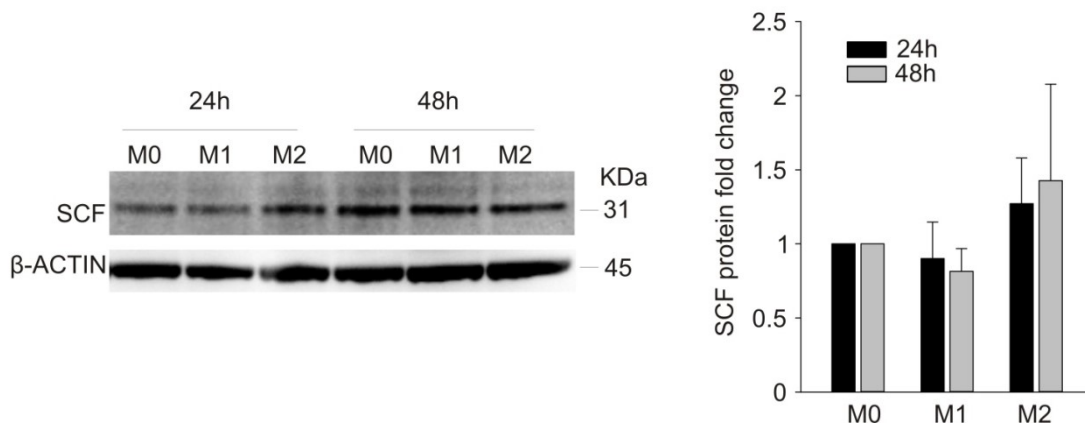


Figure 9.20. WB analysis of SCF in *in vitro* differentiated (M0), M1 and M2 macrophages after 24h and 48h from polarization. A representative blot is shown. The graph represents SCF signal normalized to β -actin. Bars represent the mean \pm S.D. (n=3).

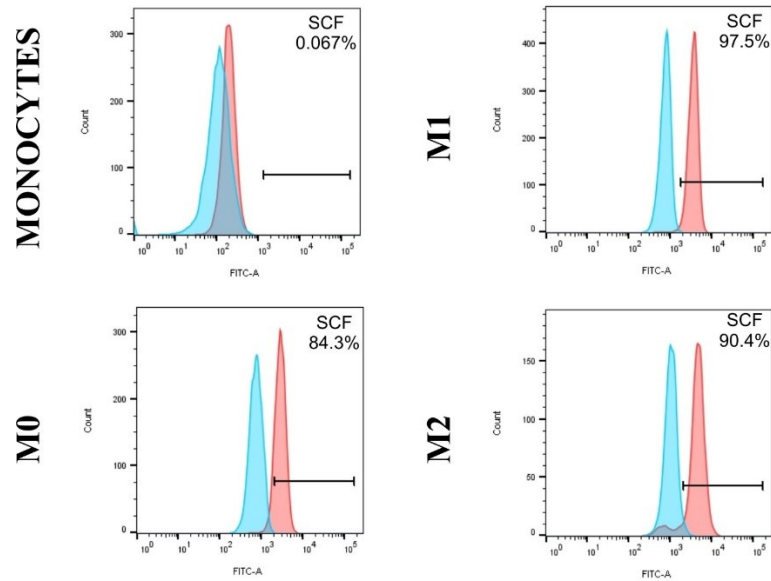


Figure 9.21. Flow cytometry analysis of SCF in *ex vivo* monocytes from healthy donors, in *in vitro* differentiated (M0), M1 and M2 macrophages after 48h from polarization. Unstained controls are shown in blue, stained samples in red.

For this reason, we collected the cell supernatant from M0, M1, and M2 macrophages after 24 and 48h from polarization and we checked whether *in vitro* differentiated and polarized macrophages were able to secrete soluble SCF, similarly to the *ex vivo* macrophages isolated from EOC ascitic effusion. ELISA analysis revealed SCF production by every cell population at both time points. M1 cells seemed to have a more rapid kinetics, as they secreted higher levels of the cytokine already after 24h, compared to M0 and M2 cells. However, differences disappeared after 48h, as M0 and M2 cells increased SCF release, equaling M1 levels (Fig. 9.22).

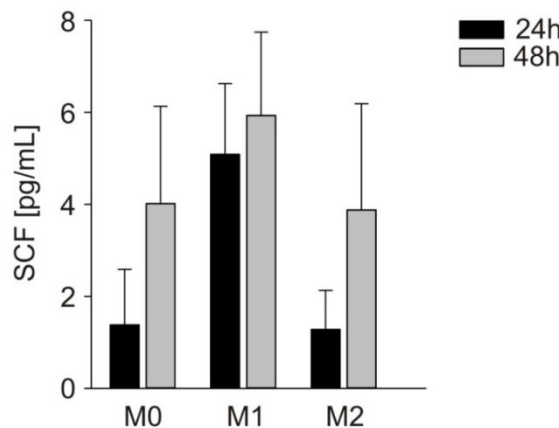


Figure 9.22. ELISA analysis of SCF in conditioned media of M0, M1, and M2 cells after 24 and 48h from polarization. The bars represent the mean \pm S.D. (n=3).

In conclusion, even though circulating monocytes from healthy controls were negative for SCF expression, their differentiation into macrophages was sufficient to induce SCF expression and secretion. However, SCF expression could not be defined as a specific hallmark of or restricted to either M1 or M2 polarized macrophages.

9.2.3. SCF 248 and SCF 220 activate the PI3K/Akt pathway in CD117⁺ cells through c-Kit activation

Next, we wondered whether soluble and membrane SCF could activate a signaling cascade in CD117⁺ cells. Because of the technical hurdles in obtaining sufficient, and vital CD44⁺CD117⁺ CSC by FACS sorting (from primary samples and PDX), in order to perform biochemical studies, which invariably require to test scalar doses of drugs, we decided to exploit another cell system. KASUMI1 is a human leukemic cell line in which the whole population is CD117⁺ and we used it as an experimental model to assess by WB and flow cytometry the effect of human recombinant SCF (hrSCF) and membrane-associated SCF stimulation, respectively.

WB analysis revealed that 5 min hrSCF stimulation induced a strong c-Kit and Akt phosphorylation (p-c-Kit and p-Akt). Interestingly, upon hrSCF treatment total c-Kit was downregulated (Fig. 9.22), most probably as a consequence of receptor internalization and degradation, a well-known RTK inactivation mechanism (252).

On the contrary, pre-treatment with imatinib, a tyrosine kinase inhibitor, hampered hrSCF-induced p-c-Kit and p-Akt at all concentrations (5, 10, 30, and 50 μ M) in a dose-dependent manner with the strongest inhibition at 30 and 50 μ M (Fig. 9.23). For this reason, we chose the dose of 30 μ M for subsequent short-term experiments.

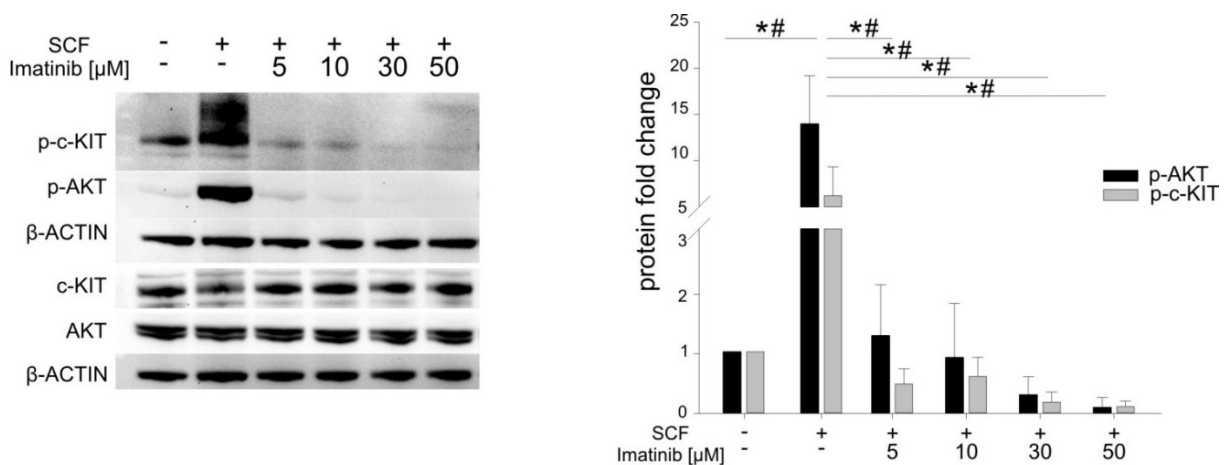


Figure 9.23. WB analysis of p-c-Kit and p-Akt in KASUMI1 cells pre-treated or not with imatinib (5, 10, 30, and 50 μ M) and stimulated with hrSCF (50 ng/mL) for 5 min. Signals were normalized to β -

Figure 9.23. (continued) actin. The graph represents p-c-Kit/c-Kit and pAkt/Akt mean ratios \pm S.D. (n=3). *p<0.05 for pAkt; #p<0.05 for p-c-Kit

WB results were corroborated by flow cytometry analysis of p-AKT in KASUMI1 cells, confirming that 5 min hrSCF stimulation increased p-Akt levels, whereas treatment with 30 μ M imatinib prior to hrSCF stimulation efficiently blocked Akt phosphorylation, reverting p-Akt levels to the baseline (Fig. 9.24).

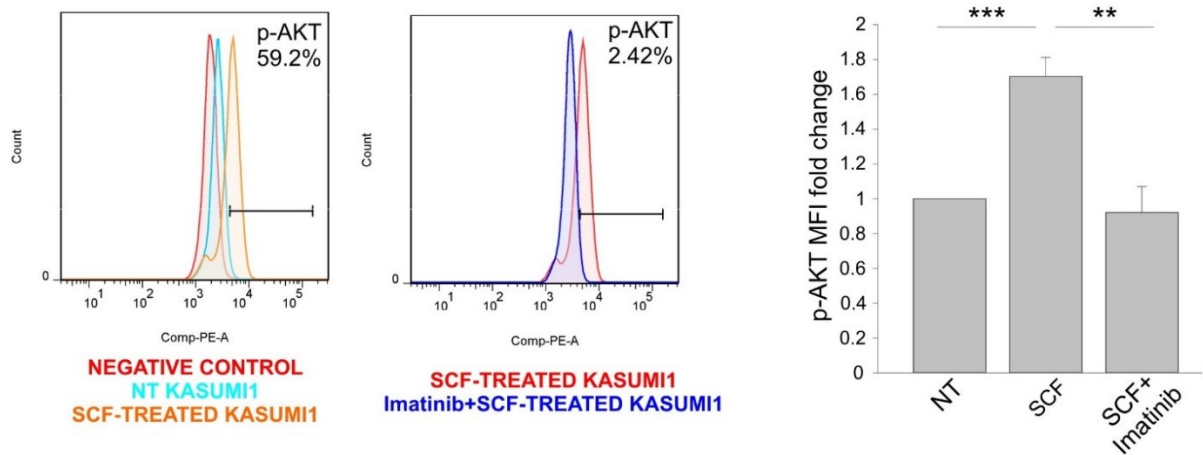


Figure 9.24. Flow cytometry analysis of p-Akt in KASUMI1 cells pre-treated or not with imatinib (30 μ M) and stimulated with hrSCF (50 ng/mL) for 5 min. The bars represent the mean \pm S.D. (n=3). **p<0.01; ***p<0.001

Next, we checked whether membrane-associated SCF could also efficiently induce Akt phosphorylation. To this end, we performed co-culture experiments with KASUMI1 cells and RAJI cells, a human B-lymphoma cell line, naturally negative for either SCF isoform (339). Hence, we firstly overexpressed in RAJI cells the non-cleavable SCF isoform, tagged with GFP (SCF-RAJI; Fig. 9.25). In order to exclude SCF-independent p-Akt induction, we challenged KASUMI1 cells with RAJI cells in which we only forced GFP expression (CTRL-RAJI). After RAJI co-culture, in order to detect p-Akt specifically in KASUMI1 cells (GFP-negative), we used flow cytometry analysis.

As a result, CTRL-RAJI could not induce p-Akt in KASUMI1 cells, as the relative curve overlapped the negative control. Accordingly, imatinib pretreatment did not determine any effect. On the contrary, 5 min co-culture with SCF-RAJI induced a significant increase of p-Akt levels in KASUMI1 cells. As expected, pretreatment with 30 μ M imatinib reverted p-Akt levels to the baseline (Fig. 9.26).

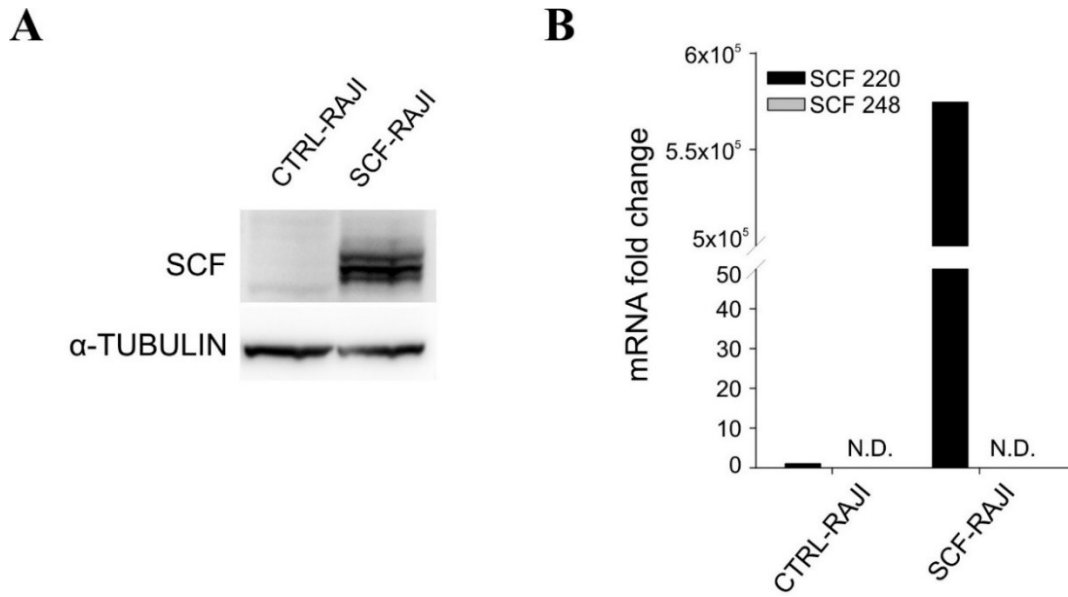


Figure 9.25. WB confirmation of SCF overexpression in SCF-RAJI cells compared to CTRL-RAJI cells (A). qRT-PCR confirmation of specific SCF 220 overexpression in SCF-RAJI cells. Data were normalized to CTRL-RAJI cells. SCF248 is not detectable (N.D.) in both populations (B).

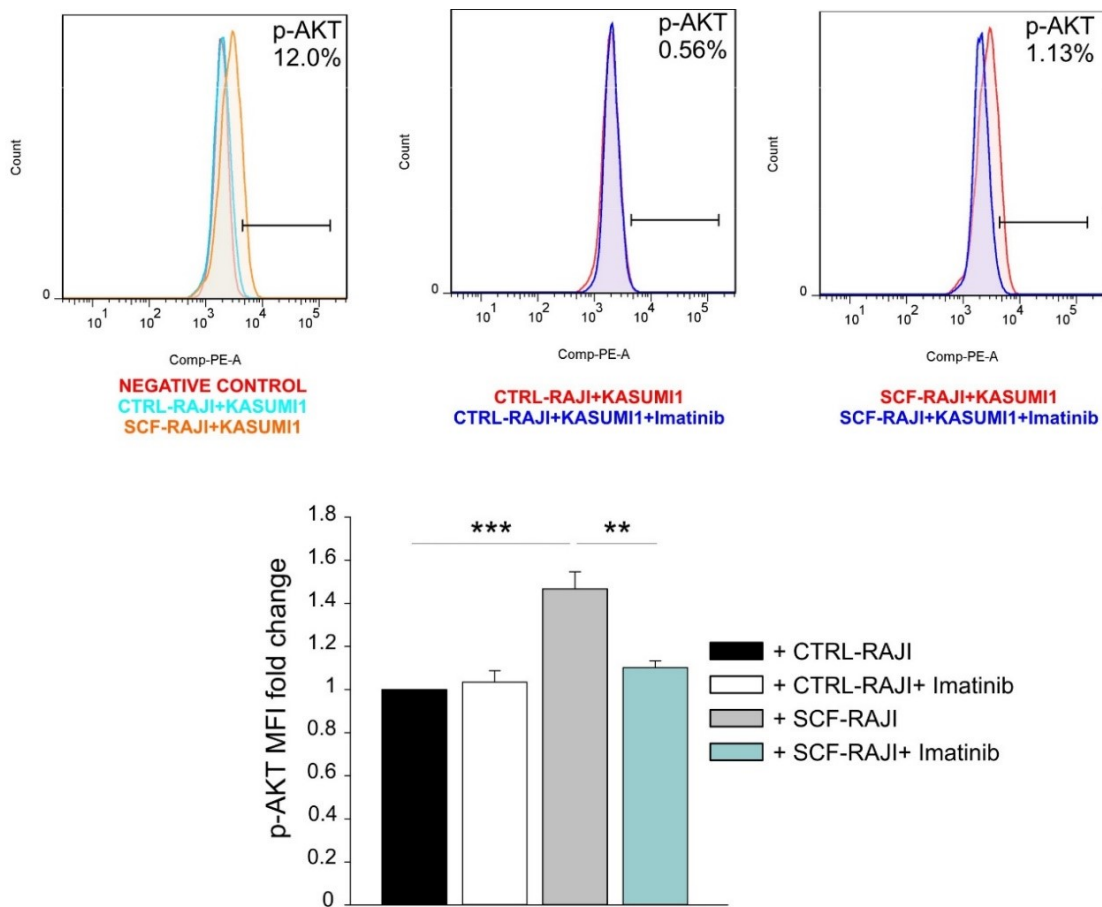


Figure 9.26. Flow cytometry analysis of p-Akt in KASUMI1 cells pretreated or not with 30 μ M imatinib and co-cultured for 5 min with CTRL-RAJI or SCF-RAJI. One representative experiment is shown in the upper panel. The bars represent the mean \pm S.D. (n=3). **p<0.01; ***p<0.001

We can conclude that 5 min treatment with both soluble and membrane-associated SCF is effective in activating Akt signaling through c-Kit phosphorylation, and imatinib pretreatment can hinder the stimulation mediated by either isoform.

9.2.4. SCF stimulation affects the canonical properties of ovarian CSC

We finally wondered whether SCF stimulation could be able to support the canonical CSC properties. To this end, EOC cells from patient ascitic effusions and PDX were cultured for two weeks under spheroid-forming conditions to enrich the amount of CD117⁺ cells (223). Hence, we verified that c-Kit expression increased after two weeks under spheroid-forming conditions, compared to the adherent counterpart (Fig. 9.27 A).

Cells were maintained in the presence of hrSCF (50 ng/mL), imatinib (5 μ M), a combination of both treatments, or left untreated. Then, equal numbers of live cells were plated according to the ELDA protocol, in the presence of the corresponding treatment. A week later, ELDA showed that SCF significantly increased the spheroid-forming ratio of EOC cells, whereas imatinib alone did not exert any effect (Fig. 9.28). The latter finding was not unexpected, since c-Kit was not phosphorylated in the absence of stimuli (Fig. 9.27 B). Interestingly, imatinib was able to abrogate hrSCF-mediated enrichment in spheroid-forming units (Fig. 9.28).

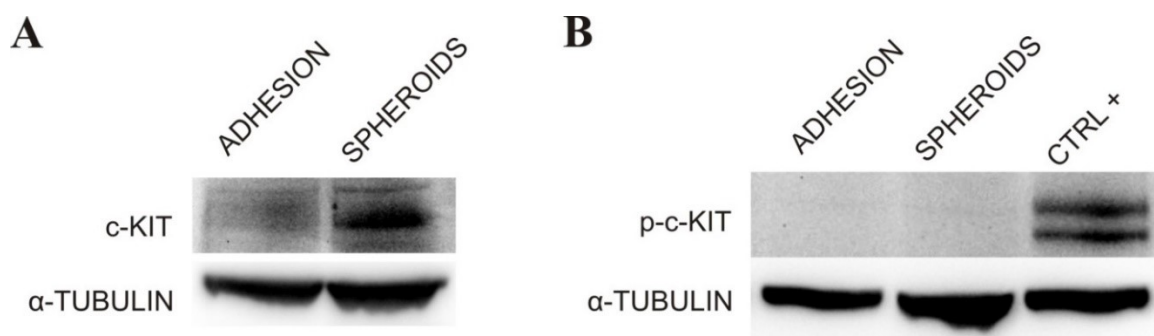


Figure 9.27. Representative WB analysis of c-Kit (A) and p-c-Kit (B) expression in EOC cells cultured either under adherent or spheroid-forming conditions (n=3).

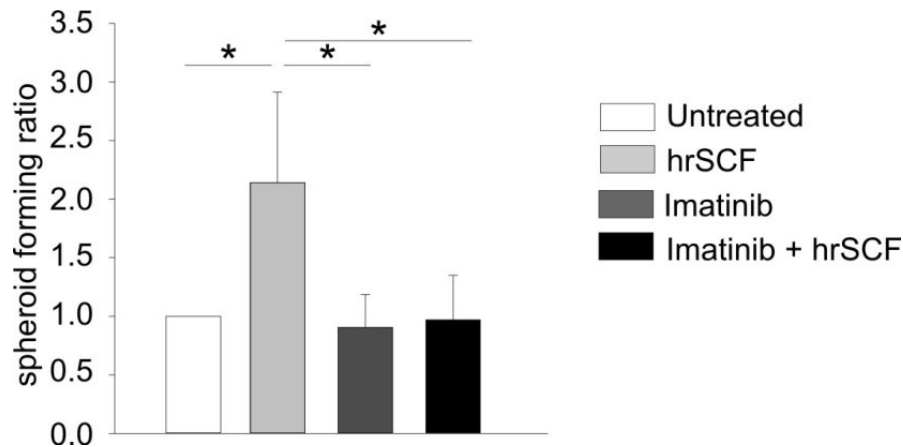


Figure 9.28. ELDA performed on EOC cells cultured for two weeks under spheroid-forming conditions in the presence of hrSCF (50 ng/mL), imatinib (5 μ M) or the combination of the two. Data are expressed as mean \pm S.D. (n=3), *p<0.05

Since PDGFR- α and - β are imatinib targets as well (340), we tested their expression in a set of primary EOC samples to confirm that our results were strictly c-Kit-dependent. As showed in Fig. 9.29, no one of the tested samples expressed either PDGFR- α or β .

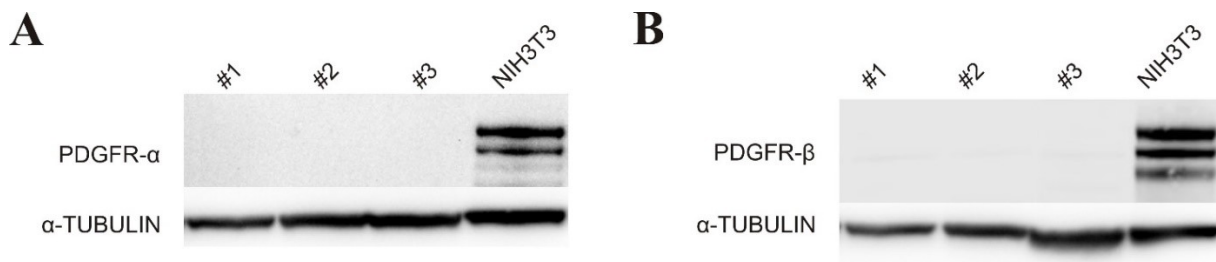


Figure 9.29. WB analysis of PDGFR- α (A) and PDGFR- β (B) expression in a panel of three EOC samples. NIH3T3 cells were used as positive control.

Eventually, we evaluated the mRNA expression of the stemness-associated genes Oct4, Sox2, and Nanog, together with c-Kit, in EOC spheroids cultured for two weeks in the presence of hrSCF, and we observed a significant increase in the mRNA levels of all the genes in presence of the growth factor (Fig. 9.30). Imatinib treatment, instead, abrogated the hrSCF-induced transcriptional regulation of all the genes, two of which in a statistically significant fashion, bringing their mRNA level to the baseline (Fig. 9.30).

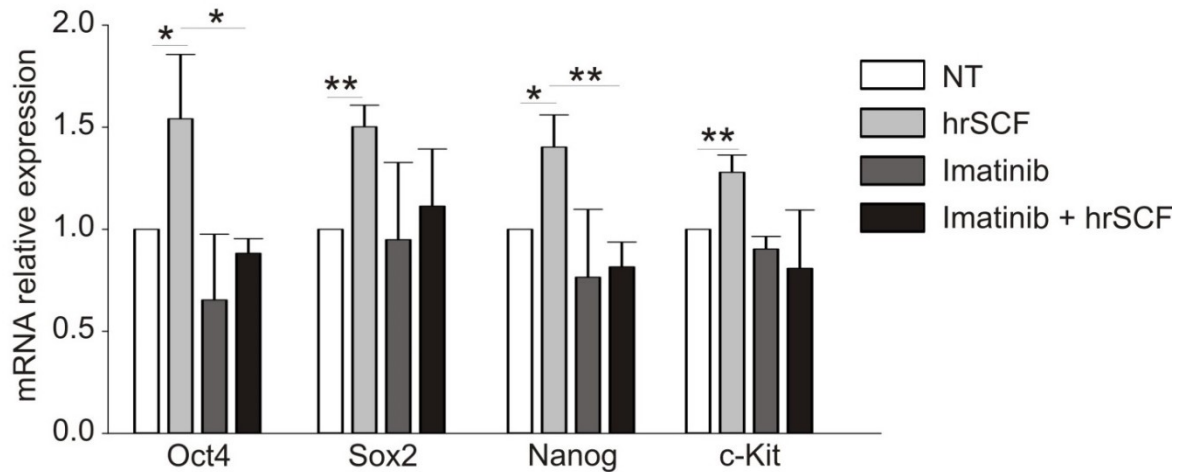


Figure 9.30. qRT-PCR analysis of Oct4 , Sox2, Nanog, and c-Kit mRNA levels in EOC cells cultured for two weeks in the presence of hrSCF (50 ng/mL), imatinib (5 μ M) or the combination of the two. Data are expressed as mean \pm S.D. (n=3), *p< 0.05, **p<0.01.

Overall, these data clearly indicate that SCF is able to affect some canonical features of ovarian CSC, while imatinib fully abolishes the effects operated by SCF. Results from the experiments performed on KASUMI1 cells suggest a pro-survival role for both soluble and membrane-associated SCF on CD117⁺ cells, due to Akt activation mediated by SCF specific interaction with its cognate receptor c-Kit. Therefore, we could infer that similar biochemical effects might be exerted by either SCF isoforms on CD44⁺CD117⁺ ovarian CSC in selective culture conditions and, more extensively, in patient ascitic fluid, leading to an increase in their survival as demonstrated by the increase in spheroid-forming units and stemness marker expression, even though a formal demonstration is lacking due to technical limitations.

9.3. CK1 δ plays a role in the regulation of cell proliferation, response to chemotherapy and migration in ovarian cancer cells

9.3.1. CK1 δ knockdown causes morphological changes in OVCAR3 cells and a growth braking in OVCAR3 and IGROV1 cells

CK1 δ has been demonstrated to have a pro-tumorigenic role in a variety of cancers, including B cell lymphoma (323), choriocarcinoma (319), pancreas ductal adenocarcinoma (324), colorectal cancer (321) and breast cancer (325). In particular, CK1 δ inhibitors efficiently slowed *in vivo* breast tumor growth (325). Moreover, it has been reported that the 4% of ovarian cancers present CSNK1D gene amplification (310). Hence, we decided to check a panel of ovarian cancer cell lines and PDX for CK1 δ protein expression. As shown in Fig. 9.31, all the cell lines and the PDX tested resulted strongly positive for CK1 δ , with the cell lines presenting a slightly higher amount of the protein.

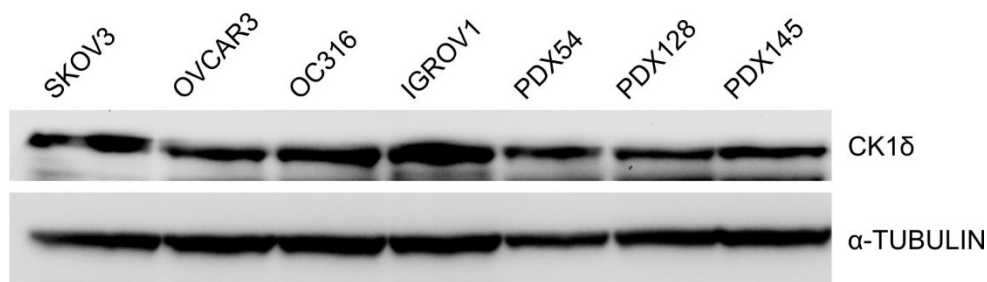


Figure 9.31. WB analysis of CK1 δ in four EOC cell lines and three PDX.

In order to verify whether CK1 δ perturbation could have any effect on some typical features of cancer cells, such as proliferation, resistance to apoptosis, migratory ability, and *in vivo* tumorigenicity, we decided to knockdown CK1 δ in two human EOC cell lines, OVCAR3 and IGROV1 cells. To this end, we transduced cells with lentiviral vectors bearing shRNA directed against CSNK1D, named sh599 and sh1552; control cells were generated by transduction with scramble shRNA (shCTRL). CSNK1D specific shRNA efficiently downregulated CK1 δ at both mRNA (Fig. 9.32) and protein levels (Fig. 9.33). Interestingly, soon after transduction, we observed a morphological change in OVCAR3 cells, *i.e.* cells appeared bigger with many protrusions (Fig. 9.34 A). On the other hand, IGROV1 cells did not display similar morphological changes, as sh599 and sh1552 transduced cells looked like the shCTRL ones (Fig. 9.34 B).

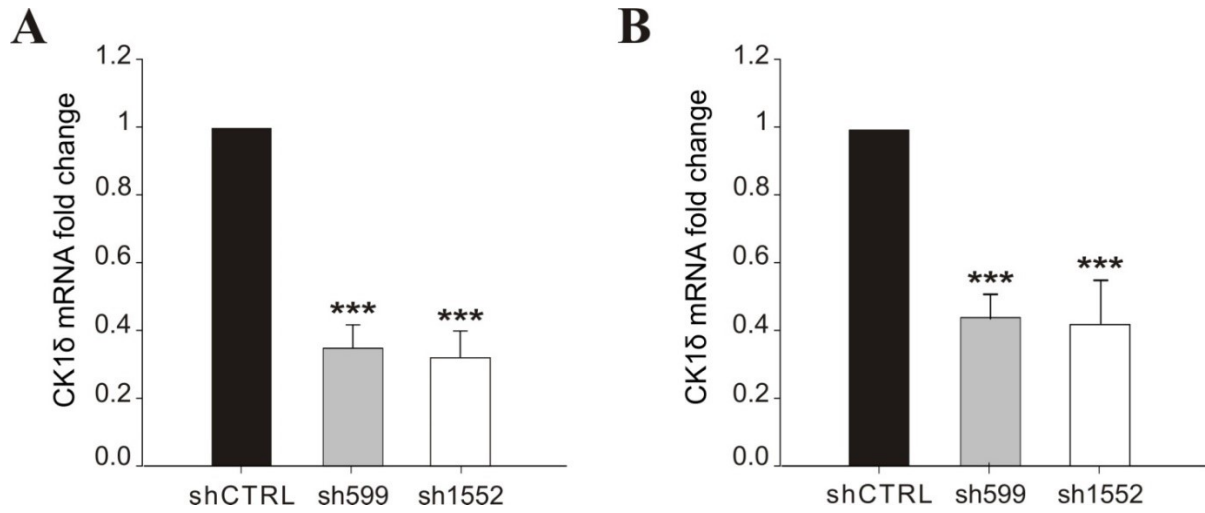


Figure 9.32. qRT-PCR confirmation of CK1δ knockdown in OVCAR3 (A) and IGROV1 (B) cells. Data were normalized to shCTRL cells. Graphs represent the mean \pm S.D. (n=5). *** p<0.001

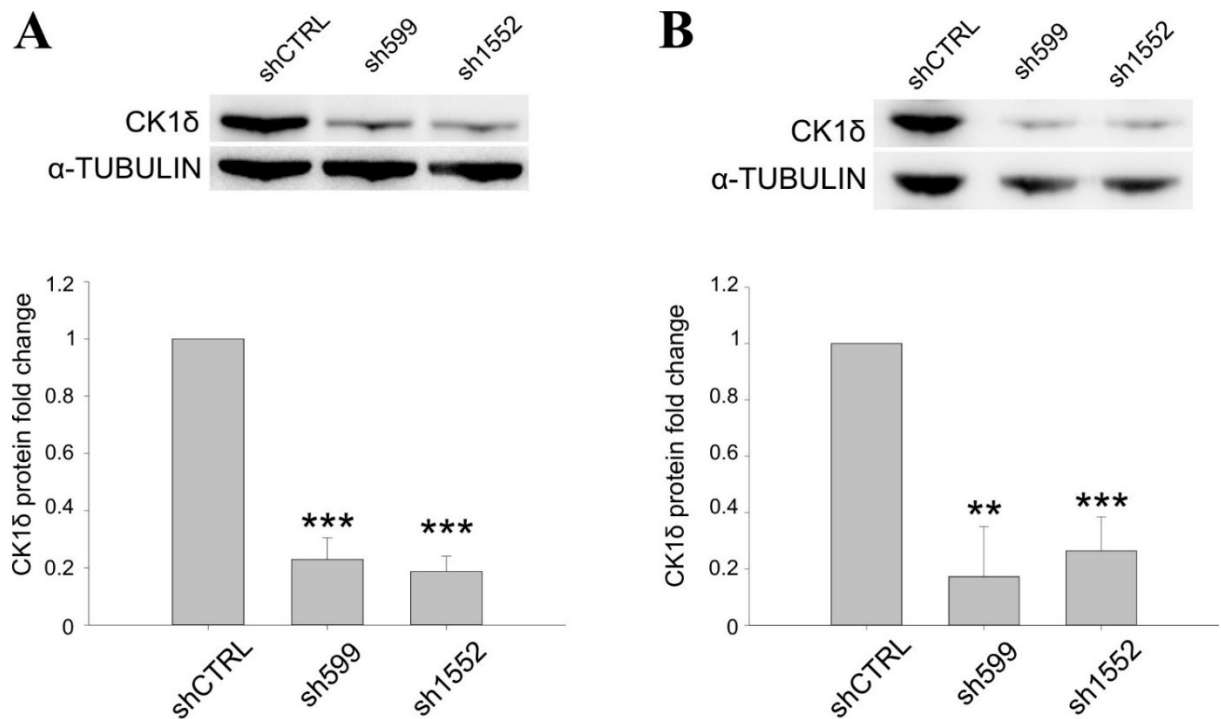


Figure 9.33. WB confirmation of CK1δ knockdown in OVCAR3 (A) and IGROV1 (B) cells. Signals were normalized to tubulin. On the top, representative blots. On the bottom, graphs represent the mean \pm S.D. (n=3). ** p<0.01; *** p<0.001

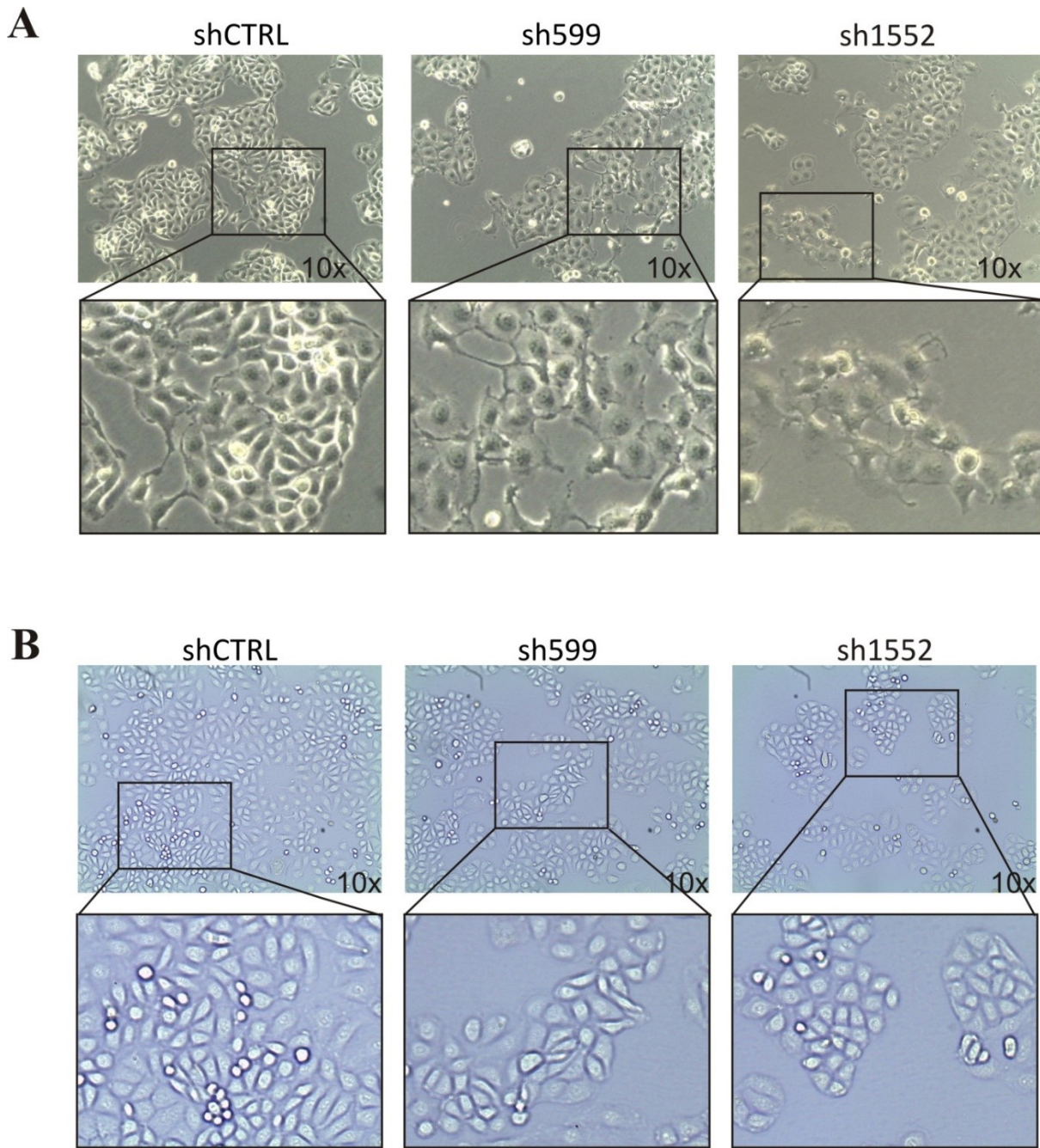


Figure 9.34. Representative pictures of OVCAR3 (A) and IGROV1 (B) cells after CK1 δ knockdown. On the bottom, magnification of the selected area.

Furthermore, cell proliferation was assessed by crystal violet assay. Growth curves showed that CK1 δ knockdown affected both cell lines in their proliferative potential (Fig. 9.35).

However, the observed differences in cell proliferation rate were not due to differences in cell viability linked to CK1 δ knockdown. Indeed, the percentage of viable cells was higher than 90% in each cell line tested (Fig. 9.36).

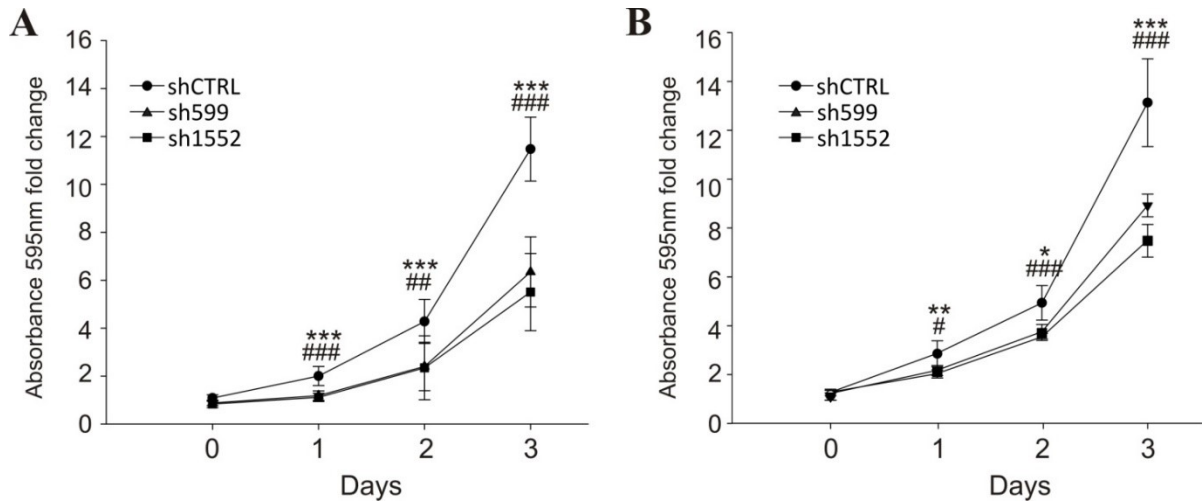


Figure 9.35. Growth curves of OVCAR3 (A) and IGROV1 (B) cells determined by crystal violet assay. Crystal violet absorbance (595 nm) was normalized to T0. Data are expressed as the mean \pm S.D. (n=6). **, ## P<0.001; ***, ### p<0.001; *sh599 vs shCTRL; #sh1552 vs shCTRL.

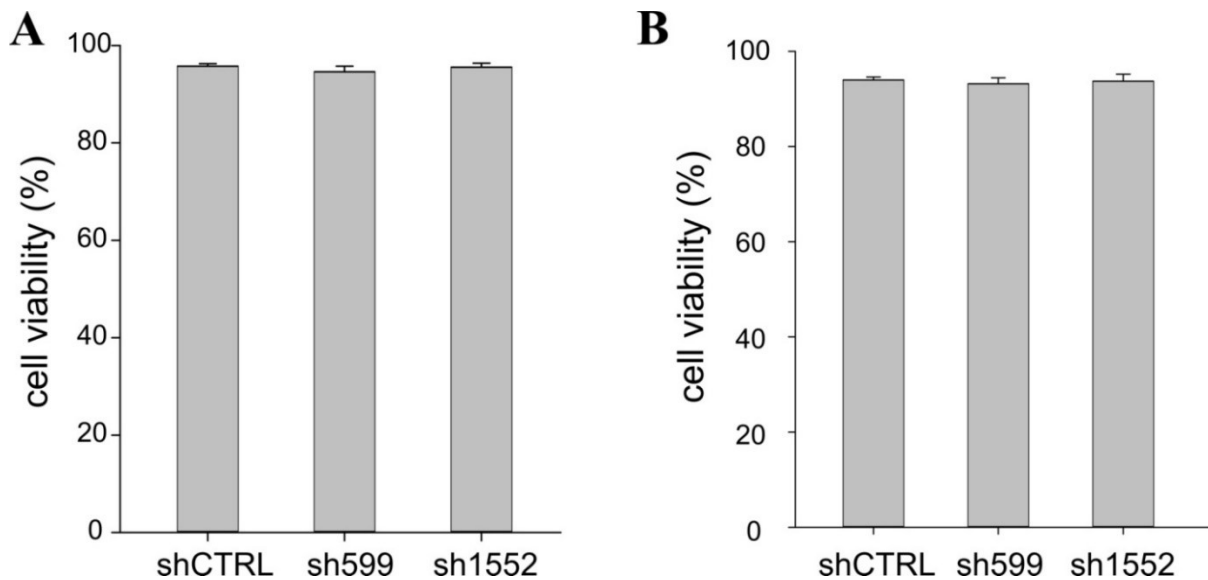


Figure 9.36. OVCAR3 (A) and IGROV1 (B) cell viability after CK1 δ knockdown. Apoptosis was assayed by Annexin-V staining. The graphs represent the mean \pm S.D. (n=5).

Eventually, we assessed the *in vivo* tumorigenic potential of knocked down OVCAR3 and IGROV1 cells injected s.c. in NSG mice. In agreement with *in vitro* experiments, and with previously published data (325), sh599 and sh1552 tumors grew slower compared to shCTRL ones (Fig. 9.37 A and 9.38 A). CK1 δ knockdown efficiency was checked at the end of the experiment (Fig. 9.37 B and 9.38 B).

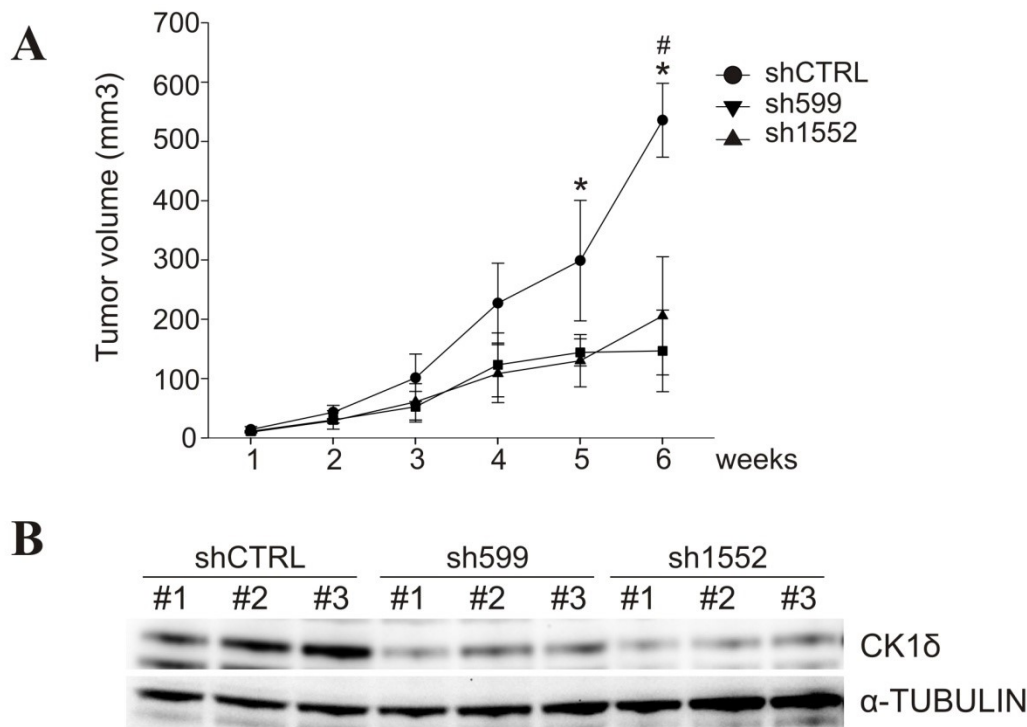


Figure 9.37. Growth curves of tumors generated by shCTRL, sh599, and sh1552 OVCAR3 cells after s.c. injection in NSG mice. Data are expressed as the mean \pm S.D. ($n=4$ /experimental group). *, # $P<0.05$; *sh599 vs shCTRL; #sh1552 vs shCTRL (A). WB analysis of CK1 δ knockdown in tumors harvested at the end of the experiment ($n=3$ /experimental group) (B).

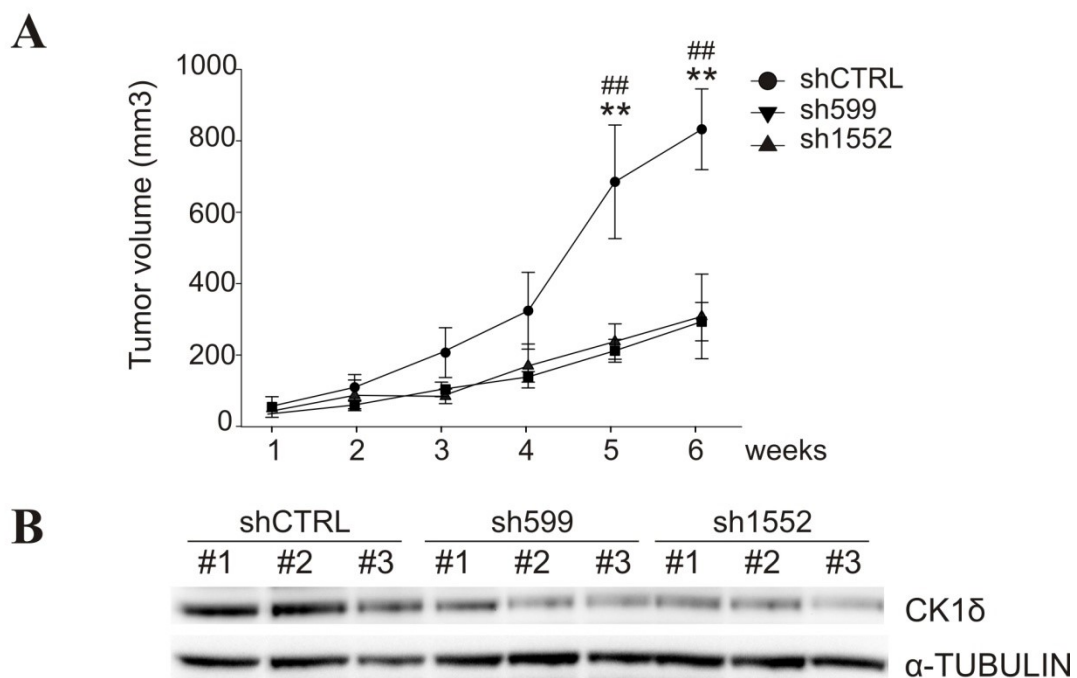


Figure 9.38. Growth curves of tumors generated by shCTRL, sh599, and sh1552 IGROV1 cells after s.c. injection in NSG mice. Data are expressed as the mean \pm S.D. ($n=5$ /experimental group). **, ## $p<0.01$; *sh599 vs shCTRL; #sh1552 vs shCTRL (A). WB analysis of CK1 δ knockdown in tumors harvested at the end of the experiment ($n=3$ /experimental group) (B).

Notably, routine checking of CK1 δ knockdown in *in vitro* cells showed that both cell lines tended to reacquire CK1 δ expression with time (Fig. 9.39). This was likely due to a counter selection of cells having low levels of CK1 δ protein. Indeed, as shown, knocked down cells were clearly disadvantaged as they were impaired in their proliferation capability.

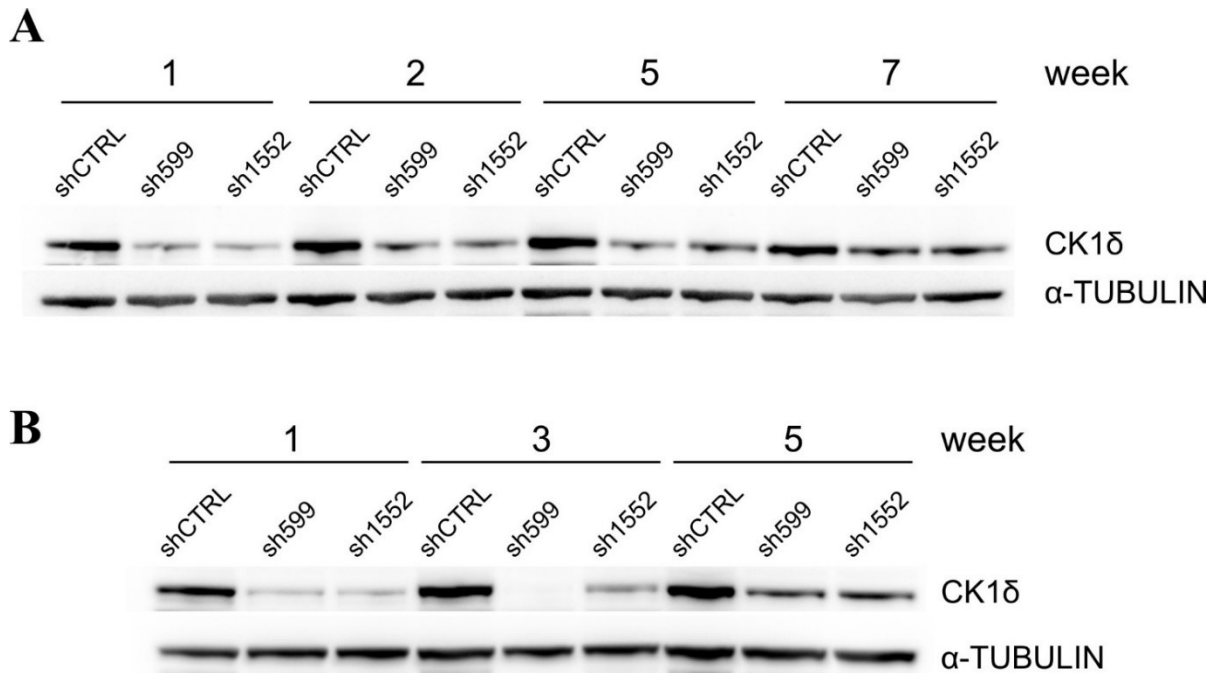


Figure 9.39. WB analysis of CK1 δ over time in shCTRL, sh599, and sh1552 OVCAR3 (A) and IGROV1 (B) cells.

9.3.2. CK1 δ knockdown is associated with p21 downregulation and sensitization to carboplatin treatment

In view of the slower growth kinetics of CK1 δ -knocked down cells, we decided to investigate the expression levels of p21(Cip1/Waf1), one of the most studied cell cycle guardians. Indeed, progression of the mammalian cell cycle is positively regulated by cyclins and cyclin-dependent kinases (CDK), while p21 disrupts the cyclin/CDK interaction and arrests the cell cycle progression at G1/S and G2/M transitions (341).

Surprisingly, we observed a significant decrease in p21 protein expression following CK1 δ knockdown in both cell lines (Fig. 9.40).

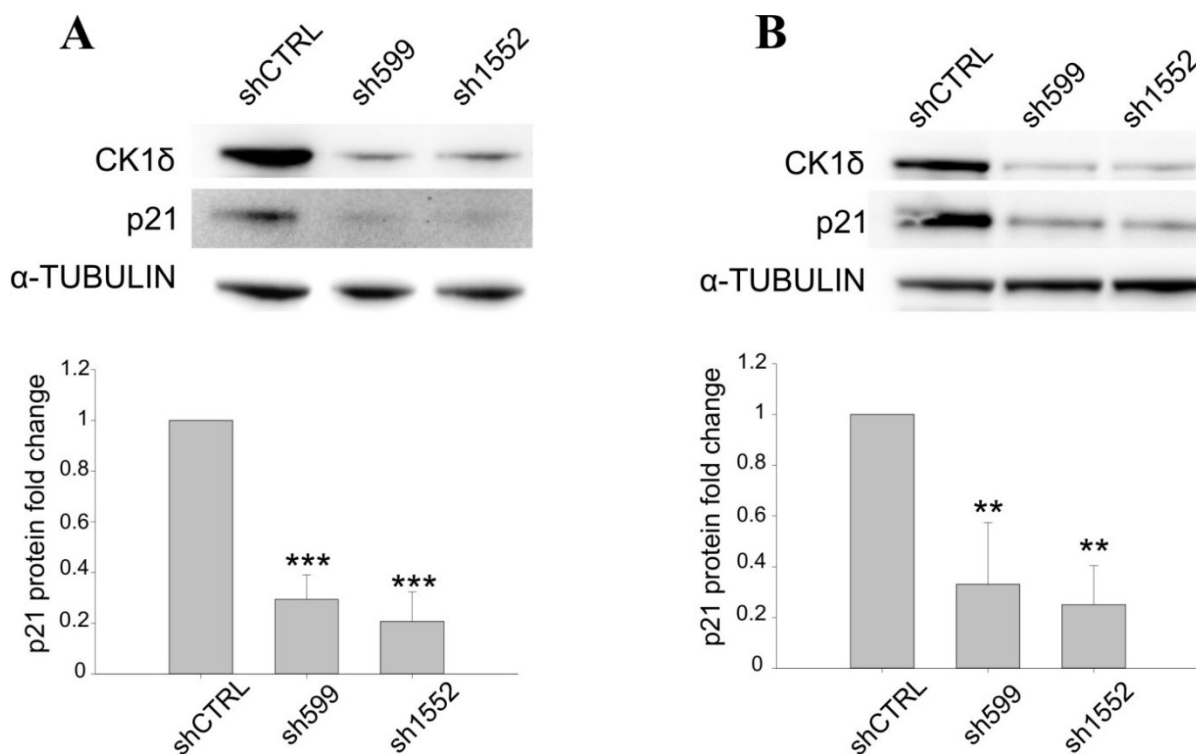


Figure 9.40. WB analysis of p21 in shCTRL, sh599, and sh1552 OVCAR3 (A) and IGROV1 (B) cells. Signals were normalized to tubulin. On the top, representative blots. On the bottom, graphs represent the mean \pm S.D. (n=3). ** p<0.01; *** p<0.001

Therefore, since p21(Cip1/Waf1) protects against apoptosis induced by DNA damage following radiation and cytotoxic agents, and as being involved in DNA repair (342), we wondered whether CK1δ-knocked down, p21(Cip1/Waf1)-deficient cells were sensitized to an alkylating agent, such as carboplatin (CPT), a first line chemotherapeutic agent for ovarian cancer patient (61). Interestingly, after 72h CPT treatment, we observed an increase in the percentage of apoptotic cells (assessed by annexin V staining) in both cell lines when CK1δ was knocked down (Fig. 9.41). As expected in a sensitization study, the greatest differences between sh599/sh1552 and shCTRL cells were observed when treated with the lowest dose tested, since at higher doses an elevated basal cell death was already present (data not shown). Hence, we can conclude that CK1δ knockdown is invariably associated to p21(Cip1/Waf1) downregulation, and, consequently, this leads to ovarian cancer cell sensitization to CPT treatment, probably due to an impaired DNA damage response and apoptosis control.

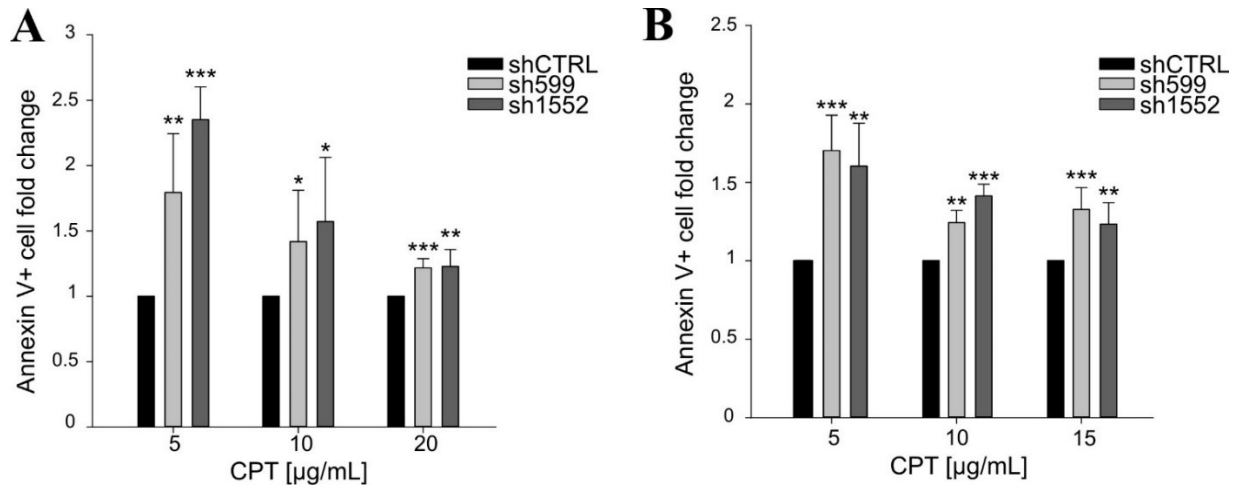


Figure 9.41. CK1 δ knockdown sensitized ovarian cancer cells to CPT treatment. ShCTRL, sh599, and sh1552 OVCAR3 (A) and IGROV1 (B) cells were challenged with scalar doses of CPT for 72h. Apoptosis was then assayed by Annexin-V staining. The graphs represent the mean \pm S.D. (n=3). Data were normalized to the corresponding shCTRL. *p<0.05; **p<0.01; ***p<0.001

9.3.3. CK1 δ knockdown affects migration in ovarian cancer cells

Since CK1 δ has been shown to regulate cell migration of triple negative breast cancer cells (343), we wanted to verify its possible involvement in the modulation of ovarian cancer cell motility. For this purpose, we performed *in vitro* wound healing and transwell assays and *in vivo* lung colonization assay.

For the wound healing assay, as shCTRL, sh599 and sh1552 OVCAR3 and IGROV1 cells reached confluence, a scratch was made in the monolayer and pictures of the wounded areas were taken at time 0 and after 24 and 48h. Interestingly, sh599 and sh1552 OVCAR3 cells were able to cover a bigger area than shCTRL cells (Fig. 9.42). Since cells were maintained in serum-free medium, cell proliferation could be excluded as a possible explanation for our observation. Therefore, CK1 δ -knocked down OVCAR3 cells were endowed with higher migratory capacity. This finding was further confirmed by transwell migration assay. Indeed, sh599 and sh1552 OVCAR3 cells moved through the transwell filter at a higher extent than shCTRL cells (Fig. 9.43).

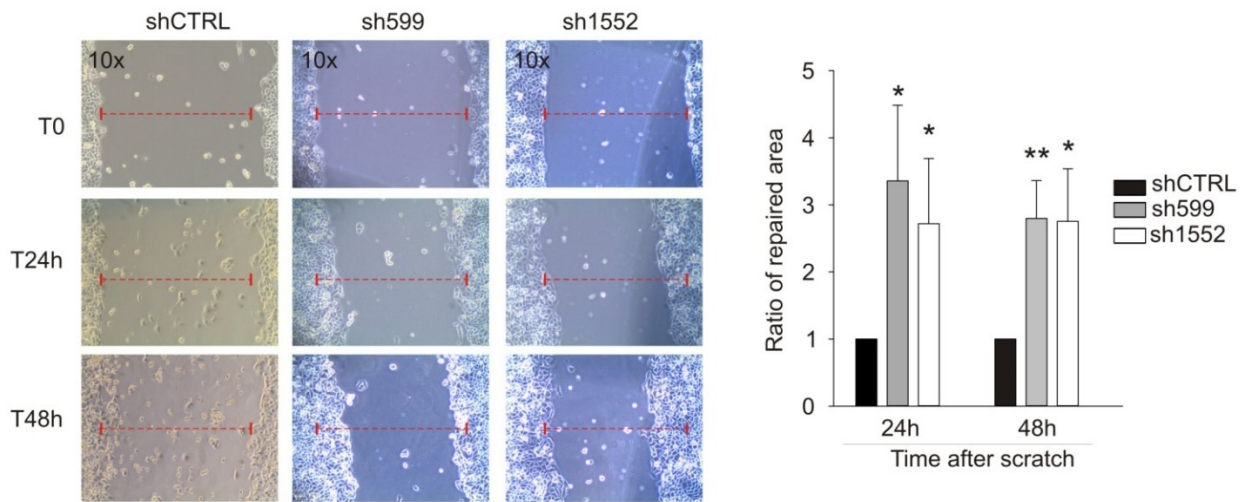


Figure 9.42. Wound healing assay performed on shCTRL, sh599, and sh1552 OVCAR3 cells. Pictures of the scratch area were taken at T0 and after 24 and 48h. Distance between the two sides of the scratch was quantified using ImageJ software. The repaired area was normalized to shCTRL. On the left, one representative experiment. On the right, the graph represents the mean of repaired area at T24 and T48h \pm S.D. (n=3). * p <0.05; ** p <0.01

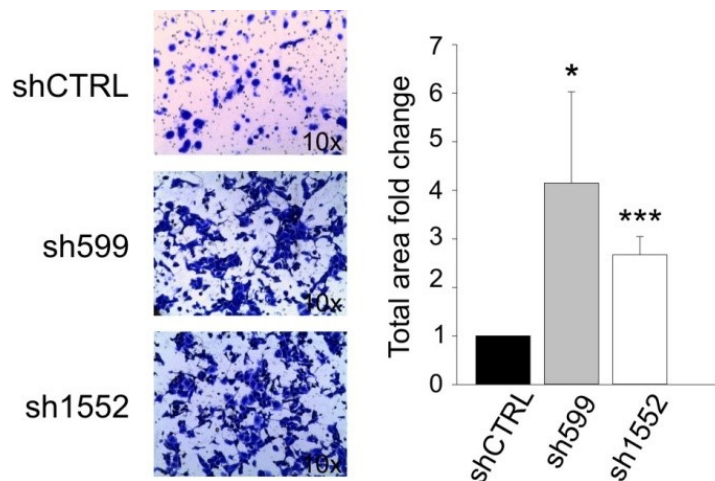


Figure 9.43. Transwell migration assay on shCTRL, sh599, and sh1552 OVCAR3 cells. On the left, representative pictures of migrated cells. On the right, the graph represents the mean fold change of total area \pm S.D. (n=3). * p <0.05; *** p <0.001

Moreover, since migration is a common trait of cells endowed with metastatic potential, we also performed an *in vivo* experimental metastasis assay. To this aim, we evaluated lung colonization ability of CK1 δ -knocked down OVCAR3 cells. First of all, firefly luciferase (Fluc)-transduced shCTRL, sh599 and sh1552 OVCAR3 cells were tested for bioluminescence intensity, showing a similar level of luciferase activity (Fig. 9.44 A). Subsequently, cells were injected into the tail vein of immunocompromised NOD/SCID mice. Imaging performed after 2h from injection showed no differences among cell lines, while 24h upon injection a higher

bioluminescence signal was observed in the lungs harvested from mice injected with sh599 or sh1552 OVCAR3 cells (Fig. 9.44 B), further proving that the absence of CK1 δ increased OVCAR3 cell motility potential.

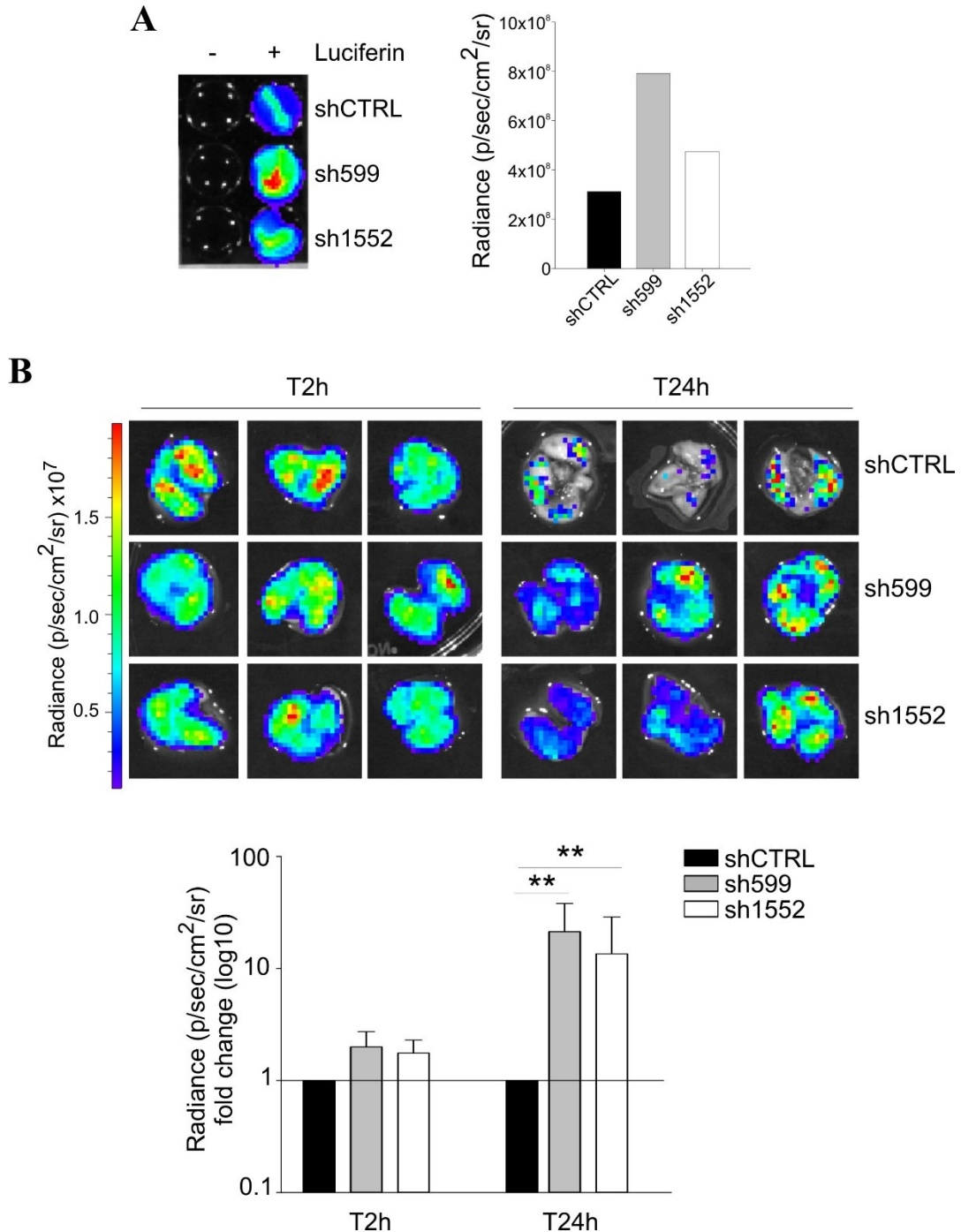


Figure 9.44. *In vitro* quantitation of bioluminescence signal in shCTRL, sh599, and sh1552 Fluc-OVCAR3 cells. On the left, pseudocolor representation of the bioluminescence intensity. Images were captured after luciferin addition. Wells without luciferin were used as negative controls. On the right, the graph represents signal quantification (A). *Ex vivo* imaging of lungs harvested at 2 and 24h after i.v. injection of shCTRL, sh599, and sh1552 Fluc-OVCAR3 cells. Representative pictures (3

Figure 9.44. (continued) mice/group) are shown at the top. At the bottom, the graph represents the mean of bioluminescence signals \pm S.D. (n=6/experimental group), normalized to shCTRL group. **p<0.01 (B)

On the contrary, wound healing (Fig. 9.45) and transwell migration assay (Fig. 9.46) revealed that shCK1 δ IGROV1 cells could migrate at a lower extent than shCTRL cells.

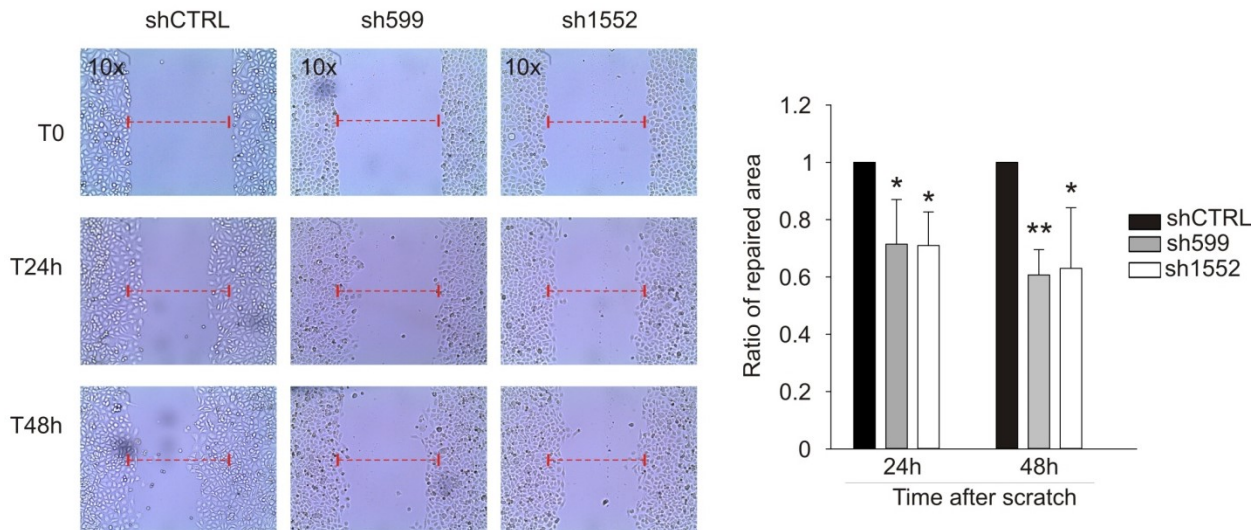


Figure 9.45. Wound healing assay performed on shCTRL, sh599, and sh1552 IGROV1 cells. Pictures of the scratch area were taken at T0 and after 24 and 48h. Distance between the two sides of the scratch was quantified using ImageJ software. The repaired area was normalized to shCTRL. On the left, one representative experiment. On the right, the graph represents the mean of repaired area at T24 and T48h \pm S.D. (n=3). *p<0.05; **p<0.01

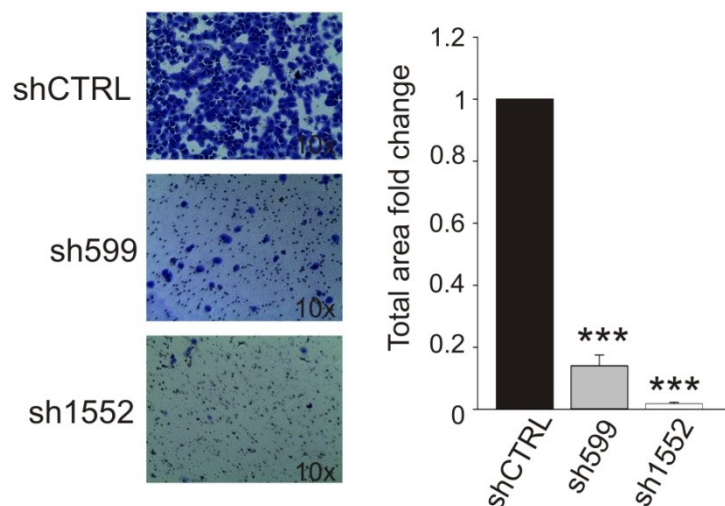


Figure 9.46. Transwell migration assay on shCTRL, sh599, and sh1552 IGROV1 cells. On the left, representative pictures of migrated cells. On the right, the graph represents the mean fold change of total area \pm S.D. (n=3). ***p<0.001

To date, we still have to perform *in vivo* lung colonization assays on IGROV1 cells, to confirm the data obtained in *in vitro* assays, that shCK1 δ IGROV1 cells have an impaired migratory capacity as compared to shCTRL cells. However, the available data suggest that, differently from growth rate, p21 expression and CPT sensitivity, CK1 δ influence on migratory capacity is more dependent on the complex cell context.

Chapter 10

**DISCUSSION AND
CONCLUSIONS**

Despite the recent advances in precision medicine, with the introduction of a variety of targeting molecules, anti-angiogenic drugs and immunologic checkpoint inhibitors (8), the standard of care for EOC is still surgery followed by chemotherapy (61). Even though the initial response rate is often high, patients finally tend to succumb to this big killer (45). This issue makes EOC a topic of intense research aimed at developing efficient screening strategies, better combination therapies and new target agents, and at discovering new Achilles' heels of the disease to overcome chemotherapy resistance.

In the last decades, cancer stem cell hypothesis has emerged to explain tumor relapse and drug resistance after initial therapeutic success and tumor regression (95). Indeed, whereas the majority of cancer cells are killed following administration of cytotoxic drugs, CSC are endowed with a series of weapons, *i.e.* detoxifying enzymes, drug extrusion pumps, efficient antioxidant systems, and the capacity of entering reversible replicative quiescence, which allow them to survive traditional therapeutic regimens (96). Since CSC represent a small fraction of the tumor bulk, these cells are undetectable by the available diagnostic instruments, and cancer seems to be cured (124). But unfortunately, as CSC are able to efficiently give rise to a whole cancer (as demonstrated by xenotransplantation assays (119)), patients can have a relapse, and the recurrent cancer is often more aggressive than the primitive one, being the result of a selection process (344). Thus, CSC targeting might be a promising strategy to overcome the many issues linked to EOC management.

Over the years, CSC have been described in a variety of solid and hematological malignancies (99-117). Since 2005, also the identification of CSC in EOC has been reported in several studies (233-241) and Authors took advantage of different surface and functional marker for CSC isolation in EOC. In particular, Zhang *et al.* validated CD44/CD117 double positive cells as *bona fide* CSC in primary samples of ovarian cancer (223). Our group confirmed this finding in our cohort of patients by isolating cancer cells from ascitic effusions (182). Moreover, in view of metabolic reprogramming as a new hallmark of cancer (326), we evaluated the metabolic fingerprint of CSC compared to the non-stem counterpart, and we found a prominent OXPHOS activity (182).

Since autophagy is another aspect of cell metabolism, we decided to investigate its possible involvement in ovarian cancer. This pathway has been shown to play relevant and contrasting roles both in tumorigenesis and cancer progression (287). In recent years, the activation of autophagy has been identified as a mechanism potentially exploited by CSC to survive stress conditions such as chemotherapy treatment (294-303). However, the precise role

of this pathway in CSC maintenance is still unknown in ovarian cancer. For this reason, we decided to evaluate autophagy activation and the effects of its perturbation in CSC from ascitic effusions collected from EOC-bearing patients and in *in vitro* CD117-enriched cell populations. Experiments revealed a higher basal autophagy activation in CSC compared to the non-CSC counterpart, as demonstrated by higher LC3-II protein levels, autophagosome staining, and lower p62 levels.

The treatment with the autophagy inhibitor chloroquine (CQ) demonstrated the importance of autophagy in sustaining the canonical CSC properties. Indeed, results indicated that CQ affected the viability and the growth of cells cultured in spheroid-forming conditions to a higher extent than in adherent culture conditions.

Autophagy is induced in established cancers as a survival mechanism in response to a variety of stress conditions, including chemo- and radiotherapy (287, 336, 345). Accordingly, besides being a molecule used in *in vitro* studies to inhibit autophagy (288), clinical trials with CQ and its derivative hydroxychloroquine (HCQ) have been undertaken to improve the response of refractory cancers to chemotherapy (293) and, thus to overcome therapy resistance (346). Since carboplatin (CPT) treatment activated autophagy in EOC cells, especially in CSC, a combination treatment with CQ was tested on spheroids exerting a synergistic effect as shown by reduced spheroid diameter and number of progenitor cells. This result was further corroborated by *in vivo* experiments in which the combined therapy significantly reduced tumor growth, compared to CQ and CPT single treatments, by affecting the CSC compartment. All these findings suggest a CSC cytotoxic role for CQ and, hence, autophagy inhibition as a strategy to mine CSC survival during chemotherapy.

The enhancement of chemotherapy effectiveness mediated by chloroquine treatment has been already observed in other cancers, such as liver (347), pancreas (348), breast (349) and colon (350). However, the impact of this treatment on CSC survival has been rarely taken into consideration. Our results suggest a possible clinical application of the CPT/CQ combined therapy in the treatment of EOC offering the possibility to counteract tumor growth and impair the CSC compartment, likely preventing tumor relapse.

In conclusion, these results, published in 2017 (242), point to the combination of autophagy inhibition with anticancer treatment as a possible strategy to overcome the limits of current therapies in the eradication of EOC CSC population.

The features of CSC are intrinsic cell properties but they can also be driven and modulated by extrinsic cues coming from the microenvironment (96, 98). Indeed, the stroma as well as cells

of myeloid origin secrete a plethora of growth factors and cytokines that sustain CSC survival and activate the key self-renewal signaling pathways and the EMT program (197, 199). Since CD117, alias c-Kit, has been identified as a CSC marker in EOC (182, 223), we wondered if, beyond being a surface marker, it could also play a functional role in maintaining and sustaining the CD117⁺ EOC cells.

To this end, we focused on SCF, the c-Kit ligand, a cytokine produced either as soluble or as a membrane-associated protein (252) both in physiological and pathological conditions (257, 274, 275). The presence of SCF in EOC ascites as well as in the ascites of patients affected by benign ovarian diseases was already reported by other groups (351). Accordingly, we found soluble SCF in the ascitic fluid of EOC-bearing patients, but its levels were much higher than those reported by Chudecka-Gláz *et al.* (1306.8 pg/mL vs 28.8 pg/mL), a discrepancy likely attributable to the different technique used to quantify the cytokine (351). Notably, to our knowledge, the presence of SCF has never been investigated in the ascites caused by other benign and malignant conditions.

After SCF detection in EOC ascites, FACS sorting allowed the isolation of cancer cells, TAM, TAF and TIL from the ascitic fluid and helped us in identifying the cell subsets responsible for soluble SCF production and release. Only TAM and TAF secreted SCF as demonstrated by ELISA assay performed on cell supernatants, while cancer cells (CSC and non-CSC) were negative for soluble SCF. Nonetheless, tumor cells presented SCF expression at the membrane level (as assessed by FACS analysis) suggesting either the unique expression of the membrane-associated isoform or, if ever, the production of very small amounts of the soluble ligand. These results are schematically summarized in Fig. 10.1.

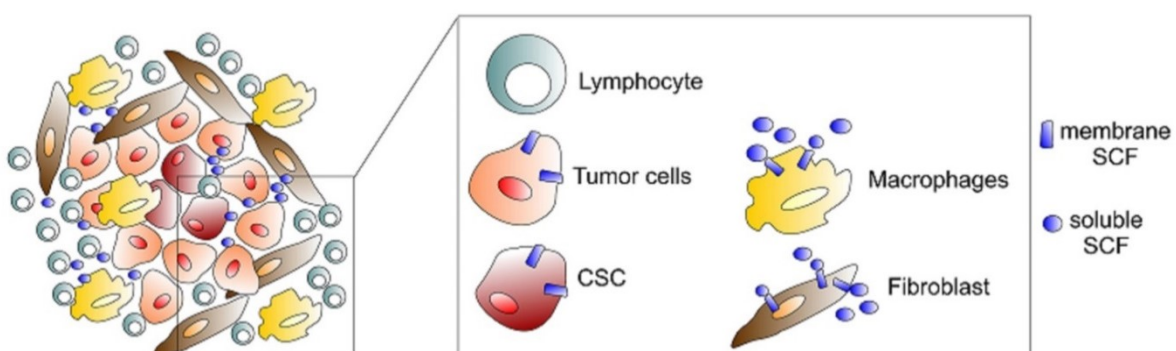


Figure 10.1. Scheme summarizing SCF production by cell subsets from EOC ascites.

It is well known from literature that SCF is mainly produced by fibroblasts (337, 352), together with endothelial cells, which release the cytokine into the bloodstream (353, 354). Recently, SCF production by TAM isolated from ascitic effusions of EOC-bearing patients was reported (355). In the same work, the Authors could detect SCF expression neither in ascites-associated T-cells nor in the cancer cells clusters (355), congruently with our findings. Since differently polarized TAM (M1 and M2) play opposite roles as tumor orchestrators, acting as anti-tumoral and pro-tumoral cells, respectively (356), we focused our attention on this cell population. First, we wondered whether *in vitro* differentiated (M0) and M1/M2 polarized macrophages were able to produce SCF and if there was any difference among the different cell populations. M0, M1 and M2 macrophages expressed SCF, while the monocytes from which macrophages were derived were completely negative. Moreover, ELISA analysis evidenced that all macrophage populations secreted soluble SCF, but M1 cells with a faster kinetics. Notably, SCF levels recorded in such an artificial differentiation system were much lower (almost one order of magnitude) than those detected in naturally occurring TAM. This discrepancy might be explained by the different cues acting on TAM in the ascitic fluid, and the restricted cytokine cocktail used *in vitro* to differentiate and polarize macrophages, that could induce different expression levels of SCF (as assessed by qRT-PCR, data not shown). Therefore, we can conclude that monocyte-to-macrophage differentiation is sufficient to induce SCF expression, irrespectively of M1 or M2 polarization.

SCF binding to its receptor c-Kit triggers the activation of different molecular cascades among which the pro-survival Akt pathway (253). Technical limitations forced us to use a cell model (the CD117⁺ KASUMI1 cell line), different from ovarian CSC to test SCF-induced pathway activation. Stimulation of KASUMI1 cells with hrSCF and membrane-associated SCF (SCF-RAJI) induced c-Kit and Akt activation, indicating receptor responsiveness to both isoforms. On the contrary, the multitarget tyrosine kinase inhibitor imatinib (272) prevented the pathway activation. Hence, SCF stimulation efficiently induces the activation of the pro-survival pathway in CD117⁺ cells and this observation can be most likely extended to ovarian CSC present in the patient ascites, even if a formal demonstration is still missing.

Nonetheless, SCF treatment of ovarian cancer cell spheroids increased the spheroid-forming ratio and the expression of the stemness master genes Oct4, Sox2 and Nanog in EOC cells, while imatinib counteracted this effect. This result is in accordance with the previous work by Chau *et al.* (244) in which c-Kit knockdown or imatinib treatment affected the canonical stemness features of ovarian cancer cells. Therefore, SCF seems to play a role in the maintenance and support of ovarian CSC by helping them to survive in a selective and hostile

environment (anchorage-independent growth) as the spheroid culture conditions and the patient ascitic fluid.

Interestingly, several phase II clinical trials have been undertaken in the last decade (245-247) relative to the use of imatinib as a maintenance treatment in EOC patients in complete regression after chemotherapy. Unfortunately, these studies showed a minimal activity, a result that could be altered by the lack of EOC patient stratification according to CD117 expression (it is detected only in the 30-40% of cases (238)). Moreover, although numerous studies indicated CD117 as the stemness marker, very little information is available regarding its biological function in ovarian CSC (357) and future efforts should be dedicated to understanding its role in these cells.

Nevertheless, our results seem to suggest a pro-survival role for SCF and the relative downstream signaling in ovarian CSC.

Besides CSC, EOC carcinogenesis is supported by numerous genetic and epigenetic alterations and aberrant signaling molecule activation (358-364). Due to its reported genetic amplification in EOC and its tumor-favoring role described in different cancers (310), we focused on CK1 δ , a member of a kinase family characterized by pleiotropic cellular functions, including cell cycle progression, p53 control, mitotic spindle arrangement, and circadian rhythm protein turnover (313). Interestingly, proteins involved in circadian rhythm control, *e.g.* PER, CRY, BMAL1, CLOCK, are highly expressed in the ovaries, where they regulate ovulation and hormonal cycles in general (360, 365), and alterations in their expression levels are associated with an increased risk of ovarian cancer and affect cancer growth, invasiveness, and drug sensitivity (366-368). Moreover, CK1 δ has been described as a positive regulator of Wnt and Hh canonical stemness signaling pathways (316), thus suggesting that its overexpression might support CSC functions and properties, even though we did not investigate this aspect in the present work.

Previous work highlighted a negative impact of CK1 δ inhibition on cell cycle progression and proper mitosis, eventually leading to apoptosis (318-321). Moreover, *in vivo* breast and pancreatic tumor growth was delayed by CK1 δ inhibitor administration (324, 325), and recently, impaired cell migration and metastases of triple negative breast cancer were also assessed (343).

In order to determine if CK1 δ plays also a role in ovarian cancer cell biology, CK1 δ expression was first checked in a panel of EOC cell lines and PDX samples displaying high protein levels in all the specimens. Genetic ablation of CK1 δ in OVCAR3 and IGROV1 ovarian cancer cells impaired cell proliferation in both cell lines, and accordingly, CK1 δ deficient cells gave rise to

smaller tumors in immunocompromised mice in agreement with previous literature (324, 325). Moreover, the expression of CK1 δ in knocked down cells was recovered with passages underlying the detrimental effect of the kinase depletion on cell proliferation and survival.

Nuclear p21(Cip1/Waf1) acts as a tumor-suppressor arresting cell cycle progression by disrupting CDK/cyclins complexes and by associating to proliferating cell nuclear antigen (PCNA), and it can be induced in a p53-dependent and independent manner (341). This motivated us to check p21 expression levels in CK1 δ -knocked down cells, and surprisingly, we found a lower protein expression. Nonetheless, high p21 protein levels in the cytoplasm have been shown to convey mitogenic signals in vascular smooth muscle cells, augmenting the transit through cell cycle, as opposite to nuclear p21 function (369), and this could link the proliferation arrest to the reduced p21 protein levels.

Besides having a role in cell cycle control, p21 is involved in DNA repair (342) and, when it localizes to the cytoplasm, it determines an apoptosis-resistant phenotype, acting as a tumor-promoting factor (370). For instance, renal cancer is usually difficult to treat because chemo-resistant, due to a highly effective DNA repair response mediated by high p21 levels (371). P21 attenuation by antisense oligonucleotides (372), small molecules (371), or sorafenib (373), is associated to increased chemo-sensitivity, with higher apoptosis rates after doxorubicin, paclitaxel and cisplatin treatment. In prostate cancer, infiltrating mast cells induced p21 expression, thus increasing docetaxel resistance (374). Accordingly, Pavan *et al.* (375) reported that IRF-1 knockdown sensitized ovarian cancer cells to cisplatin because of impaired p21 induction.

Therefore, we checked whether p21 attenuation in CK1 δ -knocked down cells similarly sensitized EOC cells to CPT treatment. Congruently, we observed a higher proportion of apoptotic cells in shCSNK1D ovarian cancer cells compared to control ones, meaning a sensitization to CPT treatment. Moreover, a recent paper reported that CK1 δ knockdown impaired breast cancer cell migration and invasion and upregulated epithelial markers such as claudin1 and occludin (343). Accordingly, specific knockdown of the CK1 δ highly related kinase, CK1 ϵ , demonstrated a 60–80% reduction in the migration ability of the EOC cell line SKOV3 (376).

Likewise, different migration assays performed on IGROV1 cells revealed a reduced migration capacity of CK1 δ knocked-down cells. On the contrary, the opposite phenomenon was observed when the same experiments were performed on OVCAR3 cells. Indeed, shCK1 δ OVCAR3 cells presented a higher migration capacity both *in vitro* and *in vivo*. So far, there is no definitive explanation of CK1 δ role in determining either a pro- or anti-migratory phenotype in EOC.

Likely, this kinase plays different roles depending on the complex cellular context, and further work is required to unveil the molecular mechanism underlying this CK1 δ -dependent phenomenon. The spiky morphology acquired by OVCAR3 cells following transduction reminded us about EMT. However, EMT marker analysis did not show any significant difference (data not shown), and thus we excluded EMT as a possible explanation.

In summary, we have identified CK1 δ as an important player in the regulation of cell proliferation and response to chemotherapeutic drugs in ovarian cancer cells. Our results would suggest CK1 δ as an attractive target for ovarian cancer treatment, but further investigation regarding its role in migration is mandatory before the introduction of CK1 δ/ϵ inhibitors into the clinics for EOC management.

AKNOWLEDGMENTS

The research was funded by the European Commission, Seventh Framework Program (FP7/2007-2013) under Grant Agreement no. 600376. This work was also supported by grants from the Italian Association for Cancer Research (AIRC) (grants #N14032) and by IOV 5 per mille.

First, I would like to thank Prof. Zanovello for giving me the opportunity of being part of the PhD school she coordinates.

Moreover, I would like to thank Prof. Amadori for being my mentor during these three years of research.

I cannot help but thank all my group: Dr. Simona Pavan, Dr. Anna Pastò, Dr. Giorgia Pilotto, Dr. Anna Pagotto, and Elisa Ceppelli. We spent together days of joy and a lot of days of sorrow. But always together. In particular, my biggest thank goes to Dr. Simona Pavan and Dr. Anna Pastò for their valuable guidance in planning, performing, and analyzing experiments. They supported me greatly both from a scientific and a human point of view. If this thesis is good from a linguistic and a conceptual point of view, Simona must be given credit: her critical reading correction made this work better.

I must thank all my PhD colleagues: Marina, Martina, Manuela, Gloria, Flavia, Giulia B., Giulia C., Rocco, Sandro, and Fabio, for the time spent together and the adventures and misadventures we shared. All the people I met at IOV deserve a particular thank: in these three years, I have been spending much more in their company than with my family.

My flatmates also deserve a particular mention: Leonardo, Sara, Mariangela, Isadora, Takatso, and Wesly. Thanks for being my Paduan family.

I cannot forget my parents. I know how much they suffer because I am not at home with them, and I appreciate that they accepted and supported my choice to attend my PhD far from home. Thank you for supporting and bearing me.

Then, there are my uncles, aunts, cousins, and friends.

Finally, the person who saw all the writing phases, assisted and encouraged me: my boyfriend Alberto, to whom this thesis is dedicated.

REFERENCES

1. <https://www.cancer.org/cancer/ovarian-cancer/about/what-is-ovarian-cancer.html#references> [
2. Boussios S, Zarkavelis G, Seraj E, Zerdes I, Tatsi K, Pentheroudakis G. Non-epithelial Ovarian Cancer: Elucidating Uncommon Gynaecological Malignancies. *Anticancer Res.* 2016;36(10):5031-42.
3. Cramer DW. The epidemiology of endometrial and ovarian cancer. *Hematol Oncol Clin North Am.* 2012;26(1):1-12.
4. Boussios S, Moschetta M, Zarkavelis G, Papadaki A, Kefas A, Tatsi K. Ovarian sex-cord stromal tumours and small cell tumours: Pathological, genetic and management aspects. *Critical Reviews in Oncology / Hematology.* 2017;120:43-51.
5. Lim D, Oliva E. Ovarian sex cord-stromal tumours: an update in recent molecular advances. *Pathology.* 2018;50(2):178-89.
6. Shih Ie M, Kurman RJ. Ovarian tumorigenesis: a proposed model based on morphological and molecular genetic analysis. *Am J Pathol.* 2004;164(5):1511-8.
7. Fukumoto M, Nakayama K. Ovarian epithelial tumors of low malignant potential: are they precursors of ovarian carcinoma? *Pathol Int.* 2006;56(5):233-9.
8. Garces AH, Dias MS, Paulino E, Ferreira CG, de Melo AC. Treatment of ovarian cancer beyond chemotherapy: are we hitting the target? *Cancer Chemother Pharmacol.* 2015;75(2):221-34.
9. Hoppenot C, Eckert MA, Tienda SM, Lengyel E. Who are the long-term survivors of high grade serous ovarian cancer? *Gynecol Oncol.* 2018;148(1):204-12.
10. Siegel RL, Miller KD, Jemal A. Cancer statistics, 2018. *CA Cancer J Clin.* 2018;68(1):7-30.
11. AIOM A. I numeri del cancro in Italia 20162016.
12. http://globocan.iarc.fr/Pages/fact_sheets_population.aspx [
13. Jayson GC, Kohn EC, Kitchener HC, Ledermann JA. Ovarian cancer. *Lancet.* 2014;384(9951):1376-88.
14. Clarke-Pearson DL. Clinical practice. Screening for ovarian cancer. *N Engl J Med.* 2009;361(2):170-7.
15. Ozols RF, Bookman MA, Connolly DC, Daly MB, Godwin AK, Schilder RJ, et al. Focus on epithelial ovarian cancer. *Cancer Cell.* 2004;5(1):19-24.

16. Titus-Ernstoff L, Perez K, Cramer DW, Harlow BL, Baron JA, Greenberg ER. Menstrual and reproductive factors in relation to ovarian cancer risk. *Br J Cancer*. 2001;84(5):714-21.
17. Chiaffarino F, Pelucchi C, Parazzini F, Negri E, Franceschi S, Talamini R, et al. Reproductive and hormonal factors and ovarian cancer. *Ann Oncol*. 2001;12(3):337-41.
18. Purdie DM, Bain CJ, Siskind V, Webb PM, Green AC. Ovulation and risk of epithelial ovarian cancer. *Int J Cancer*. 2003;104(2):228-32.
19. La Vecchia C. Ovarian cancer: epidemiology and risk factors. *Eur J Cancer Prev*. 2017;26(1):55-62.
20. Ness RB, Dodge RC, Edwards RP, Baker JA, Moysich KB. Contraception methods, beyond oral contraceptives and tubal ligation, and risk of ovarian cancer. *Ann Epidemiol*. 2011;21(3):188-96.
21. Fathalla MF. Incessant ovulation and ovarian cancer - a hypothesis re-visited. *Facts Views Vis Obgyn*. 2013;5(4):292-7.
22. Ness RB, Cottreau C. Possible role of ovarian epithelial inflammation in ovarian cancer. *J Natl Cancer Inst*. 1999;91(17):1459-67.
23. Balkwill F, Charles KA, Mantovani A. Smoldering and polarized inflammation in the initiation and promotion of malignant disease. *Cancer Cell*. 2005;7(3):211-7.
24. Green A, Purdie D, Bain C, Siskind V, Russell P, Quinn M, et al. Tubal sterilisation, hysterectomy and decreased risk of ovarian cancer. Survey of Women's Health Study Group. *Int J Cancer*. 1997;71(6):948-51.
25. Cramer DW, Liberman RF, Titus-Ernstoff L, Welch WR, Greenberg ER, Baron JA, et al. Genital talc exposure and risk of ovarian cancer. *Int J Cancer*. 1999;81(3):351-6.
26. Berge W, Mundt K, Luu H, Boffetta P. Genital use of talc and risk of ovarian cancer: a meta-analysis. *Eur J Cancer Prev*. 2018;27(3):248-57.
27. Narod SA. Talc and ovarian cancer. *Gynecol Oncol*. 2016;141(3):410-2.
28. Houghton SC, Reeves KW, Hankinson SE, Crawford L, Lane D, Wactawski-Wende J, et al. Perineal powder use and risk of ovarian cancer. *J Natl Cancer Inst*. 2014;106(9).
29. Cramer DW, Titus-Ernstoff L, McKolanis JR, Welch WR, Vitonis AF, Berkowitz RS, et al. Conditions associated with antibodies against the tumor-associated antigen MUC1 and their relationship to risk for ovarian cancer. *Cancer Epidemiol Biomarkers Prev*. 2005;14(5):1125-31.
30. Pearce CL, Chung K, Pike MC, Wu AH. Increased ovarian cancer risk associated with menopausal estrogen therapy is reduced by adding a progestin. *Cancer*. 2009;115(3):531-9.

31. Stewart LM, Holman CD, Finn JC, Preen DB, Hart R. In vitro fertilization is associated with an increased risk of borderline ovarian tumours. *Gynecol Oncol.* 2013;129(2):372-6.
32. Stewart LM, Holman CD, Aboagye-Sarfo P, Finn JC, Preen DB, Hart R. In vitro fertilization, endometriosis, nulliparity and ovarian cancer risk. *Gynecol Oncol.* 2013;128(2):260-4.
33. Leitzmann MF, Koebnick C, Danforth KN, Brinton LA, Moore SC, Hollenbeck AR, et al. Body mass index and risk of ovarian cancer. *Cancer.* 2009;115(4):812-22.
34. Beral V, Gaitskell K, Hermon C, Moser K, Reeves G, Peto R. Ovarian cancer and smoking: individual participant meta-analysis including 28,114 women with ovarian cancer from 51 epidemiological studies. *Lancet Oncol.* 2012;13(9):946-56.
35. Bartosch C, Clarke B, Bosse T. Gynaecological neoplasms in common familial syndromes (Lynch and HBOC). *Pathology.* 2018;50(2):222-37.
36. Watson P, Vasen HFA, Mecklin JP, Bernstein I, Aarnio M, Jarvinen HJ, et al. The risk of extra-colonic, extra-endometrial cancer in the Lynch syndrome. *Int J Cancer.* 2008;123(2):444-9.
37. Malander S, Rambech E, Kristoffersson U, Halvarsson B, Ridderheim M, Borg A, et al. The contribution of the hereditary nonpolyposis colorectal cancer syndrome to the development of ovarian cancer. *Gynecol Oncol.* 2006;101(2):238-43.
38. Lu FI, Gilks CB, Mulligan AM, Ryan P, Allo G, Sy K, et al. Prevalence of loss of expression of DNA mismatch repair proteins in primary epithelial ovarian tumors. *Int J Gynecol Pathol.* 2012;31(6):524-31.
39. King MC, Marks JH, Mandell JB. Breast and ovarian cancer risks due to inherited mutations in BRCA1 and BRCA2. *Science.* 2003;302(5645):643-6.
40. Simchoni S, Friedman E, Kaufman B, Gershoni-Baruch R, Orr-Urtreger A, Kedar-Barnes I, et al. Familial clustering of site-specific cancer risks associated with BRCA1 and BRCA2 mutations in the Ashkenazi Jewish population. *Proc Natl Acad Sci U S A.* 2006;103(10):3770-4.
41. Zhang S, Royer R, Li S, McLaughlin JR, Rosen B, Risch HA, et al. Frequencies of BRCA1 and BRCA2 mutations among 1,342 unselected patients with invasive ovarian cancer. *Gynecol Oncol.* 2011;121(2):353-7.
42. Cunningham JM, Cicek MS, Larson NB, Davila J, Wang C, Larson MC, et al. Clinical characteristics of ovarian cancer classified by BRCA1, BRCA2, and RAD51C status. *Sci Rep.* 2014;4:4026.

43. Baldwin RL, Nemeth E, Tran H, Shvartsman H, Cass I, Narod S, et al. BRCA1 promoter region hypermethylation in ovarian carcinoma: a population-based study. *Cancer Res.* 2000;60(19):5329-33.
44. Daly MB, Pilarski R, Berry M, Buys SS, Farmer M, Friedman S, et al. NCCN Guidelines Insights: Genetic/Familial High-Risk Assessment: Breast and Ovarian, Version 2.2017. *J Natl Compr Canc Netw.* 2017;15(1):9-20.
45. Openshaw MR, Fotopoulou C, Blagden S, Gabra H. The next steps in improving the outcomes of advanced ovarian cancer. *Womens Health (Lond).* 2015;11(3):355-67.
46. Norquist BM, Harrell MI, Brady MF, Walsh T, Lee MK, Gulsuner S, et al. Inherited Mutations in Women With Ovarian Carcinoma. *JAMA Oncol.* 2016;2(4):482-90.
47. Prat J. Staging classification for cancer of the ovary, fallopian tube, and peritoneum. *Int J Gynaecol Obstet.* 2014;124(1):1-5.
48. UICC. TNM classification of malignant tumours. Eighth edition ed2017.
49. <http://www.cancerresearchuk.org/about-cancer/ovarian-cancer/stages-grades/about-stages-and-grades>.
50. Aletti GD, Peiretti M. Quality control in ovarian cancer surgery. *Best Pract Res Clin Obstet Gynaecol.* 2017;41:96-107.
51. Lim AW, Mesher D, Gentry-Maharaj A, Balogun N, Jacobs I, Menon U, et al. Predictive value of symptoms for ovarian cancer: comparison of symptoms reported by questionnaire, interview, and general practitioner notes. *J Natl Cancer Inst.* 2012;104(2):114-24.
52. Jacobs IJ, Menon U. Progress and challenges in screening for early detection of ovarian cancer. *Mol Cell Proteomics.* 2004;3(4):355-66.
53. <https://www.mayoclinic.org/diseases-conditions/ovarian-cancer/diagnosis-treatment/drc-20375946>.
54. Jacobs I, Oram D, Fairbanks J, Turner J, Frost C, Grudzinskas JG. A risk of malignancy index incorporating CA 125, ultrasound and menopausal status for the accurate preoperative diagnosis of ovarian cancer. *Br J Obstet Gynaecol.* 1990;97(10):922-9.
55. Yamamoto Y, Yamada R, Oguri H, Maeda N, Fukaya T. Comparison of four malignancy risk indices in the preoperative evaluation of patients with pelvic masses. *Eur J Obstet Gynecol Reprod Biol.* 2009;144(2):163-7.
56. Jelovac D. Recent Progress in the Diagnosis and Treatment of Ovarian Cancer. 2011;61(3):183-203.
57. Kuhn E, Kurman RJ, Shih IM. Ovarian Cancer Is an Imported Disease: Fact or Fiction? *Curr Obstet Gynecol Rep.* 2012;1(1):1-9.

58. Piek JM, van Diest PJ, Verheijen RH. Ovarian carcinogenesis: an alternative hypothesis. *Adv Exp Med Biol.* 2008;622:79-87.
59. Henderson JT, Webber EM, Sawaya GF. Screening for Ovarian Cancer: Updated Evidence Report and Systematic Review for the US Preventive Services Task Force. *Jama.* 2018;319(6):595-606.
60. Rosenthal AN, Fraser L, Manchanda R, Badman P, Philpott S, Mozersky J, et al. Results of annual screening in phase I of the United Kingdom familial ovarian cancer screening study highlight the need for strict adherence to screening schedule. *J Clin Oncol.* 2013;31(1):49-57.
61. Marchetti C, Pisano C, Facchini G, Bruni GS, Magazzino FP, Losito S, et al. First-line treatment of advanced ovarian cancer: current research and perspectives. *Expert Rev Anticancer Ther.* 2010;10(1):47-60.
62. Narod S. Can advanced-stage ovarian cancer be cured? *Nat Rev Clin Oncol.* 2016;13(4):255-61.
63. Lim HJ, Ledger W. Targeted therapy in ovarian cancer. *Womens Health (Lond).* 2016;12(3):363-78.
64. Ozols RF. Treatment goals in ovarian cancer. *Int J Gynecol Cancer.* 2005;15 Suppl 1:3-11.
65. McGuire WP, Hoskins WJ, Brady MF, Kucera PR, Partridge EE, Look KY, et al. Cyclophosphamide and cisplatin compared with paclitaxel and cisplatin in patients with stage III and stage IV ovarian cancer. *N Engl J Med.* 1996;334(1):1-6.
66. Bookman MA, Greer BE, Ozols RF. Optimal therapy of advanced ovarian cancer: carboplatin and paclitaxel vs. cisplatin and paclitaxel (GOG 158) and an update on GOG0 182-ICON5. *Int J Gynecol Cancer.* 2003;13(6):735-40.
67. <https://www.cancer.org/cancer/ovarian-cancer/detection-diagnosis-staging/survival-rates.html>.
68. Rosen B, Laframboise S, Ferguson S, Dodge J, Bernardini M, Murphy J, et al. The impacts of neoadjuvant chemotherapy and of debulking surgery on survival from advanced ovarian cancer. *Gynecol Oncol.* 2014;134(3):462-7.
69. Rustin GJ, van der Burg ME, Griffin CL, Guthrie D, Lamont A, Jayson GC, et al. Early versus delayed treatment of relapsed ovarian cancer (MRC OV05/EORTC 55955): a randomised trial. *Lancet.* 2010;376(9747):1155-63.
70. Armstrong DK, Bundy B, Wenzel L, Huang HQ, Baergen R, Lele S, et al. Intraperitoneal cisplatin and paclitaxel in ovarian cancer. *N Engl J Med.* 2006;354(1):34-43.

71. Provencher DM, Gallagher CJ, Parulekar WR, Ledermann JA, Armstrong DK, Brundage M, et al. OV21/PETROC: a randomized Gynecologic Cancer Intergroup phase II study of intraperitoneal versus intravenous chemotherapy following neoadjuvant chemotherapy and optimal debulking surgery in epithelial ovarian cancer. *Ann Oncol.* 2018;29(2):431-8.
72. Tewari D, Java JJ, Salani R, Armstrong DK, Markman M, Herzog T, et al. Long-term survival advantage and prognostic factors associated with intraperitoneal chemotherapy treatment in advanced ovarian cancer: a gynecologic oncology group study. *J Clin Oncol.* 2015;33(13):1460-6.
73. Eskander RN, Cripe J, Bristow RE. Intraperitoneal chemotherapy from Armstrong to HIPEC: challenges and promise. *Curr Treat Options Oncol.* 2014;15(1):27-40.
74. van Driel WJ, Koole SN, Sikorska K, Schagen van Leeuwen JH, Schreuder HWR, Hermans RHM, et al. Hyperthermic Intraperitoneal Chemotherapy in Ovarian Cancer. *N Engl J Med.* 2018;378(3):230-40.
75. Radl B, Mlineritsch B. ASCO 2017-highlights of gynecological cancer. *Memo.* 2017;10(4):237-9.
76. Katsumata N. Dose-dense approaches to ovarian cancer treatment. *Curr Treat Options Oncol.* 2015;16(5):21.
77. Katsumata N, Yasuda M, Isonishi S, Takahashi F, Michimae H, Kimura E, et al. Long-term results of dose-dense paclitaxel and carboplatin versus conventional paclitaxel and carboplatin for treatment of advanced epithelial ovarian, fallopian tube, or primary peritoneal cancer (JGOG 3016): a randomised, controlled, open-label trial. *Lancet Oncol.* 2013;14(10):1020-6.
78. Chan JK, Brady MF, Penson RT, Huang H, Birrer MJ, Walker JL, et al. Weekly vs. Every-3-Week Paclitaxel and Carboplatin for Ovarian Cancer. *N Engl J Med.* 2016;374(8):738-48.
79. Pignata S, Scambia G, Katsaros D, Gallo C, Pujade-Lauraine E, De Placido S, et al. Carboplatin plus paclitaxel once a week versus every 3 weeks in patients with advanced ovarian cancer (MITO-7): a randomised, multicentre, open-label, phase 3 trial. *Lancet Oncol.* 2014;15(4):396-405.
80. Ledermann JA, Harter P, Gourley C, Friedlander M, Vergote I, Rustin G, et al. Overall survival in patients with platinum-sensitive recurrent serous ovarian cancer receiving olaparib maintenance monotherapy: an updated analysis from a randomised, placebo-controlled, double-blind, phase 2 trial. *Lancet Oncol.* 2016;17(11):1579-89.

81. Mirza MR, Monk BJ, Herrstedt J, Oza AM, Mahner S, Redondo A, et al. Niraparib Maintenance Therapy in Platinum-Sensitive, Recurrent Ovarian Cancer. *N Engl J Med*. 2016;375(22):2154-64.
82. Markman M. Antiangiogenic drugs in ovarian cancer. *Expert Opin Pharmacother*. 2009;10(14):2269-77.
83. Kolomainen DF, Daponte A, Barton DP, Pennert K, Ind TE, Bridges JE, et al. Outcomes of surgical management of bowel obstruction in relapsed epithelial ovarian cancer (EOC). *Gynecol Oncol*. 2012;125(1):31-6.
84. Aghajanian C, Blank SV, Goff BA, Judson PL, Teneriello MG, Husain A, et al. OCEANS: a randomized, double-blind, placebo-controlled phase III trial of chemotherapy with or without bevacizumab in patients with platinum-sensitive recurrent epithelial ovarian, primary peritoneal, or fallopian tube cancer. *J Clin Oncol*. 2012;30(17):2039-45.
85. Bookman MA, Darcy KM, Clarke-Pearson D, Boothby RA, Horowitz IR. Evaluation of monoclonal humanized anti-HER2 antibody, trastuzumab, in patients with recurrent or refractory ovarian or primary peritoneal carcinoma with overexpression of HER2: a phase II trial of the Gynecologic Oncology Group. *J Clin Oncol*. 2003;21(2):283-90.
86. Vergote IB, Jimeno A, Joly F, Katsaros D, Coens C, Despierre E, et al. Randomized phase III study of erlotinib versus observation in patients with no evidence of disease progression after first-line platin-based chemotherapy for ovarian carcinoma: a European Organisation for Research and Treatment of Cancer-Gynaecological Cancer Group, and Gynecologic Cancer Intergroup study. *J Clin Oncol*. 2014;32(4):320-6.
87. Naumann RW, Coleman RL, Burger RA, Sausville EA, Kutarska E, Ghamande SA, et al. PRECEDENT: a randomized phase II trial comparing vintafolide (EC145) and pegylated liposomal doxorubicin (PLD) in combination versus PLD alone in patients with platinum-resistant ovarian cancer. *J Clin Oncol*. 2013;31(35):4400-6.
88. Jelovac D, Armstrong DK. Role of farletuzumab in epithelial ovarian carcinoma. *Curr Pharm Des*. 2012;18(25):3812-5.
89. Janku F, Wheler JJ, Westin SN, Moulder SL, Naing A, Tsimberidou AM, et al. PI3K/AKT/mTOR inhibitors in patients with breast and gynecologic malignancies harboring PIK3CA mutations. *J Clin Oncol*. 2012;30(8):777-82.
90. Behbakht K, Sill MW, Darcy KM, Rubin SC, Mannel RS, Waggoner S, et al. Phase II trial of the mTOR inhibitor, temsirolimus and evaluation of circulating tumor cells and tumor biomarkers in persistent and recurrent epithelial ovarian and primary peritoneal malignancies: a Gynecologic Oncology Group study. *Gynecol Oncol*. 2011;123(1):19-26.

91. Farley J, Brady WE, Vathipadiekal V, Lankes HA, Coleman R, Morgan MA, et al. Selumetinib in women with recurrent low-grade serous carcinoma of the ovary or peritoneum: an open-label, single-arm, phase 2 study. *Lancet Oncol.* 2013;14(2):134-40.
92. Mhawech-Fauceglia P, Afkhami M, Pejovic T. MET/HGF Signaling Pathway in Ovarian Carcinoma: Clinical Implications and Future Direction. *Patholog Res Int.* 2012;2012:960327.
93. Berek J, Taylor P, McGuire W, Smith LM, Schultes B, Nicodemus CF. Oregovomab maintenance monoimmunotherapy does not improve outcomes in advanced ovarian cancer. *J Clin Oncol.* 2009;27(3):418-25.
94. Nassar D, Blanpain C. Cancer Stem Cells: Basic Concepts and Therapeutic Implications. *Annu Rev Pathol.* 2016;11:47-76.
95. Clevers H. The cancer stem cell: premises, promises and challenges. *Nat Med.* 2011;17(3):313-9.
96. Pattabiraman DR, Weinberg RA. Tackling the cancer stem cells - what challenges do they pose? *Nat Rev Drug Discov.* 13. England2014. p. 497-512.
97. Singh A, Settleman J. EMT, cancer stem cells and drug resistance: an emerging axis of evil in the war on cancer. *Oncogene.* 2010;29(34):4741-51.
98. Batlle E, Clevers H. Cancer stem cells revisited. *Nat Med.* 2017;23(10):1124-34.
99. Lapidot T, Sirard C, Vormoor J, Murdoch B, Hoang T, Caceres-Cortes J, et al. A cell initiating human acute myeloid leukaemia after transplantation into SCID mice. *Nature.* 1994;367(6464):645-8.
100. Bonnet D, Dick JE. Human acute myeloid leukemia is organized as a hierarchy that originates from a primitive hematopoietic cell. *Nat Med.* 1997;3(7):730-7.
101. Kondo M, Wagers AJ, Manz MG, Prohaska SS, Scherer DC, Beilhack GF, et al. Biology of hematopoietic stem cells and progenitors: implications for clinical application. *Annu Rev Immunol.* 2003;21:759-806.
102. Dalerba P, Cho RW, Clarke MF. Cancer stem cells: models and concepts. *Annu Rev Med.* 2007;58:267-84.
103. Al-Hajj M, Wicha MS, Benito-Hernandez A, Morrison SJ, Clarke MF. Prospective identification of tumorigenic breast cancer cells. *Proc Natl Acad Sci U S A.* 2003;100(7):3983-8.
104. Singh SK, Clarke ID, Terasaki M, Bonn VE, Hawkins C, Squire J, et al. Identification of a cancer stem cell in human brain tumors. *Cancer Res.* 2003;63(18):5821-8.

105. Chen R, Nishimura MC, Bumbaca SM, Kharbanda S, Forrest WF, Kasman IM, et al. A hierarchy of self-renewing tumor-initiating cell types in glioblastoma. *Cancer Cell*. 2010;17(4):362-75.
106. Patrawala L, Calhoun T, Schneider-Broussard R, Li H, Bhatia B, Tang S, et al. Highly purified CD44+ prostate cancer cells from xenograft human tumors are enriched in tumorigenic and metastatic progenitor cells. *Oncogene*. 2006;25(12):1696-708.
107. Collins AT, Berry PA, Hyde C, Stower MJ, Maitland NJ. Prospective identification of tumorigenic prostate cancer stem cells. *Cancer Res*. 2005;65(23):10946-51.
108. Fang D, Nguyen TK, Leishear K, Finko R, Kulp AN, Hotz S, et al. A tumorigenic subpopulation with stem cell properties in melanomas. *Cancer Res*. 2005;65(20):9328-37.
109. Boiko AD, Razorenova OV, van de Rijn M, Swetter SM, Johnson DL, Ly DP, et al. Human melanoma-initiating cells express neural crest nerve growth factor receptor CD271. *Nature*. 2010;466(7302):133-7.
110. Schatton T, Murphy GF, Frank NY, Yamaura K, Waaga-Gasser AM, Gasser M, et al. Identification of cells initiating human melanomas. *Nature*. 2008;451(7176):345-9.
111. Eramo A, Lotti F, Sette G, Piloizzi E, Biffoni M, Di Virgilio A, et al. Identification and expansion of the tumorigenic lung cancer stem cell population. *Cell Death Differ*. 2008;15(3):504-14.
112. Jiang F, Qiu Q, Khanna A, Todd NW, Deepak J, Xing L, et al. Aldehyde dehydrogenase 1 is a tumor stem cell-associated marker in lung cancer. *Mol Cancer Res*. 2009;7(3):330-8.
113. Dalerba P, Dylla SJ, Park IK, Liu R, Wang X, Cho RW, et al. Phenotypic characterization of human colorectal cancer stem cells. *Proc Natl Acad Sci U S A*. 2007;104(24):10158-63.
114. Carpentino JE, Hynes MJ, Appelman HD, Zheng T, Steindler DA, Scott EW, et al. Aldehyde dehydrogenase-expressing colon stem cells contribute to tumorigenesis in the transition from colitis to cancer. *Cancer Res*. 2009;69(20):8208-15.
115. Pasto A, Marchesi M, Diamantini A, Frasson C, Curtarello M, Lago C, et al. PKH26 staining defines distinct subsets of normal human colon epithelial cells at different maturation stages. *PLoS One*. 2012;7(8):e43379.
116. Vermeulen L, Todaro M, de Sousa Mello F, Sprick MR, Kemper K, Perez Alea M, et al. Single-cell cloning of colon cancer stem cells reveals a multi-lineage differentiation capacity. *Proc Natl Acad Sci U S A*. 2008;105(36):13427-32.
117. Li C, Heidt DG, Dalerba P, Burant CF, Zhang L, Adsay V, et al. Identification of pancreatic cancer stem cells. *Cancer Res*. 2007;67(3):1030-7.

118. Jordan CT, Guzman ML, Noble M. Cancer stem cells. *N Engl J Med.* 2006;355(12):1253-61.
119. Magee JA, Piskounova E, Morrison SJ. Cancer stem cells: impact, heterogeneity, and uncertainty. *Cancer Cell.* 2012;21(3):283-96.
120. Williams RT, den Besten W, Sherr CJ. Cytokine-dependent imatinib resistance in mouse BCR-ABL+, Arf-null lymphoblastic leukemia. *Genes Dev.* 2007;21(18):2283-7.
121. Quintana E, Shackleton M, Sabel MS, Fullen DR, Johnson TM, Morrison SJ. Efficient tumour formation by single human melanoma cells. *Nature.* 2008;456(7222):593-8.
122. Pece S, Tosoni D, Confalonieri S, Mazzarol G, Vecchi M, Ronzoni S, et al. Biological and molecular heterogeneity of breast cancers correlates with their cancer stem cell content. *Cell.* 2010;140(1):62-73.
123. Li X, Lewis MT, Huang J, Gutierrez C, Osborne CK, Wu MF, et al. Intrinsic resistance of tumorigenic breast cancer cells to chemotherapy. *J Natl Cancer Inst.* 2008;100(9):672-9.
124. Subramaniam D, Ramalingam S, Houchen CW, Anant S. Cancer stem cells: a novel paradigm for cancer prevention and treatment. *Mini Rev Med Chem.* 2010;10(5):359-71.
125. Oskarsson T, Batlle E, Massague J. Metastatic stem cells: sources, niches, and vital pathways. *Cell Stem Cell.* 2014;14(3):306-21.
126. Mitra A, Mishra L, Li S. EMT, CTCs and CSCs in tumor relapse and drug-resistance. *Oncotarget.* 2015;6(13):10697-711.
127. Hatzikirou H, Basanta D, Simon M, Schaller K, Deutsch A. 'Go or grow': the key to the emergence of invasion in tumour progression? *Math Med Biol.* 2012;29(1):49-65.
128. Garg M. Epithelial plasticity and cancer stem cells: Major mechanisms of cancer pathogenesis and therapy resistance. *World J Stem Cells.* 2017;9(8):118-26.
129. Kurrey NK, Jalgaonkar SP, Joglekar AV, Ghanate AD, Chaskar PD, Doiphode RY, et al. Snail and slug mediate radioresistance and chemoresistance by antagonizing p53-mediated apoptosis and acquiring a stem-like phenotype in ovarian cancer cells. *Stem Cells.* 2009;27(9):2059-68.
130. Cai Z, Cao Y, Luo Y, Hu H, Ling H. Signalling mechanism(s) of epithelial–mesenchymal transition and cancer stem cells in tumour therapeutic resistance. *Clinica Chimica Acta.* 2018;483:156-63.
131. Cheng Y, Cheung AK, Ko JM, Phoon YP, Chiu PM, Lo PH, et al. Physiological beta-catenin signaling controls self-renewal networks and generation of stem-like cells from nasopharyngeal carcinoma. *BMC Cell Biol.* 2013;14:44.

132. Guo Y, Liu S, Wang P, Zhao S, Wang F, Bing L, et al. Expression profile of embryonic stem cell-associated genes Oct4, Sox2 and Nanog in human gliomas. *Histopathology*. 2011;59(4):763-75.
133. Takahashi K, Yamanaka S. Induction of pluripotent stem cells from mouse embryonic and adult fibroblast cultures by defined factors. *Cell*. 2006;126(4):663-76.
134. <http://www.uniprot.org/uniprot/P48431>.
135. Niwa H, Ogawa K, Shimosato D, Adachi K. A parallel circuit of LIF signalling pathways maintains pluripotency of mouse ES cells. *Nature*. 2009;460:118.
136. Hussenet T, Dali S, Exinger J, Monga B, Jost B, Dembelé D, et al. SOX2 Is an Oncogene Activated by Recurrent 3q26.3 Amplifications in Human Lung Squamous Cell Carcinomas. *PLoS ONE*. 2010;5(1):e8960.
137. Rodda DJ, Chew JL, Lim LH, Loh YH, Wang B, Ng HH, et al. Transcriptional regulation of nanog by OCT4 and SOX2. *J Biol Chem*. 2005;280(26):24731-7.
138. Zaehres H, Lensch MW, Daheron L, Stewart SA, Itskovitz-Eldor J, Daley GQ. High-efficiency RNA interference in human embryonic stem cells. *Stem Cells*. 2005;23(3):299-305.
139. Wu G, Scholer HR. Role of Oct4 in the early embryo development. *Cell Regen (Lond)*. 2014;3(1):7.
140. Hochedlinger K, Yamada Y, Beard C, Jaenisch R. Ectopic Expression of *Oct-4* Blocks Progenitor-Cell Differentiation and Causes Dysplasia in Epithelial Tissues. *Cell*. 2005;121(3):465-77.
141. Chambers I, Colby D, Robertson M, Nichols J, Lee S, Tweedie S, et al. Functional expression cloning of Nanog, a pluripotency sustaining factor in embryonic stem cells. *Cell*. 2003;113(5):643-55.
142. Piestun D, Kochupurakkal BS, Jacob-Hirsch J, Zeligson S, Koudritsky M, Domany E, et al. Nanog transforms NIH3T3 cells and targets cell-type restricted genes. *Biochem Biophys Res Commun*. 2006;343(1):279-85.
143. Iv Santaliz-Ruiz LE, Xie X, Old M, Teknos TN, Pan Q. Emerging role of nanog in tumorigenesis and cancer stem cells. *Int J Cancer*. 2014;135(12):2741-8.
144. Gong S, Li Q, Jeter CR, Fan Q, Tang DG, Liu B. Regulation of NANOG in cancer cells. *Molecular carcinogenesis*. 2015;54(9):679-87.
145. Wang M-L, Chiou S-H, Wu C-W. Targeting cancer stem cells: emerging role of Nanog transcription factor. *OncoTargets and therapy*. 2013;6:1207-20.
146. Vaz AP, Ponnusamy MP, Seshacharyulu P, Batra SK. A concise review on the current understanding of pancreatic cancer stem cells. *J Cancer Stem Cell Res*. 2014;2.

147. https://www.genome.jp/dbget-bin/www_bget?pathway+hsa04310.
148. <http://web.stanford.edu/group/nusselab/cgi-bin/wnt/node/269>.
149. https://web.stanford.edu/group/nusselab/cgi-bin/wnt/target_genes.
150. Moserle L, Ghisi M, Amadori A, Indraccolo S. Side population and cancer stem cells: therapeutic implications. *Cancer Lett.* 2010;288(1):1-9.
151. Haraguchi N, Utsunomiya T, Inoue H, Tanaka F, Mimori K, Barnard GF, et al. Characterization of a side population of cancer cells from human gastrointestinal system. *Stem Cells.* 2006;24(3):506-13.
152. Hu Y, Fu L. Targeting cancer stem cells: a new therapy to cure cancer patients. *Am J Cancer Res.* 2012;2(3):340-56.
153. https://www.genome.jp/dbget-bin/www_bget?pathway+hsa04340.
154. Ingham PW, McMahon AP. Hedgehog signaling in animal development: paradigms and principles. *Genes Dev.* 2001;15(23):3059-87.
155. Katoh Y, Katoh M. Hedgehog target genes: mechanisms of carcinogenesis induced by aberrant hedgehog signaling activation. *Curr Mol Med.* 2009;9(7):873-86.
156. Peacock CD, Wang Q, Gesell GS, Corcoran-Schwartz IM, Jones E, Kim J, et al. Hedgehog signaling maintains a tumor stem cell compartment in multiple myeloma. *Proc Natl Acad Sci U S A.* 2007;104(10):4048-53.
157. Liu S, Dontu G, Wicha MS. Mammary stem cells, self-renewal pathways, and carcinogenesis. *Breast Cancer Res.* 2005;7(3):86-95.
158. Borggreffe T, Oswald F. The Notch signaling pathway: transcriptional regulation at Notch target genes. *Cell Mol Life Sci.* 2009;66(10):1631-46.
159. https://www.genome.jp/dbget-bin/www_bget?pathway+hsa04330.
160. Duncan AW, Rattis FM, DiMascio LN, Congdon KL, Pazianos G, Zhao C, et al. Integration of Notch and Wnt signaling in hematopoietic stem cell maintenance. *Nat Immunol.* 2005;6(3):314-22.
161. Katoh M. WNT antagonist, DKK2, is a Notch signaling target in intestinal stem cells: augmentation of a negative regulation system for canonical WNT signaling pathway by the Notch-DKK2 signaling loop in primates. *Int J Mol Med.* 2007;19(1):197-201.
162. Pasto A, Serafin V, Pilotto G, Lago C, Bellio C, Trusolino L, et al. NOTCH3 signaling regulates MUSASHI-1 expression in metastatic colorectal cancer cells. *Cancer Res.* 2014;74(7):2106-18.

163. Fan X, Matsui W, Khaki L, Stearns D, Chun J, Li YM, et al. Notch pathway inhibition depletes stem-like cells and blocks engraftment in embryonal brain tumors. *Cancer Res.* 2006;66(15):7445-52.
164. Keysar SB, Jimeno A. More than markers: biological significance of cancer stem cell-defining molecules. *Mol Cancer Ther.* 2010;9(9):2450-7.
165. Stuelten CH, Mertins SD, Busch JI, Gowens M, Scudiero DA, Burkett MW, et al. Complex display of putative tumor stem cell markers in the NCI60 tumor cell line panel. *Stem Cells.* 2010;28(4):649-60.
166. Zhang H-F, Hu P, Fang S-Q. Understanding the role of CD44V6 in ovarian cancer. *Oncology Letters.* 2017;14(2):1989-92.
167. Aigner S, Sthoeger ZM, Fogel M, Weber E, Zarn J, Ruppert M, et al. CD24, a Mucin-Type Glycoprotein, Is a Ligand for P-Selectin on Human Tumor Cells. *Blood.* 1997;89(9):3385.
168. Runz S, Mierke CT, Joumaa S, Behrens J, Fabry B, Altevogt P. CD24 induces localization of beta1 integrin to lipid raft domains. *Biochem Biophys Res Commun.* 2008;365(1):35-41.
169. Hadnagy A, Gaboury L, Beaulieu R, Balicki D. SP analysis may be used to identify cancer stem cell populations. *Exp Cell Res.* 2006;312(19):3701-10.
170. Lee CH, Yu CC, Wang BY, Chang WW. Tumorsphere as an effective in vitro platform for screening anti-cancer stem cell drugs. *Oncotarget.* 2016;7(2):1215-26.
171. Goodell MA, Brose K, Paradis G, Conner AS, Mulligan RC. Isolation and functional properties of murine hematopoietic stem cells that are replicating in vivo. *J Exp Med.* 1996;183(4):1797-806.
172. Deshmukh A, Deshpande K, Arfuso F, Newsholme P, Dharmarajan A. Cancer stem cell metabolism: a potential target for cancer therapy. *Mol Cancer.* 2016;15(1):69.
173. Peiris-Pages M, Martinez-Outschoorn UE, Pestell RG, Sotgia F, Lisanti MP. Cancer stem cell metabolism. *Breast Cancer Res.* 2016;18(1):55.
174. Sancho P, Barneda D, Heeschen C. Hallmarks of cancer stem cell metabolism. *Br J Cancer.* 2016;114(12):1305-12.
175. Vazquez-Martin A, Oliveras-Ferraros C, Cufi S, Del Barco S, Martin-Castillo B, Menendez JA. Metformin regulates breast cancer stem cell ontogeny by transcriptional regulation of the epithelial-mesenchymal transition (EMT) status. *Cell Cycle.* 2010;9(18):3807-14.
176. Wang YC, Chao TK, Chang CC, Yo YT, Yu MH, Lai HC. Drug screening identifies niclosamide as an inhibitor of breast cancer stem-like cells. *PLoS One.* 2013;8(9):e74538.

177. Dong C, Yuan T, Wu Y, Wang Y, Fan TW, Miriyala S, et al. Loss of FBP1 by Snail-mediated repression provides metabolic advantages in basal-like breast cancer. *Cancer Cell*. 2013;23(3):316-31.
178. Ye XQ, Li Q, Wang GH, Sun FF, Huang GJ, Bian XW, et al. Mitochondrial and energy metabolism-related properties as novel indicators of lung cancer stem cells. *Int J Cancer*. 2011;129(4):820-31.
179. Janiszewska M, Suva ML, Riggi N, Houtkooper RH, Auwerx J, Clement-Schatlo V, et al. Imp2 controls oxidative phosphorylation and is crucial for preserving glioblastoma cancer stem cells. *Genes Dev*. 2012;26(17):1926-44.
180. Yo YT, Lin YW, Wang YC, Balch C, Huang RL, Chan MW, et al. Growth inhibition of ovarian tumor-initiating cells by niclosamide. *Mol Cancer Ther*. 2012;11(8):1703-12.
181. Anderson AS, Roberts PC, Frisard MI, Hulver MW, Schmelz EM. Ovarian tumor-initiating cells display a flexible metabolism. *Exp Cell Res*. 2014;328(1):44-57.
182. Pasto A, Bellio C, Pilotto G, Ciminale V, Silic-Benussi M, Guzzo G, et al. Cancer stem cells from epithelial ovarian cancer patients privilege oxidative phosphorylation, and resist glucose deprivation. *Oncotarget*. 2014;5(12):4305-19.
183. Lagadinou ED, Sach A, Callahan K, Rossi RM, Neering SJ, Minhajuddin M, et al. BCL-2 inhibition targets oxidative phosphorylation and selectively eradicates quiescent human leukemia stem cells. *Cell Stem Cell*. 2013;12(3):329-41.
184. Shen YA, Lin CH, Chi WH, Wang CY, Hsieh YT, Wei YH, et al. Resveratrol Impedes the Stemness, Epithelial-Mesenchymal Transition, and Metabolic Reprogramming of Cancer Stem Cells in Nasopharyngeal Carcinoma through p53 Activation. *Evid Based Complement Alternat Med*. 2013;2013:590393.
185. Shen YA, Wang CY, Hsieh YT, Chen YJ, Wei YH. Metabolic reprogramming orchestrates cancer stem cell properties in nasopharyngeal carcinoma. *Cell Cycle*. 2015;14(1):86-98.
186. Sancho P, Burgos-Ramos E, Tavera A, Bou Kheir T, Jagust P, Schoenhals M, et al. MYC/PGC-1alpha Balance Determines the Metabolic Phenotype and Plasticity of Pancreatic Cancer Stem Cells. *Cell Metab*. 2015;22(4):590-605.
187. Chen CL, Uthaya Kumar DB, Punj V, Xu J, Sher L, Tahara SM, et al. NANOG Metabolically Reprograms Tumor-Initiating Stem-like Cells through Tumorigenic Changes in Oxidative Phosphorylation and Fatty Acid Metabolism. *Cell Metab*. 2016;23(1):206-19.

188. Folmes CD, Martinez-Fernandez A, Faustino RS, Yamada S, Perez-Terzic C, Nelson TJ, et al. Nuclear reprogramming with c-Myc potentiates glycolytic capacity of derived induced pluripotent stem cells. *J Cardiovasc Transl Res.* 2013;6(1):10-21.
189. Yuan S, Lu Y, Yang J, Chen G, Kim S, Feng L, et al. Metabolic activation of mitochondria in glioma stem cells promotes cancer development through a reactive oxygen species-mediated mechanism. *Stem Cell Res Ther.* 2015;6:198.
190. Katajisto P, Dohla J, Chaffer CL, Pentimikko N, Marjanovic N, Iqbal S, et al. Stem cells. Asymmetric apportioning of aged mitochondria between daughter cells is required for stemness. *Science.* 2015;348(6232):340-3.
191. Yeh CT, Su CL, Huang CY, Lin JK, Lee WH, Chang PM, et al. A preclinical evaluation of antimycin a as a potential antitumor cancer stem cell agent. *Evid Based Complement Alternat Med.* 2013;2013:910451.
192. Gupta PB, Onder TT, Jiang G, Tao K, Kuperwasser C, Weinberg RA, et al. Identification of selective inhibitors of cancer stem cells by high-throughput screening. *Cell.* 2009;138(4):645-59.
193. Lamb R, Ozsvari B, Lisanti CL, Tanowitz HB, Howell A, Martinez-Outschoorn UE, et al. Antibiotics that target mitochondria effectively eradicate cancer stem cells, across multiple tumor types: treating cancer like an infectious disease. *Oncotarget.* 2015;6(7):4569-84.
194. Fiorillo M, Lamb R, Tanowitz HB, Mutti L, Krstic-Demonacos M, Cappello AR, et al. Repurposing atovaquone: targeting mitochondrial complex III and OXPHOS to eradicate cancer stem cells. *Oncotarget.* 2016;7(23):34084-99.
195. Gupta PB, Fillmore CM, Jiang G, Shapira SD, Tao K, Kuperwasser C, et al. Stochastic state transitions give rise to phenotypic equilibrium in populations of cancer cells. *Cell.* 2011;146(4):633-44.
196. Clevers H. The intestinal crypt, a prototype stem cell compartment. *Cell.* 2013;154(2):274-84.
197. Borovski T, De Sousa EMF, Vermeulen L, Medema JP. Cancer stem cell niche: the place to be. *Cancer Res.* 2011;71(3):634-9.
198. Ritchie KE, Nor JE. Perivascular stem cell niche in head and neck cancer. *Cancer Lett.* 2013;338(1):41-6.
199. Sica A, Porta C, Amadori A, Pasto A. Tumor-associated myeloid cells as guiding forces of cancer cell stemness. *Cancer Immunol Immunother.* 2017;66(8):1025-36.

200. Kurtova AV, Xiao J, Mo Q, Pazhanisamy S, Krasnow R, Lerner SP, et al. Blocking PGE2-induced tumour repopulation abrogates bladder cancer chemoresistance. *Nature*. 2015;517(7533):209-13.
201. Nile AH, Hannoush RN. Fatty acylation of Wnt proteins. *Nat Chem Biol*. 2016;12(2):60-9.
202. <https://clinicaltrials.gov/ct2/show/NCT01957007>.
203. Jimeno A, Gordon M, Chugh R, Messersmith W, Mendelson D, Dupont J, et al. A First-in-Human Phase I Study of the Anticancer Stem Cell Agent Ipafricept (OMP-54F28), a Decoy Receptor for Wnt Ligands, in Patients with Advanced Solid Tumors. *Clin Cancer Res*. 2017;23(24):7490-7.
204. Fischer MM, Cancilla B, Yeung VP, Cattaruzza F, Chartier C, Murriel CL, et al. WNT antagonists exhibit unique combinatorial antitumor activity with taxanes by potentiating mitotic cell death. *Sci Adv*. 2017;3(6):e1700090.
205. Kühnle M, Egger M, Müller C, Mahringer A, Bernhardt G, Fricker G, et al. Potent and selective inhibitors of breast cancer resistance protein (ABCG2) derived from the p-glycoprotein (ABCB1) modulator tariquidar. *J Med Chem*. 2009;52(4):1190-7.
206. Butler LM, Webb Y, Agus DB, Higgins B, Tolentino TR, Kutko MC, et al. Inhibition of transformed cell growth and induction of cellular differentiation by pyroxamide, an inhibitor of histone deacetylase. *Clin Cancer Res*. 2001;7(4):962-70.
207. Piccirillo SG, Reynolds BA, Zanetti N, Lamorte G, Binda E, Broggi G, et al. Bone morphogenetic proteins inhibit the tumorigenic potential of human brain tumour-initiating cells. *Nature*. 2006;444(7120):761-5.
208. Jozan S, Paute S, Courtade-Saidi M, Julie S, Vidal S, Bugat R, et al. All trans retinoic acid enhances CDDP-induced apoptosis: modulation of the CDDP effect on cell cycle progression. *Int J Oncol*. 2002;20(6):1289-95.
209. Lim YC, Kang HJ, Kim YS, Choi EC. All-trans-retinoic acid inhibits growth of head and neck cancer stem cells by suppression of Wnt/beta-catenin pathway. *Eur J Cancer*. 2012;48(17):3310-8.
210. Ying M, Wang S, Sang Y, Sun P, Lal B, Goodwin CR, et al. Regulation of glioblastoma stem cells by retinoic acid: role for Notch pathway inhibition. *Oncogene*. 2011;30(31):3454-67.
211. Qiu L, Kelso MJ, Hansen C, West ML, Fairlie DP, Parsons PG. Anti-tumour activity in vitro and in vivo of selective differentiating agents containing hydroxamate. *Br J Cancer*. 1999;80(8):1252-8.

212. Harris WJ, Huang X, Lynch JT, Spencer GJ, Hitchin JR, Li Y, et al. The histone demethylase KDM1A sustains the oncogenic potential of MLL-AF9 leukemia stem cells. *Cancer Cell*. 2012;21(4):473-87.
213. Ma X, Holt D, Kundu N, Reader J, Goloubeva O, Take Y, et al. A prostaglandin E (PGE) receptor EP4 antagonist protects natural killer cells from PGE2-mediated immunosuppression and inhibits breast cancer metastasis. *Oncoimmunology*. 2013;2(1):e22647.
214. Lin L, Amin R, Gallicano GI, Glasgow E, Jogunoori W, Jessup JM, et al. The STAT3 inhibitor NSC 74859 is effective in hepatocellular cancers with disrupted TGF-beta signaling. *Oncogene*. 2009;28(7):961-72.
215. MacDonald KP, Palmer JS, Cronau S, Seppanen E, Olver S, Raffelt NC, et al. An antibody against the colony-stimulating factor 1 receptor depletes the resident subset of monocytes and tissue- and tumor-associated macrophages but does not inhibit inflammation. *Blood*. 2010;116(19):3955-63.
216. DeNardo DG, Brennan DJ, Rexhepaj E, Ruffell B, Shiao SL, Madden SF, et al. Leukocyte complexity predicts breast cancer survival and functionally regulates response to chemotherapy. *Cancer Discov*. 2011;1(1):54-67.
217. Germano G, Frapolli R, Belgiovine C, Anselmo A, Pesce S, Liguori M, et al. Role of macrophage targeting in the antitumor activity of trabectedin. *Cancer Cell*. 2013;23(2):249-62.
218. Shah MM, Landen CN. Ovarian cancer stem cells: are they real and why are they important? *Gynecol Oncol*. 2014;132(2):483-9.
219. Bapat SA. Human ovarian cancer stem cells. *Reproduction*. 2010;140(1):33-41.
220. Baba T, Convery PA, Matsumura N, Whitaker RS, Kondoh E, Perry T, et al. Epigenetic regulation of CD133 and tumorigenicity of CD133+ ovarian cancer cells. *Oncogene*. 2009;28(2):209-18.
221. Curley MD, Therrien VA, Cummings CL, Sergent PA, Koulouris CR, Friel AM, et al. CD133 expression defines a tumor initiating cell population in primary human ovarian cancer. *Stem Cells*. 2009;27(12):2875-83.
222. Alvero AB, Chen R, Fu HH, Montagna M, Schwartz PE, Rutherford T, et al. Molecular phenotyping of human ovarian cancer stem cells unravels the mechanisms for repair and chemoresistance. *Cell Cycle*. 2009;8(1):158-66.
223. Zhang S, Balch C, Chan MW, Lai HC, Matei D, Schilder JM, et al. Identification and characterization of ovarian cancer-initiating cells from primary human tumors. *Cancer Res*. 2008;68(11):4311-20.

224. Shi MF, Jiao J, Lu WG, Ye F, Ma D, Dong QG, et al. Identification of cancer stem cell-like cells from human epithelial ovarian carcinoma cell line. *Cell Mol Life Sci.* 2010;67(22):3915-25.
225. Gao MQ, Choi YP, Kang S, Youn JH, Cho NH. CD24⁺ cells from hierarchically organized ovarian cancer are enriched in cancer stem cells. *Oncogene.* 2010;29(18):2672-80.
226. Landen CN, Jr., Goodman B, Katre AA, Steg AD, Nick AM, Stone RL, et al. Targeting aldehyde dehydrogenase cancer stem cells in ovarian cancer. *Mol Cancer Ther.* 2010;9(12):3186-99.
227. Silva IA, Bai S, McLean K, Yang K, Griffith K, Thomas D, et al. Aldehyde dehydrogenase in combination with CD133 defines angiogenic ovarian cancer stem cells that portend poor patient survival. *Cancer Res.* 2011;71(11):3991-4001.
228. Kryczek I, Liu S, Roh M, Vatan L, Szeliga W, Wei S, et al. Expression of aldehyde dehydrogenase and CD133 defines ovarian cancer stem cells. *Int J Cancer.* 2012;130(1):29-39.
229. Szotek PP, Pieretti-Vanmarcke R, Masiakos PT, Dinulescu DM, Connolly D, Foster R, et al. Ovarian cancer side population defines cells with stem cell-like characteristics and Mullerian Inhibiting Substance responsiveness. *Proc Natl Acad Sci U S A.* 2006;103(30):11154-9.
230. Hu L, McArthur C, Jaffe RB. Ovarian cancer stem-like side-population cells are tumourigenic and chemoresistant. *Br J Cancer.* 2010;102(8):1276-83.
231. Dou J, Jiang C, Wang J, Zhang X, Zhao F, Hu W, et al. Using ABCG2-molecule-expressing side population cells to identify cancer stem-like cells in a human ovarian cell line. *Cell Biol Int.* 2011;35(3):227-34.
232. Kobayashi Y, Seino K, Hosonuma S, Ohara T, Itamochi H, Isonishi S, et al. Side population is increased in paclitaxel-resistant ovarian cancer cell lines regardless of resistance to cisplatin. *Gynecol Oncol.* 2011;121(2):390-4.
233. Bapat SA, Mali AM, Koppikar CB, Kurrey NK. Stem and progenitor-like cells contribute to the aggressive behavior of human epithelial ovarian cancer. *Cancer Res.* 2005;65(8):3025-9.
234. Ferrandina G, Bonanno G, Pierelli L, Perillo A, Procoli A, Mariotti A, et al. Expression of CD133-1 and CD133-2 in ovarian cancer. *Int J Gynecol Cancer.* 2008;18(3):506-14.
235. Kusumbe AP, Mali AM, Bapat SA. CD133-expressing stem cells associated with ovarian metastases establish an endothelial hierarchy and contribute to tumor vasculature. *Stem Cells.* 2009;27(3):498-508.

236. Steffensen KD, Alvero AB, Yang Y, Waldstrom M, Hui P, Holmberg JC, et al. Prevalence of epithelial ovarian cancer stem cells correlates with recurrence in early-stage ovarian cancer. *J Oncol.* 2011;2011:620523.
237. Steg AD, Bevis KS, Katre AA, Ziebarth A, Dobbin ZC, Alvarez RD, et al. Stem cell pathways contribute to clinical chemoresistance in ovarian cancer. *Clin Cancer Res.* 2012;18(3):869-81.
238. Luo L, Zeng J, Liang B, Zhao Z, Sun L, Cao D, et al. Ovarian cancer cells with the CD117 phenotype are highly tumorigenic and are related to chemotherapy outcome. *Exp Mol Pathol.* 2011;91(2):596-602.
239. Kusumbe AP, Bapat SA. Cancer stem cells and aneuploid populations within developing tumors are the major determinants of tumor dormancy. *Cancer Res.* 2009;69(24):9245-53.
240. Ma L, Lai D, Liu T, Cheng W, Guo L. Cancer stem-like cells can be isolated with drug selection in human ovarian cancer cell line SKOV3. *Acta Biochim Biophys Sin (Shanghai).* 2010;42(9):593-602.
241. Wang L, Mezencev R, Bowen NJ, Matyunina LV, McDonald JF. Isolation and characterization of stem-like cells from a human ovarian cancer cell line. *Mol Cell Biochem.* 2012;363(1-2):257-68.
242. Pagotto A, Pilotto G, Mazzoldi EL, Nicoletto MO, Frezzini S, Pasto A, et al. Autophagy inhibition reduces chemoresistance and tumorigenic potential of human ovarian cancer stem cells. *Cell Death Dis.* 2017;8(7):e2943.
243. Auzenne E, Ghosh SC, Khodadadian M, Rivera B, Farquhar D, Price RE, et al. Hyaluronic acid-paclitaxel: antitumor efficacy against CD44(+) human ovarian carcinoma xenografts. *Neoplasia.* 2007;9(6):479-86.
244. Chau WK, Ip CK, Mak AS, Lai HC, Wong AS. c-Kit mediates chemoresistance and tumor-initiating capacity of ovarian cancer cells through activation of Wnt/beta-catenin-ATP-binding cassette G2 signaling. *Oncogene.* 2013;32(22):2767-81.
245. Schilder RJ, Sill MW, Lee RB, Shaw TJ, Senterman MK, Klein-Szanto AJ, et al. Phase II evaluation of imatinib mesylate in the treatment of recurrent or persistent epithelial ovarian or primary peritoneal carcinoma: a Gynecologic Oncology Group Study. *J Clin Oncol.* 2008;26(20):3418-25.
246. Juretzka M, Hensley ML, Tew W, Konner J, Aghajanian C, Leitao M, et al. A phase 2 trial of oral imatinib in patients with epithelial ovarian, fallopian tube, or peritoneal carcinoma in second or greater remission. *Eur J Gynaecol Oncol.* 2008;29(6):568-72.

247. Matei D, Emerson RE, Schilder J, Menning N, Baldrige LA, Johnson CS, et al. Imatinib mesylate in combination with docetaxel for the treatment of patients with advanced, platinum-resistant ovarian cancer and primary peritoneal carcinomatosis : a Hoosier Oncology Group trial. *Cancer*. 2008;113(4):723-32.
248. Burgos-Ojeda D, Rueda BR, Buckanovich RJ. Ovarian cancer stem cell markers: prognostic and therapeutic implications. *Cancer Lett*. 2012;322(1):1-7.
249. Dyllal S, Gayther SA, Dafou D. Cancer stem cells and epithelial ovarian cancer. *J Oncol*. 2010;2010:105269.
250. Conic I, Dimov I, Tasic-Dimov D, Djordjevic B, Stefanovic V. Ovarian epithelial cancer stem cells. *ScientificWorldJournal*. 2011;11:1243-69.
251. Foster R, Buckanovich RJ, Rueda BR. Ovarian cancer stem cells: working towards the root of stemness. *Cancer Lett*. 2013;338(1):147-57.
252. Lennartsson J, Ronnstrand L. Stem cell factor receptor/c-Kit: from basic science to clinical implications. *Physiol Rev*. 2012;92(4):1619-49.
253. Stankov K, Popovic S, Mikov M. C-KIT signaling in cancer treatment. *Curr Pharm Des*. 2014;20(17):2849-80.
254. Trieselmann NZ, Soboloff J, Berger SA. Mast cells stimulated by membrane-bound, but not soluble, steel factor are dependent on phospholipase C activation. *Cell Mol Life Sci*. 2003;60(4):759-66.
255. Keshet E, Lyman SD, Williams DE, Anderson DM, Jenkins NA, Copeland NG, et al. Embryonic RNA expression patterns of the c-kit receptor and its cognate ligand suggest multiple functional roles in mouse development. *Embo j*. 1991;10(9):2425-35.
256. Lev S, Blechman JM, Givol D, Yarden Y. Steel factor and c-kit protooncogene: genetic lessons in signal transduction. *Crit Rev Oncog*. 1994;5(2-3):141-68.
257. Lammie A, Drobnjak M, Gerald W, Saad A, Cote R, Cordon-Cardo C. Expression of c-kit and kit ligand proteins in normal human tissues. *J Histochem Cytochem*. 1994;42(11):1417-25.
258. Yarden Y, Kuang WJ, Yang-Feng T, Coussens L, Munemitsu S, Dull TJ, et al. Human proto-oncogene c-kit: a new cell surface receptor tyrosine kinase for an unidentified ligand. *Embo j*. 1987;6(11):3341-51.
259. Montero JC, Lopez-Perez R, San Miguel JF, Pandiella A. Expression of c-Kit isoforms in multiple myeloma: differences in signaling and drug sensitivity. *Haematologica*. 2008;93(6):851-9.

260. Caruana G, Cambareri AC, Ashman LK. Isoforms of c-KIT differ in activation of signalling pathways and transformation of NIH3T3 fibroblasts. *Oncogene*. 1999;18(40):5573-81.
261. Sun J, Pedersen M, Ronnstrand L. Gab2 is involved in differential phosphoinositide 3-kinase signaling by two splice forms of c-Kit. *J Biol Chem*. 2008;283(41):27444-51.
262. Lyman SD, Jacobsen SE. c-kit ligand and Flt3 ligand: stem/progenitor cell factors with overlapping yet distinct activities. *Blood*. 1998;91(4):1101-34.
263. Lennartsson J, Jelacic T, Linnekin D, Shivakrupa R. Normal and oncogenic forms of the receptor tyrosine kinase kit. *Stem Cells*. 2005;23(1):16-43.
264. Jahn T, Sindhu S, Gooch S, Seipel P, Lavori P, Leifheit E, et al. Direct interaction between Kit and the interleukin-7 receptor. *Blood*. 2007;110(6):1840-7.
265. Wu H, Klingmuller U, Besmer P, Lodish HF. Interaction of the erythropoietin and stem-cell-factor receptors. *Nature*. 1995;377(6546):242-6.
266. Okada S, Nakauchi H, Nagayoshi K, Nishikawa S, Miura Y, Suda T. Enrichment and characterization of murine hematopoietic stem cells that express c-kit molecule. *Blood*. 1991;78(7):1706-12.
267. Wehrle-Haller B. The role of Kit-ligand in melanocyte development and epidermal homeostasis. *Pigment Cell Res*. 2003;16(3):287-96.
268. Loveland KL, Schlatt S. Stem cell factor and c-kit in the mammalian testis: lessons originating from Mother Nature's gene knockouts. *J Endocrinol*. 1997;153(3):337-44.
269. Maeda H, Yamagata A, Nishikawa S, Yoshinaga K, Kobayashi S, Nishi K. Requirement of c-kit for development of intestinal pacemaker system. *Development*. 1992;116(2):369-75.
270. Sun L, Lee J, Fine HA. Neuronally expressed stem cell factor induces neural stem cell migration to areas of brain injury. *J Clin Invest*. 2004;113(9):1364-74.
271. Foster BM, Zaidi D, Young TR, Mobley ME, Kerr BA. CD117/c-kit in Cancer Stem Cell-Mediated Progression and Therapeutic Resistance. *Biomedicines*. 2018;6(1).
272. Croom KF, Perry CM. Imatinib mesylate: in the treatment of gastrointestinal stromal tumours. *Drugs*. 2003;63(5):513-22; discussion 23-4.
273. Demetri GD. Differential properties of current tyrosine kinase inhibitors in gastrointestinal stromal tumors. *Semin Oncol*. 2011;38 Suppl 1:S10-9.
274. Fatrai S, van Schelven SJ, Ubink I, Govaert KM, Raats D, Koster J, et al. Maintenance of Clonogenic KIT(+) Human Colon Tumor Cells Requires Secretion of Stem Cell Factor by Differentiated Tumor Cells. *Gastroenterology*. 2015;149(3):692-704.

275. Levina V, Marrangoni A, Wang T, Parikh S, Su Y, Herberman R, et al. Elimination of human lung cancer stem cells through targeting of the stem cell factor-c-kit autocrine signaling loop. *Cancer Res.* 2010;70(1):338-46.
276. Wang L, Wang J, Li Z, Liu Y, Jiang M, Li Y, et al. Silencing stem cell factor attenuates stemness and inhibits migration of cancer stem cells derived from Lewis lung carcinoma cells. *Tumour Biol.* 2016;37(6):7213-27.
277. Pedersen M, Lofstedt T, Sun J, Holmquist-Mengelbier L, Pahlman S, Ronnstrand L. Stem cell factor induces HIF-1alpha at normoxia in hematopoietic cells. *Biochem Biophys Res Commun.* 2008;377(1):98-103.
278. Yang Z, Klionsky DJ. Eaten alive: a history of macroautophagy. *Nat Cell Biol.* 2010;12(9):814-22.
279. Glick D, Barth S, Macleod KF. Autophagy: cellular and molecular mechanisms. *J Pathol.* 2010;221(1):3-12.
280. Mizushima N, Yoshimori T, Ohsumi Y. The role of Atg proteins in autophagosome formation. *Annu Rev Cell Dev Biol.* 2011;27:107-32.
281. Clark SL, Jr. Cellular differentiation in the kidneys of newborn mice studies with the electron microscope. *J Biophys Biochem Cytol.* 1957;3(3):349-62.
282. Novikoff AB. The proximal tubule cell in experimental hydronephrosis. *J Biophys Biochem Cytol.* 1959;6(1):136-8.
283. Ashford TP, Porter KR. Cytoplasmic components in hepatic cell lysosomes. *J Cell Biol.* 1962;12:198-202.
284. De Duve C, Wattiaux R. Functions of lysosomes. *Annu Rev Physiol.* 1966;28:435-92.
285. Takeshige K, Baba M, Tsuboi S, Noda T, Ohsumi Y. Autophagy in yeast demonstrated with proteinase-deficient mutants and conditions for its induction. *J Cell Biol.* 1992;119(2):301-11.
286. Yang Z, Klionsky DJ. Mammalian autophagy: core molecular machinery and signaling regulation. *Curr Opin Cell Biol.* 2010;22(2):124-31.
287. Kimmelman AC. The dynamic nature of autophagy in cancer. *Genes Dev.* 2011;25(19):1999-2010.
288. Klionsky DJ, Abdelmohsen K, Abe A, Abedin MJ, Abeliovich H, Acevedo Arozena A, et al. Guidelines for the use and interpretation of assays for monitoring autophagy (3rd edition). *Autophagy.* 2016;12(1):1-222.
289. Jiang P, Mizushima N. LC3- and p62-based biochemical methods for the analysis of autophagy progression in mammalian cells. *Methods.* 2015;75:13-8.

290. <http://www.enzolifesciences.com/ENZ-51031/cyto-id-autophagy-detection-kit/>.
291. White E. Deconvoluting the context-dependent role for autophagy in cancer. *Nat Rev Cancer*. 2012;12(6):401-10.
292. White E. The role for autophagy in cancer. *J Clin Invest*. 2015;125(1):42-6.
293. Amaravadi RK, Lippincott-Schwartz J, Yin XM, Weiss WA, Takebe N, Timmer W, et al. Principles and current strategies for targeting autophagy for cancer treatment. *Clin Cancer Res*. 2011;17(4):654-66.
294. Ojha R, Bhattacharyya S, Singh SK. Autophagy in Cancer Stem Cells: A Potential Link Between Chemoresistance, Recurrence, and Metastasis. *Biores Open Access*. 2015;4(1):97-108.
295. Lin YH, Huang YC, Chen LH, Chu PM. Autophagy in cancer stem/progenitor cells. *Cancer Chemother Pharmacol*. 2015;75(5):879-86.
296. Chatterjee M, van Golen KL. Breast cancer stem cells survive periods of farnesyl-transferase inhibitor-induced dormancy by undergoing autophagy. *Bone Marrow Res*. 2011;2011:362938.
297. Filippi-Chiela EC, Villodre ES, Zamin LL, Lenz G. Autophagy interplay with apoptosis and cell cycle regulation in the growth inhibiting effect of resveratrol in glioma cells. *PLoS One*. 2011;6(6):e20849.
298. Gong C, Bauvy C, Tonelli G, Yue W, Delomenie C, Nicolas V, et al. Beclin 1 and autophagy are required for the tumorigenicity of breast cancer stem-like/progenitor cells. *Oncogene*. 2013;32(18):2261-72, 72e.1-11.
299. Cufi S, Vazquez-Martin A, Oliveras-Ferreros C, Martin-Castillo B, Vellon L, Menendez JA. Autophagy positively regulates the CD44(+) CD24(-/low) breast cancer stem-like phenotype. *Cell Cycle*. 2011;10(22):3871-85.
300. Zhu H, Wang D, Liu Y, Su Z, Zhang L, Chen F, et al. Role of the Hypoxia-inducible factor-1 alpha induced autophagy in the conversion of non-stem pancreatic cancer cells into CD133+ pancreatic cancer stem-like cells. *Cancer Cell Int*. 2013;13(1):119.
301. Bellodi C, Lidonnici MR, Hamilton A, Helgason GV, Soliera AR, Ronchetti M, et al. Targeting autophagy potentiates tyrosine kinase inhibitor-induced cell death in Philadelphia chromosome-positive cells, including primary CML stem cells. *J Clin Invest*. 2009;119(5):1109-23.
302. Ojha R, Jha V, Singh SK, Bhattacharyya S. Autophagy inhibition suppresses the tumorigenic potential of cancer stem cell enriched side population in bladder cancer. *Biochim Biophys Acta*. 2014;1842(11):2073-86.

303. Galavotti S, Bartesaghi S, Faccenda D, Shaked-Rabi M, Sanzone S, McEvoy A, et al. The autophagy-associated factors DRAM1 and p62 regulate cell migration and invasion in glioblastoma stem cells. *Oncogene*. 2013;32(6):699-712.
304. Jiang H, Gomez-Manzano C, Aoki H, Alonso MM, Kondo S, McCormick F, et al. Examination of the therapeutic potential of Delta-24-RGD in brain tumor stem cells: role of autophagic cell death. *J Natl Cancer Inst*. 2007;99(18):1410-4.
305. Zhao Y, Huang Q, Yang J, Lou M, Wang A, Dong J, et al. Autophagy impairment inhibits differentiation of glioma stem/progenitor cells. *Brain Res*. 2010;1313:250-8.
306. Zhuang W, Li B, Long L, Chen L, Huang Q, Liang Z. Induction of autophagy promotes differentiation of glioma-initiating cells and their radiosensitivity. *Int J Cancer*. 2011;129(11):2720-31.
307. Francipane MG, Lagasse E. Selective targeting of human colon cancer stem-like cells by the mTOR inhibitor Torin-1. *Oncotarget*. 2013;4(11):1948-62.
308. Sharif T, Martell E, Dai C, Kennedy BE, Murphy P, Clements DR, et al. Autophagic homeostasis is required for the pluripotency of cancer stem cells. *Autophagy*. 2017;13(2):264-84.
309. Pan H, Cai N, Li M, Liu GH, Izpisua Belmonte JC. Autophagic control of cell 'stemness'. *EMBO Mol Med*. 2013;5(3):327-31.
310. Schitteck B, Sinnberg T. Biological functions of casein kinase 1 isoforms and putative roles in tumorigenesis. *Mol Cancer*. 2014;13:231.
311. Ahmad KA, Wang G, Unger G, Slaton J, Ahmed K. Protein Kinase CK2 - A Key Suppressor of Apoptosis. *Advances in enzyme regulation*. 2008;48:179-87.
312. Ruzzene M, Bertacchini J, Toker A, Marmioli S. Cross-talk between the CK2 and AKT signaling pathways in cancer. *Advances in Biological Regulation*. 2017;64:1-8.
313. Knippschild U, Gocht A, Wolff S, Huber N, Lohler J, Stoter M. The casein kinase 1 family: participation in multiple cellular processes in eukaryotes. *Cell Signal*. 2005;17(6):675-89.
314. Bischof J, Randoll SJ, Sussner N, Henne-Bruns D, Pinna LA, Knippschild U. CK1delta kinase activity is modulated by Chk1-mediated phosphorylation. *PLoS One*. 2013;8(7):e68803.
315. Zhang L, Jia J, Wang B, Amanai K, Wharton KA, Jr., Jiang J. Regulation of wingless signaling by the CKI family in *Drosophila* limb development. *Dev Biol*. 2006;299(1):221-37.
316. Jiang J. CK1 in Developmental Signaling: Hedgehog and Wnt. *Curr Top Dev Biol*. 2017;123:303-29.

317. Venerando A, Marin O, Cozza G, Bustos VH, Sarno S, Pinna LA. Isoform specific phosphorylation of p53 by protein kinase CK1. *Cell Mol Life Sci.* 2010;67(7):1105-18.
318. Behrend L, Milne DM, Stoter M, Deppert W, Campbell LE, Meek DW, et al. IC261, a specific inhibitor of the protein kinases casein kinase 1-delta and -epsilon, triggers the mitotic checkpoint and induces p53-dependent postmitotic effects. *Oncogene.* 2000;19(47):5303-13.
319. Stoter M, Bamberger AM, Aslan B, Kurth M, Speidel D, Loning T, et al. Inhibition of casein kinase I delta alters mitotic spindle formation and induces apoptosis in trophoblast cells. *Oncogene.* 2005;24(54):7964-75.
320. Bibian M, Rahaim RJ, Choi JY, Noguchi Y, Schurer S, Chen W, et al. Development of highly selective casein kinase 1delta/1epsilon (CK1delta/epsilon) inhibitors with potent antiproliferative properties. *Bioorg Med Chem Lett.* 2013;23(15):4374-80.
321. Richter J, Ullah K, Xu P, Alscher V, Blatz A, Peifer C, et al. Effects of altered expression and activity levels of CK1delta and varepsilon on tumor growth and survival of colorectal cancer patients. *Int J Cancer.* 2015;136(12):2799-810.
322. Penas C, Ramachandran V, Simanski S, Lee C, Madoux F, Rahaim RJ, et al. Casein kinase 1delta-dependent Wee1 protein degradation. *J Biol Chem.* 2014;289(27):18893-903.
323. Maritzen T, Lohler J, Deppert W, Knippschild U. Casein kinase I delta (CK1delta) is involved in lymphocyte physiology. *Eur J Cell Biol.* 2003;82(7):369-78.
324. Brockschmidt C, Hirner H, Huber N, Eismann T, Hillenbrand A, Giamas G, et al. Anti-apoptotic and growth-stimulatory functions of CK1 delta and epsilon in ductal adenocarcinoma of the pancreas are inhibited by IC261 in vitro and in vivo. *Gut.* 2008;57(6):799-806.
325. Rosenberg LH, Lafitte M, Quereda V, Grant W, Chen W, Bibian M, et al. Therapeutic targeting of casein kinase 1delta in breast cancer. *Sci Transl Med.* 2015;7(318):318ra202.
326. Hanahan D, Weinberg RA. Hallmarks of cancer: the next generation. *Cell.* 2011;144(5):646-74.
327. Anderson DM, Williams DE, Tushinski R, Gimpel S, Eisenman J, Cannizzaro LA, et al. Alternate splicing of mRNAs encoding human mast cell growth factor and localization of the gene to chromosome 12q22-q24. *Cell Growth Differ.* 1991;2(8):373-8.
328. Schneider CA, Rasband WS, Eliceiri KW. NIH Image to ImageJ: 25 years of image analysis. *Nat Methods.* 2012;9(7):671-5.
329. <http://bioinf.wehi.edu.au/software/elda>.
330. Chou TC. Drug combination studies and their synergy quantification using the Chou-Talalay method. *Cancer Res.* 2010;70(2):440-6.

331. Martinez FO, Gordon S, Locati M, Mantovani A. Transcriptional profiling of the human monocyte-to-macrophage differentiation and polarization: new molecules and patterns of gene expression. *J Immunol.* 2006;177(10):7303-11.
332. Tarique AA, Logan J, Thomas E, Holt PG, Sly PD, Fantino E. Phenotypic, functional, and plasticity features of classical and alternatively activated human macrophages. *Am J Respir Cell Mol Biol.* 2015;53(5):676-88.
333. Soldano S, Pizzorni C, Paolino S, Trombetta AC, Montagna P, Brizzolara R, et al. Alternatively Activated (M2) Macrophage Phenotype Is Inducible by Endothelin-1 in Cultured Human Macrophages. *PLoS One.* 2016;11(11):e0166433.
334. Di Noto G, Chiarini M, Paolini L, Mazzoldi EL, Giustini V, Radeghieri A, et al. Immunoglobulin Free Light Chains and GAGs Mediate Multiple Myeloma Extracellular Vesicles Uptake and Secondary NfκB Nuclear Translocation. *Front Immunol.* 2014;5:517.
335. Justus CR, Leffler N, Ruiz-Echevarria M, Yang LV. In vitro cell migration and invasion assays. *J Vis Exp.* 2014(88).
336. Zhang Y, Cheng Y, Ren X, Zhang L, Yap KL, Wu H, et al. NAC1 Modulates Sensitivity of Ovarian Cancer Cells to Cisplatin via Altering the HMGB1-Mediated Autophagic Response. *Oncogene.* 2012;31(8):1055-64.
337. Fireman E, Kivity S, Shahar I, Reshef T, Mekori YA. Secretion of stem cell factor by alveolar fibroblasts in interstitial lung diseases. *Immunol Lett.* 1999;67(3):229-36.
338. Ries CH, Cannarile MA, Hoves S, Benz J, Wartha K, Runza V, et al. Targeting tumor-associated macrophages with anti-CSF-1R antibody reveals a strategy for cancer therapy. *Cancer Cell.* 2014;25(6):846-59.
339. Inoue M, Kyo S, Fujita M, Enomoto T, Kondoh G. Coexpression of the c-kit receptor and the stem cell factor in gynecological tumors. *Cancer Res.* 1994;54(11):3049-53.
340. Buchdunger E, Cioffi CL, Law N, Stover D, Ohno-Jones S, Druker BJ, et al. Abl protein-tyrosine kinase inhibitor STI571 inhibits in vitro signal transduction mediated by c-kit and platelet-derived growth factor receptors. *J Pharmacol Exp Ther.* 2000;295(1):139-45.
341. Karimian A, Ahmadi Y, Yousefi B. Multiple functions of p21 in cell cycle, apoptosis and transcriptional regulation after DNA damage. *DNA Repair.* 2016;42:63-71.
342. Georgakilas AG, Martin OA, Bonner WM. p21: A Two-Faced Genome Guardian. *Trends Mol Med.* 2017;23(4):310-9.
343. Bar I, Merhi A, Larbanoix L, Constant M, Haussy S, Laurent S, et al. Silencing of casein kinase 1 delta reduces migration and metastasis of triple negative breast cancer cells. *Oncotarget.* 2018;9(56):30821-36.

344. Deng J, Wang L, Chen H, Hao J, Ni J, Chang L, et al. Targeting epithelial-mesenchymal transition and cancer stem cells for chemoresistant ovarian cancer. *Oncotarget*. 2016;7(34):55771-88.
345. Koukourakis MI, Kalamida D, Mitrakas A, Pouliliou S, Kalamida S, Sivridis E, et al. Intensified autophagy compromises the efficacy of radiotherapy against prostate cancer. *Biochem Biophys Res Commun*. 2015;461(2):268-74.
346. Levy JM, Thorburn A. Targeting autophagy during cancer therapy to improve clinical outcomes. *Pharmacol Ther*. 2011;131(1):130-41.
347. Guo XL, Li D, Hu F, Song JR, Zhang SS, Deng WJ, et al. Targeting autophagy potentiates chemotherapy-induced apoptosis and proliferation inhibition in hepatocarcinoma cells. *Cancer Lett*. 2012;320(2):171-9.
348. Yang MC, Wang HC, Hou YC, Tung HL, Chiu TJ, Shan YS. Blockade of autophagy reduces pancreatic cancer stem cell activity and potentiates the tumoricidal effect of gemcitabine. *Mol Cancer*. 2015;14:179.
349. Bousquet G, El Bouchtaoui M, Sophie T, Leboeuf C, de Bazelaire C, Ratajczak P, et al. Targeting autophagic cancer stem-cells to reverse chemoresistance in human triple negative breast cancer. *Oncotarget*. 2017;8(21):35205-21.
350. Li J, Hou N, Faried A, Tsutsumi S, Kuwano H. Inhibition of autophagy augments 5-fluorouracil chemotherapy in human colon cancer in vitro and in vivo model. *Eur J Cancer*. 2010;46(10):1900-9.
351. Chudecka-Glaz AM, Cymbaluk-Ploska AA, Menkiszak JL, Pius-Sadowska E, Machalinski BB, Sompolska-Rzechula A, et al. Assessment of selected cytokines, proteins, and growth factors in the peritoneal fluid of patients with ovarian cancer and benign gynecological conditions. *Onco Targets Ther*. 2015;8:471-85.
352. Li PH, Liu LH, Chang CC, Gao R, Leung CH, Ma DL, et al. Silencing Stem Cell Factor Gene in Fibroblasts to Regulate Paracrine Factor Productions and Enhance c-Kit Expression in Melanocytes on Melanogenesis. *Int J Mol Sci*. 2018;19(5).
353. Ding L, Saunders TL, Enikolopov G, Morrison SJ. Endothelial and perivascular cells maintain haematopoietic stem cells. *Nature*. 2012;481(7382):457-62.
354. Xu C, Gao X, Wei Q, Nakahara F, Zimmerman SE, Mar J, et al. Stem cell factor is selectively secreted by arterial endothelial cells in bone marrow. *Nat Commun*. 2018;9(1):2449.
355. Worzfeld T, Finkernagel F, Reinartz S, Konzer A, Adhikary T, Nist A, et al. Proteotranscriptomics Reveal Signaling Networks in the Ovarian Cancer Microenvironment. *Mol Cell Proteomics*. 2018;17(2):270-89.

356. Yang L, Zhang Y. Tumor-associated macrophages: from basic research to clinical application. *J Hematol Oncol.* 2017;10(1):58.
357. Lupia M, Cavallaro U. Ovarian cancer stem cells: still an elusive entity? *Mol Cancer.* 2017;16(1):64.
358. Gov E, Kori M, Arga KY. RNA-based ovarian cancer research from 'a gene to systems biomedicine' perspective. *Syst Biol Reprod Med.* 2017;63(4):219-38.
359. Xing BL, Li T, Tang ZH, Jiao L, Ge SM, Qiang X, et al. Cumulative methylation alternations of gene promoters and protein markers for diagnosis of epithelial ovarian cancer. *Genet Mol Res.* 2015;14(2):4532-40.
360. Jim HS, Lin HY, Tyrer JP, Lawrenson K, Dennis J, Chornokur G, et al. Common Genetic Variation in Circadian Rhythm Genes and Risk of Epithelial Ovarian Cancer (EOC). *J Genet Genome Res.* 2015;2(2).
361. Caiola E, Brogginini M, Marabese M. Genetic markers for prediction of treatment outcomes in ovarian cancer. *Pharmacogenomics J.* 2014;14(5):401-10.
362. Al Bakir M, Gabra H. The molecular genetics of hereditary and sporadic ovarian cancer: implications for the future. *Br Med Bull.* 2014;112(1):57-69.
363. Kurman RJ, Shih Ie M. Molecular pathogenesis and extraovarian origin of epithelial ovarian cancer--shifting the paradigm. *Hum Pathol.* 2011;42(7):918-31.
364. Smolle E, Taucher V, Pichler M, Petru E, Lax S, Haybaeck J. Targeting signaling pathways in epithelial ovarian cancer. *Int J Mol Sci.* 2013;14(5):9536-55.
365. Fahrenkrug J, Georg B, Hannibal J, Hindersson P, Gras S. Diurnal rhythmicity of the clock genes *Per1* and *Per2* in the rat ovary. *Endocrinology.* 2006;147(8):3769-76.
366. Sun Y, Jin L, Sui YX, Han LL, Liu JH. Circadian Gene *CLOCK* Affects Drug-Resistant Gene Expression and Cell Proliferation in Ovarian Cancer SKOV3/DDP Cell Lines Through Autophagy. *Cancer Biother Radiopharm.* 2017;32(4):139-46.
367. Xu H, Wang Z, Mo G, Chen H. Association between circadian gene *CLOCK* and cisplatin resistance in ovarian cancer cells: A preliminary study. *Oncol Lett.* 2018;15(6):8945-50.
368. Wang Z, Li L, Wang Y. Effects of *Per2* overexpression on growth inhibition and metastasis, and on *MTA1*, *nm23-H1* and the autophagy-associated *PI3K/PKB* signaling pathway in nude mice xenograft models of ovarian cancer. *Mol Med Rep.* 2016;13(6):4561-8.
369. Dong Y, Chi SL, Borowsky AD, Fan Y, Weiss RH. Cytosolic *p21Waf1/Cip1* increases cell cycle transit in vascular smooth muscle cells. *Cell Signal.* 2004;16(2):263-9.

370. Asada M, Yamada T, Ichijo H, Delia D, Miyazono K, Fukumuro K, et al. Apoptosis inhibitory activity of cytoplasmic p21(Cip1/WAF1) in monocytic differentiation. *Embo j.* 1999;18(5):1223-34.
371. Park SH, Wang X, Liu R, Lam KS, Weiss RH. High throughput screening of a small molecule one-bead-one-compound combinatorial library to identify attenuators of p21 as chemotherapy sensitizers. *Cancer Biol Ther.* 2008;7(12):2015-22.
372. Park SH, Park JY, Weiss RH. Antisense attenuation of p21 sensitizes kidney cancer to apoptosis in response to conventional DNA damaging chemotherapy associated with enhancement of phospho-p53. *J Urol.* 2008;180(1):352-60.
373. Inoue H, Hwang SH, Wecksler AT, Hammock BD, Weiss RH. Sorafenib attenuates p21 in kidney cancer cells and augments cell death in combination with DNA-damaging chemotherapy. *Cancer Biol Ther.* 2011;12(9):827-36.
374. Xie H, Li C, Dang Q, Chang LS, Li L. Infiltrating mast cells increase prostate cancer chemotherapy and radiotherapy resistances via modulation of p38/p53/p21 and ATM signals. *Oncotarget.* 2016;7(2):1341-53.
375. Pavan S, Olivero M, Cora D, Di Renzo MF. IRF-1 expression is induced by cisplatin in ovarian cancer cells and limits drug effectiveness. *Eur J Cancer.* 2013;49(4):964-73.
376. Rodriguez N, Yang J, Hasselblatt K, Liu S, Zhou Y, Rauh-Hain JA, et al. Casein kinase I epsilon interacts with mitochondrial proteins for the growth and survival of human ovarian cancer cells. *EMBO Mol Med.* 2012;4(9):952-63.